EVALUATION OF CONCRETE STRENGTH AND PERMEABILITY WITH TIME

by

PAUL M. TACKETT

B.S., The University of Kansas, 2011

A THESIS

submitted in partial fulfillment of the requirements for the degree

MASTER OF SCIENCE

Department of Civil Engineering

College of Engineering

KANSAS STATE UNIVERSITY

Manhattan, Kansas

2013

Approved by:

Major Professor

Dr. Kyle Riding

Abstract

The relationship between in-place concrete strength and permeability with concrete cylinder strength and permeability with time is of interest - especially when supplementary cementitious materials (SCMs) are used. A joint research project between The University of Kansas was undergone to quantify these relationships. The permeability of concrete is directly tied to its ability to mitigate certain failure mechanisms such as corrosion and sulfate attack.

The three concrete mixtures being tested by Kansas State University (KSU) vary in cementitious content as follows: (1) 100% ordinary portland cement (OPC), (2) 25% Class F fly ash (F-ash) and 75% OPC, (3) 25% Class C fly ash (C-Ash) and 75% OPC. The mixtures were also placed in three different seasons to present differing curing environmental effects. The summer slabs were cast during July and August. The fall slabs were cast in October and November. The final set of slabs were cast in March and April. Three sets of concrete specimens (lab cured, field cured and in-situ core specimens) were tested at 28, 56, 90, 180, and 360 days for strength and permeability properties. The permeability performance tests being utilized are ASTM C1202 and ASTM C642.

The results have shown very desirable permeability and strength data for the mixes using blended fly ash cements. The F-ash exhibited the best high early strength and low permeability data for the summer placement season and slower strength and permeability performance at cold weather. The C-ash performed the best overall for all seasons and had the least environmental effects. The OPC performed the worst in regards to permeability and did not reach as high long term strength.

Table of Contents

List of Figures

List of Tables

Acknowledgements

I would first like to thank Dr. Kyle Riding for his guidance on the project. I also want to thank the Kansas Department of Transportation for the research funding through its Kansas Transportation Research and New-Developments (K-TRAN) program. There are also many graduate students at Kansas State University that have helped with the placement of the concrete slabs and cylinders without whose help I would not have been able to accomplish this research. Finally, I would like to thank my parents, Robert and Becky Tackett and my brother Brandon and his wife Bonnie for always encouraging me to think deeply about academics, life and worldview.

Chapter 1 - Introduction

With the construction industry becoming more diverse and many more parties being involved, much more focus has been put on reliable, cost effective and sustainable projects. In order for this to become a reality, more insight on material behavior and how quality control and quality assurance protocols can measure material behavior is needed. Particular needs have arisen in concrete construction for lower owner and maintenance costs and better projections of project service life. Service life modeling is becoming more prevalent in design contracts and, with this prevalence, designers and manufacturers have then had to assume more risk and contractual liability. In order for this risk to be minimized, higher confidence is needed in material behavior and therefore in how the material is tested to meet the desired behavior.

A paradigm shift can be noticed in most building and construction codes where an emphasis is now being placed on material performance and durability. For instance, ACI 318 was revised in 2008, making categories for exposure classes as well as maximum and minimum requirements of concrete mixture designs and the materials in them. With this change, the structural and transportation engineering professions have also had to transition from their traditional design philosophies in order to incorporate designs and mitigations for durability (ACI 318 2008).

The pavement and bridge industries also have transitioned from their traditional strength-based criterion, which can be very easily met without durability considerations, to performance and prescriptive design specifications. Material performance in freeze-thaw conditions and environments in which the concrete is exposed to materials having deleterious effects now often control the design of the concrete mixture. In many situations, the environment the concrete is placed in cannot be helped. De-icing salts and chemicals are placed during the winter to ensure

public safety and other environments are constantly exposed to other harmful chemicals. These are major durability concerns if the substances are able to penetrate into the concrete, hence concrete performance is directly related to the ease of ingress of harmful materials. If the permeability of the concrete is able to be lowered, less deleterious materials have the opportunity to affect the function and service life of the concrete.

Concrete durability is the ability of concrete to retain its original form, performance and serviceability in its environment (ACI 201 2008). The research being investigated herein focuses on two performance based quality control standards, (1) ASTM C1202 commonly referred to as the Rapid Chloride Permeability Test, (2) ASTM C642 commonly referred to as Volume of Permeable Voids. The permeability of the concrete is greatly affected by its curing environment and its degree of hydration. In order to quantify these, three different cementitious blends were used in an identically proportioned concrete mixture. The first blend was normal ordinary portland cement (OPC), the second blend was 75% OPC and 25% by mass type F fly-ash (F-ash) and the third blend was a 75% OPC and 25% by mass type C fly-ash (C-ash). These blends were placed during three different seasons and exposed only to in-situ curing in slabs, field curing or lab curing over a two year period. The mixes were tested at 28, 56, 90, 180 and 360 days for both permeability performance tests and also for compressive strength in order to gain further insight into the effects of curing environments and the performance of blended cements in concrete over an extended period of time.

The research objectives of this investigation are to evaluate the three concrete mixes on three criteria: (1) how casting season affects the long term properties of each mix, (2) compare different curing environments and the difference in them for quality assurance and acceptance and (3) investigate the differences in the performance tests used to evaluate permeability.

Chapter two gives an overview of developed test methods in the literature and brief introductions into failure mechanisms and concrete chemistry. Chapter three details the materials used in the research. Chapter four explains the methods used for placement and evaluation of the material. Chapter five presents the findings of all seasons 360 day tests. Chapter six gives insight into the variance among the seasons, the impacts of curing environments and analysis of the relationships between the performance tests. Chapter seven gives conclusions, recommendations and future research needs.

Chapter 2 - Literature Review

2.1 - Importance of Strength and Durability

The majority of acceptance criterion for State Department of Transportations in the U.S. and other entities that adhere to the American Concrete Institute specifications (herein referred to as DOT's and ACI respectively) are based upon the compressive strength of the concrete. (Castro, Spragg and Weiss 2010). The compressive strength of concrete is established by ASTM C39 (2012). Concrete's mechanical properties are determined as functions of its 28 day compressive strength (f'c). For most design purposes, the modulus of elasticity, modulus of rupture, tensile strength etc. are all taken as functions of concretes unit weight and ultimate compressive strength (Mindess, Young and Darwin 2003).

This is of particular importance for concrete pavements. Pavements will almost never see loads that cause concrete crushing to be the governing failure mechanism of the material – if extreme loading events e.g. crashes and impact/impulse loads are neglected. The primary reason for strength failure in concrete is due to a lack of tensile strength. Reductions in the tensile strength can arise from fatigue and durability effects. Concrete pavements can be idealized as a beam, or plate, resting on an elastic foundation. With the pavement undergoing hysteretic loading, flexural cracking occurs. Since concrete's tensile strength is usually between 10 and 15 percent of its current compressive strength, this is the controlling factor for strength reduction. Once the concrete cracks, it loses strength capacity because of the reduction of its available cross-sectional area.

Concrete is then designed not to experience cracking at these loads. As the concrete strength increases, the water to cement ratio (w/c) decreases. As the w/c ratio decreases the permeability of the concrete also decreases. Lower permeability in concrete aides the concrete in

keeping out deleterious substances that cause negative material effects, like softening and disintegration of cement paste, corroding of materials and ensuing mechanical stress from chemical action. From a purely strength of materials approach, lowering the permeability of a concrete section creates a section having less voids and more effective area to transfer stresses.

2.1.1 - Failure Mechanisms of Concrete Related to Permeability

It is very well established that there is vast variety of concrete aggregates, cementitious materials and concrete mix design philosophies used - dating all the way back to the Roman Empire. Although much has changed and progressed since that time, one thing that has not changed is how concrete, as a material, reacts to differing stresses and the mechanisms causing it to fail. The main governing factor affecting the durability of concrete is the water to cement ratio (w/c). As stated previously, as the w/c ratio decreases, as a general rule the permeability of the concrete decreases. Decreasing the permeability makes it much more difficult for the ingress of detrimental substances/processes. Three common mechanisms of failure are: freeze-thaw damage, corrosion, and sulfate attack. These can be categorized in two ways, physical attack and chemical attack. Freeze-thaw and sulfate attack can have both physical and chemical means of deteriorating concrete, whereas corrosion is primarily chemical in nature (Mindess, Young and Darwin 2003).

Freeze-thaw damage is much more complicated than the accepted phenomenon of water expanding when it freezes due to its polar nature (usually around 9% per volume). This does account for some development of tensile stresses, but not the sole cause of the deformation of the material. The freezing point of water is often lowered in concrete because of the small diameter of its pores and capillaries and the presence of other minerals through the process of freezing point depression. Even when concrete is only partially saturated and there are more than enough

air-entrained voids to accommodate the expansion of water, significant strain on the material is still encountered. This contributes to pressure and fluid properties, i.e. osmosis, osmotic pressure and desorption. The last of these is worth explaining in more detail because the stress is not as easily apparent, but still quite impactful. Desorption during freezing is the process by which water leaves the hydrated cement paste and spontaneously moves towards freezing sites. This causes the cement paste to dry and shrink – creating expansion and contraction near each other (Mindess, Young and Darwin 2003). Perhaps the greatest obstacle with freeze-thaw damage is the cyclical nature of the problem. Once micro-cracks form, more water can enter the concrete. The more the water that enters, the more the expansion and cracking that can occur. Many tests have been done on concrete pavements that have been in service for fifty or more years, and many concretes that have lower permeability are still in service and in good condition. An example of this is stretches of I-94 outside of Detroit (Castro, Spragg and Weiss 2010).

Perhaps the most widespread and easily seen failure mechanism is corrosion. The normal corrosion mechanism involves the flow of an electrical current in order for oxidation and reduction reactions to occur. At some point in normal ferrous steel, the iron will oxidize and produce two electrons and a ferrous ion as shown in *Eq. 2.1.1a.*

$$\mathrm{Fe} \rightleftharpoons 2\mathrm{e}^- + \mathrm{Fe}^{2+} \tag{2.1.1a}$$

The following reaction in *Eq. 2.1.1b* then occurs at the cathode.

$$\frac{1}{2}\mathrm{O}_2 + \mathrm{H}_2\mathrm{O} + 2\mathrm{e}^- \rightleftharpoons 2\mathrm{OH}^- \tag{2.1.1b}$$

With the flow of electrons and the ability of OH^- hydroxyl ions to migrate between the cathode and the anode, equalizing the electrical current, ferrous hydroxide forms at the anode. The final result is shown in *Eq. 2.1.2a.*

$$\mathrm{Fe}^{2+} + 2(\mathrm{OH})^- \longrightarrow \mathrm{Fe}(\mathrm{OH})_2 \tag{2.1.2a}$$

If the migration of the hydroxyl ions is stopped the reaction does not happen. It is difficult to stop the migration entirely, but having denser microstructure in concrete can significantly slow the migration rate and the dependent corrosion rate (Mindess, Young and Darwin 2003). With the presence of water and air available, ferrous hydroxide will oxidize to hydrated ferric oxide, i.e. rust. Ferric rust gives a large volume expansion of anywhere between two and six times greater than the base iron volume before corrosion (Bertolini, et al. 2013). While corrosion of steel cannot be completely avoided by low permeability concrete (especially if carbonation has dropped the pH below the passive protection oxide layer), it can significantly slow down the corrosion rate.

Sulfate attack can have devastating effects on the concrete integrity. It can involve most of the hydration products and can lead to expansion and cracking of concrete and negatively impact properties of the cement paste. Two of the more common attacks are sulfoaluminate corrosion and gypsum corrosion. The sulfoaluminate reaction in cement chemistry oxide notation is shown in *Eq. 2.1.3*.

$$C_4A\bar{S}H_{12} + 2C\bar{S}H_2 + 16H \longrightarrow C_6A\bar{S}_3H_{32} \qquad (2.1.3)$$

Note: In inorganic chemistry, the capital of the oxide element is used instead of the full element abbreviation, where: C = CaO; S = SiO_2; A = Al_2O_3; F = Fe_2O_3; M = MgO; K = K_2O;

N = Na_2O; H = H_2O; $\bar{S}$ = SO_3

The reaction is concurrent with a solid volume increase of 55%, which creates very large internal stresses. The sulfoaluminate reaction originates in the interaction of sulfates and the calcium hydroxides as presented in *Eq. 2.1.4*.

$$CH + SO_4^{2-}(aq) \rightleftharpoons +C\bar{S}H_2 + 2OH^-(aq) \qquad (2.1.4)$$

Eq. 2.1.4 is referred to as gypsum corrosion and is characteristic of a 120% increase of solid volume. Gypsum corrosion is often secondary for relatively young concrete and can become the primary mechanism for concrete greater than 10 years of age. It must be remembered that even though gypsum corrosion has a larger percent increase in solid volume, there is much more sulfoaluminate present than the other components in the concrete. Therefore, the total volume increase of the concrete will be more with sulfoaluminate because of the large volume fraction of sulfoaluminate compared to the volume fraction of gypsum. *Eq. 2.1.4* is important because it shows with low sulfate exposure the sulfates still penetrate and are able to concentrate and react with the sulfoaluminate. Even without large volume expansion, sulfate attack can cause durability issues by disintegration and decalcification of the cement paste – the cement paste becomes softer and more plastic (Mindess, Young and Darwin 2003). These are both controlled and mitigated by the ability of the sulfates to ingress or diffuse into the pores of the concrete solution. Low permeability concrete will help reduce the rate of sulfate ion ingress into the concrete and greatly slow down the deterioration.

2.2 - Cement Chemistry and Pozzolans

2.2.1 - Normal Portland Cement Hydration

Non-hydraulic cements were among the first to appear in Egypt when the Egyptians used gypsum mortars. Impure gypsum was calcinated and then combined later with a small amount of water that would have been driven off by the calcination process which recombines it into a new form. Gypsum mortars required a lower burning temperature to calcinate (~130˚C) than limestone (calcium-carbonate) mortars. Limestone motors were formed with a burning temperature of ~1000˚C and hardened by the drying of air. Both the gypsum and lime mortars

are somewhat impermeable to water after they have hardened, but are classified as non-hydraulic cements because they will not form/harden underwater (Mindess, Young and Darwin 2003).

Hydraulic cements were produced by the Romans and Greeks. It was noticed that when limestone was calcined in the presence of clayey impurities and mixed with volcanic ash, lime and sand much stronger mortars were produced. The term pozzolan is derived from this practice, because the Romans used volcanic ash found near the village of Pozzuoli - which was adjacent to Mt. Vesuvius (Mindess, Young and Darwin 2003). These new cements were hydraulic cements and could withstand hardening in water; this hardening occurred through the process of cement hydration.

The two major strength contributors for modern portland cement strength are tri-calcium silicate and di-calcium silicate, C_3S and C_2S. The strength effects of tri-calcium silicate begin after setting whereas the di-calcium silicate begins acting at later ages. Impure C_3S and C_2S typically found in portland cement are referred to as alite and belite respectively. Their chemical reactions are shown in *Eq. 2.2.1a,b.*

$$2C_3S + 11H \rightarrow C_3S_2H_8 + 3CH \quad (2.2.1a)$$

$$2C_2S + 9H \rightarrow C_3S_2H_8 + 3CH \quad (2.2.1b)$$

Calcium-silicate-hydroxide (C-S-H) is formed from the hydrated cement grains and is the principle binding agent that holds the concrete together (Mindess, Young and Darwin 2003).

2.2.2 - Pozzolan Classification and Hydration

Pozzolans can be naturally occurring or byproducts of industry. Fly ash is a byproduct of modern coal fired power plants. The ash is the noncombustible residual coal material that is discharged out of the furnace in the flue gas – which is where the term fly ash comes from, compared to bottom ash left in the furnace. As the fly ash is being discharged with the flue gas it

travels through electrostatic precipitators, or bag houses, where the fly ash is collected and stored. ASTM C618 (2012) classifies fly ash into two categories, Class F and Class C. Class F fly ash is usually obtained from anthracite or bituminous coal. Class C fly ash is usually from lignite or subbituminous coal. (Mindess, Young and Darwin 2003). The main requirement for chemical composition is to ensure the major acidic oxidizers do not comprise less than 70% for F-ash and 50% for C-ash. ASTM C618 (2012) states the compressive strength of mortar cubes made with a partial replacement of portland cement up to 20% fly ash must be within 75% of the compressive strength of cubes with no fly ash at 7 or 28 day indexes. Pozzolanic reactions follow the principal reaction shown in *Eq. 2.2.2*.

$$\mathrm{CH} + \mathrm{S} + \mathrm{H} \rightarrow \mathrm{C} - \mathrm{S} - \mathrm{H} \qquad (2.2.2)$$

The fly ash particles themselves have close to the same average size as normal portland cement grains (~10-15μm), but the surface area of the fly ash is between 1 and 2 m^2/g compared to normal portland cement which is less than 1 m^2/g. The cement grains, however, are irregular and granular while the fly ash grains are mostly spherical – hence the larger surface area of the fly ash. Since cement incorporating fly ash also has spherical grains, the matrix can be made denser by particle packing and from additional C-S-H formation from the pozzolanic reaction. The pozzolanic reaction also reduces the CH content by consuming it in the reaction. CH crystals usually occupy about 20% of cement volume and form very weak failure planes in the interfacial transition zone. Replacing them with C-S-H is very desirable for strength and durability (Mindess, Young and Darwin 2003). Fly ash reduces the porosity, although this reduction is dependent on a healthy curing environment for the fly ash. Low calcium fly ash (F-ash) also adds more workability to the concrete. Another reason for the addition of fly ash in concretes is to mitigate the Alkali-Silica Reaction (ASR) as seen by research by Halstead (1986).

Fly ash can also reduce the rate and total amount of heat released during hydration. In mass concreting applications this is usually an advantage, and for general concrete lower heat reduces thermal cracking. However, mixtures incorporating fly ash have slower initial strength gain. Fly ash (especially high calcium C-ash) can also have interaction problems with chemical admixtures leading to extended setting problems (Monteiro 2006).This requires mixtures containing high amounts of fly ash be tested to ensure these problems will not occur at both the low and high temperatures expected in the field.

2.3 - Water and Ion Transport in Concrete

2.3.1 - Permeability D'Arcy's Law

D'Arcy's Law is a constitutive equation used to model the flow of water through any porous media and is given by *Eq. 2.3.1.*

$$v = K_p \frac{h}{x} \tag{2.3.1}$$

Where: v = velocity of water (ft./s)

h = pressure head of water (ft.)

x = thickness of specimen (ft.)

K_p = permeability coefficient (ft./s)

While D'Arcy's Law is widely applied to soil mechanics and other constant media, the K_p for concrete paste changes largely with w/c ratio and with the age of cement paste as more hydration proceeds. Therefore, applying D'Arcy's Law is usually not practical for most quality control and quality assurance purposes (Mindess, Young and Darwin 2003).

2.3.2 - Diffusion (Ficks 2nd Law)

Fick's Second law applies where no (or little) pressure head exists to drive the ions through the concrete. Instead it is the concentration gradient that provides the transport method of diffusion, the governing linear, second order partial differential equation is shown in *Eq. 2.3.2a* and the solution in *Eq. 2.3.2b* – it could become a nonlinear, second order partial differential equation if expressions for K_d with time where able to be quantified.

$$\frac{\partial C}{\partial t} = K_d \frac{\partial^2 C}{\partial x^2} \qquad (2.3.2a)$$

Where: C = concentration (lbs./in.^{3})

T = time (s)

K_d = diffusion coefficient (in.^{2}/s)

x = depth of interest in specimen (in.)

$$C(x,t) = C_0\left[1 - \text{erf}\left(\frac{x}{2\sqrt{K_d t}}\right)\right] \qquad (2.3.2b)$$

Where: $C(x,t)$ = concentration at depth, x (in.) and time, t (days from exposure)

C_0 = concentration at surface (lbs./in.^{3})

$erf(\ )$ = error function

The solution in *Eq. 2.3.2b* utilizes the error function, which uses a constant diffusion coefficient that does not change with time. It is well known that the diffusion coefficient does change with time. The diffusion coefficient calculated using the error function gives an average diffusion coefficient over the time period analyzed. To combat this, Berke and Hicks (1996) used an iterative method of measuring chloride concentrations at varying depths and then solved for the

corresponding diffusion coefficients. Chloride profiles were than generated to predict concentrations at future times. The models they developed for a parking garage in the Midwest correlated very well for measured vs. calculated chloride levels at different depths. The diffusion coefficient can also be found using the Nernst-Einstein equation relating diffusivity to electrical conductivity *Eq. 2.3.2c*.

$$\frac{K_d}{K_0} = \frac{k}{k_0} = \beta\phi \qquad (2.3.2c)$$

Where: K_0 = diffusivity pore solution (in.^{2}/s)

k_0 = conductivity pore solution (1/ohms)

K_d, k = diffusivity and conductivity of concrete respectively

β = tortuosity of capillaries (in./in.)

ϕ = concrete capillary porosity (in.^{3}/lb.)

Some object to the accuracy of this by pointing out the material is not all homogeneous (rebar etc.), the diffusivity changes with time and concentration and possible chemical reactions could bind the ions. The diffusion coefficient calculated from fitting concentrations with depth is termed an “apparent” diffusion coefficient since it includes the effects of both diffusion and chloride binding.

2.3.3 - Electro-migration

Migration is simply the transport of charged particles within a substance subject to Brownian motion. The transport method is a potential energy difference, in this case, voltage. The corresponding voltage will drive the chloride ions into the concrete in solution, or once the steel starts to corrode it creates a potential (direct current) that wants to draw down more chlorides. Electro-migration is measured by concrete resistivity and can only be measured by this

property rather than with conduction band electrons as in metal electrical conduction (Claisse 2005).

2.3.4 - Thermal Migration

Thermal migration arises from the thermodynamic principle where water will move from regions of high temperature to cold temperature. Likewise, ions or molecules in the water will also be transported by the water. The rate of this transport is also a function of the permeability of the substance. Thermal migration in concrete occurs commonly with application of de-icing salts. The salt depresses the freezing point of the surface water and a temperature gradient develops with the sun shining on the surface. The salt saturated solution on the surface will migrate into the concrete, and even if the salts do not penetrate deep enough to encounter the steel, the salt solution is now in the pore structure of the concrete and can be transported by other mechanisms (Claisse 2005).

2.3.5 - Variables Affecting Transport

Adsorption is a key chemical concept by which ions adhere to the cement matrix and are no longer able to flow through the media. Since these ions are locked in the matrix they are no longer able to create as strong chemical, electrical or pressure gradients and thus no longer contribute to the deleterious effects. Adsorption in concrete normally proceeds from the interaction between the ions and the aluminate in the cement. The adhesion capacity for concrete media is thus dependent on the cement content, and believed to increase with the inclusion of fly ash (Claisse 2005).

Capillary action phenomena can be described as the wicking or drawing up of water (or liquid) into narrow tubes. The height of the rise or decrease in a capillary is a function of the net

forces it is opposing and dependent on viscosity. Water, for instance, has very strong attractions or adhesion forces to oxygen and hydroxyl groups that are very common in glass. The cohesion of water to itself is known to be very low because of its low viscosity. This is why the meniscus in water capillaries is concaved, but liquids with strong cohesion forces and week adhesion force, like mercury, have a convex shape (Atkins and Jones 2005). Capillary action can affect the shrinkage of concrete and is highly dependent on the moisture condition of the concrete – the smaller the capillary diameter the more energy required to overcome adhesion. Some hydrostatic surface tension forces can create corresponding compressive forces on the capillary solid skeleton. For materials like cement that are able to have particle reorientation (viscoelastic), some pores/capillaries can become smaller (Mindess, Young and Darwin 2003). The most obvious way capillary action affects concrete detrimentally is by drawing up or down water containing deleterious materials such as sulfates and chlorides. If the concrete is more dry, it adsorbs more solution if it is present – as seen in many bridge cases over water with high humidity.

Osmosis is the process by which a solvent flows through a semipermeable membrane to a solution. Being a thermodynamic property, osmosis is driven by the enthalpy and entropy changes that occur when a solute is present in solution - since a solute lowers the free energy of the solution. This is the vehicle by which solutions of weaker concentration flow into solutions of higher concentrations (Atkins and Jones 2005). This arises in concrete when the solution on the surface is much weaker than that of the pore solution, therefore an osmotic gradient is created and the surface solution ingresses into the concrete carrying sulfates and chlorides etc. (Claisse 2005). Osmotic gradients also exist in the concrete itself. When water begins to freeze in concrete, nucleation sites occur and increase the surrounding solute concentration not directly

involved with the nucleation. With the creation of strong solutions there is, in turn, an osmotic pressure created that can crack the surrounding cement paste. Similar effects happen from vapor pressure gradients between frozen water and supercooled water. Water is consequently drawn out of the C-S-H and it incurs stresses from shrinkage (Mindess, Young and Darwin 2003).

2.4 - Quality Control Methods

2.4.1 - AASHTO T259: Standard Method of Test for Resistance of Concrete to Chloride Ion Penetration

The AASHTO T259 (2007) herein referred to as "salt ponding test" or "ponding test" is a quality control measure used to develop a chloride ingress profile through the cross-section of a slab. Slabs must be a minimum of 75 mm thick and have a surface area of 300 mm^2 .The test requires a minimum of three replicate specimens. The specimens are moist cured for 14 days and then kept in a room with 50% relative humidity for 28 days. A 3% sodium chloride solution is then ponded on top of the specimen after the sides have been sealed to ensure there is only one-directional ingress. The bottom is still exposed to the environment as seen in the *Figure 2-1*.

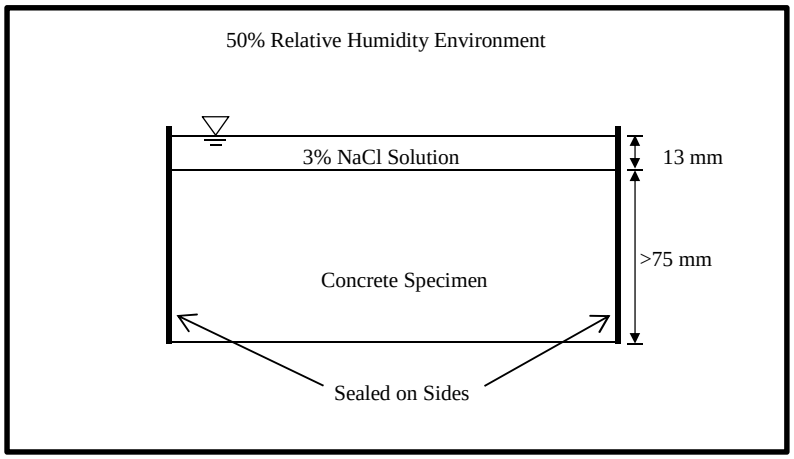

Figure 2-1 AASHTO T259 Ponding Test, after McGrath and Hooton **(1999)**

After the 90 day ponding time has elapsed, samples are then taken and evaluated at 0.5 in. cuts following AASHTO T260 (2009). Clearly for the 0.5 in. cuts obtained, the chloride ingress is quantified as the average per length of the cut. Thus the distribution profile of chloride ingress is undistinguishable for each cut and only the change between two cuts may be observed. The ponding test involves three mechanisms of penetration. The first being intrusion through adsorption. The second is the long term ingress of ions through diffusion. The third, known as wicking, comes from the change in vapor pressure from the top ponded section to the 50% relative humidity exposed bottom surface –which ideally simulates the underside of a bridge deck. There exists some ambiguity among researchers and engineers about the relative importance and the strongest ingress mechanism. McGrath and Hooton (1999) believe the absorption effects are inflated compared to the actual ingress in this test.

2.4.2 - Bulk Diffusion (ASTM C1156 & NordTest NT Build 443)

While the bulk diffusion procedures described in ASTM C1156 (2011) and NT Build 443 (1995) differ slightly, the measuring goal of the tests are the same. The minimum specimen requirement according to ASTM C1156 is that the finished surface must be a minimum of 75 mm (~3 in.) and the depth must also be a minimum of 75 mm (~3 in.). With the AASHTO ponding test having other variables than pure diffusion, the bulk diffusion tests try to rectify this by sealing all of the sides of the sample except the top finished surface. This is done to eliminate any gradients that would exist in the specimen and/or flow through the specimen. The specimen is then placed in a lime saturated solution until a stable mass is reached. With the specimen being fully saturated before it is placed in the sodium chloride solution the effects of initial sorption are

considered negligible. Profile grinding is then done according to AASHTO T260 (2009) and Fick's Second Law is applied to the data to fit a diffusion coefficient.

These tests do alleviate some of the concerns with the ASSHTO ponding test, but they still require 35 days of salt exposure in addition to the grinding and sampling times. Moreover, specified mixes with low w/c ratios and high performance mixes incorporating supplementary cementitious materials should have extended exposure time as recommended by ASTM C1156 and NTBuild 443.

2.4.3 - ASTM C642: Density, Absorption and Voids in Hardened Concrete

ASTM C642 (2006), commonly referred to as "the boil test" by most DOTs and herein as volume of permeable voids, is a test that produces the total volume of permeable voids in the sample. This is a key distinction from the two previous tests mentioned prior because they are measuring two different constitutive properties. The ponding test and bulk diffusion tests are measuring the physical amount of chlorides that have penetrated into the specimen. The boil test evaluates only the total volume of voids/pores and reveals nothing about the connectivity of the pores or the resistance to ion and water flow through the pores as illustrated in *Figure 2-2*.

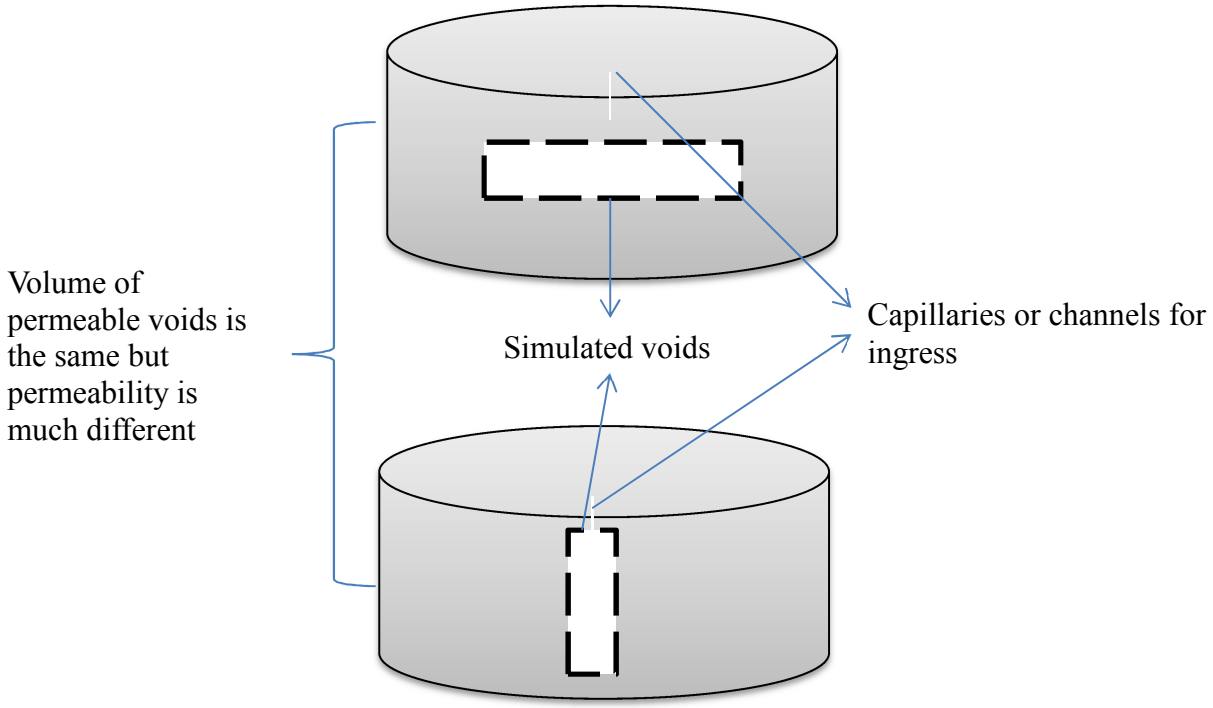

Figure 2-2 Volume of permeable voids does not correlate directly with ingress

The boil test is used to evaluate density, percent absorption and total volume of voids/pores. The term voids/pores will henceforth be referred to as pores due to the total volume of water that resides in both the gel pores, capillary pores and entrapped air voids in a saturated condition. The test evaluates the total volume of pores by measuring the oven dry mass, the saturated surface dry mass (SSD) after immersion, the saturated submersed mass, and the saturated surface dry mass after boiling the specimen in water. The determination of the volume of the pore space is given by *Eq. 2.4.3.*

$$\% \text{ Voids} = (g_2 - g_1)/g_2 * 100 = [(C-A)/(C-D)] * 100 \quad (2.4.3)$$

Where: A = mass of oven dried sample in air (lbs.)

B = mass of surface dry sample in air after immersion (lbs.)

C = mass of surface dry sample in air after immersion and boiling (lbs.)

D = apparent mass of sample in water after immersion and boiling (lbs.)

g_1 = dry bulk density (lbs./in.^{3})

g_2 = apparent density (lbs./in.^{3})

The placement of the specimen into boiling water for a minimum of five hours is intended to excite any air that is entrapped in the small microstructure and force water to penetrate into that space. This is implicitly stated in the comparison of the difference between the dry bulk density and the apparent density normalized over the apparent density.

The boil test is often favored because of the very simple procedure that does not require special equipment or knowledge. The total test can be run in a work week and is repeatable. It also is able to measure gel pores, capillary pores and air entrained pores. The test however is insufficient in providing information regarding pore connectivity and ingress rates (Castro, Spragg and Weiss 2010). Many DOTs may use this as the only quality control measure needed to be checked if they are using a prequalified mix that has been used very often and trends between the boil test and other permeability measures that show rate of ingress or pore connectivity have been established.

2.4.4 - ASTM C1202: Electrical Indication of Concrete's Ability to Resist Chloride Ion Penetration (Rapid Chloride Permeability Test, AASHTO T277)

The rapid chloride test is also an indirect measure of permeability wherein it assesses the permeability of the concrete by calculating the total charge passed during a six hour period when 60 V is applied to a two inch thick concrete specimen. The potential difference supplied by a voltage differential is applied at both ends of the specimen with solutions of sodium hydroxide and sodium chloride being placed on either end. The rapid chloride permeability test (RCPT) is referred to as a "rapid" even though it takes around six hours to run, but in comparison to long term diffusion/ponding tests it is much more rapid. The test set up is depicted in *Figure 2-3.*

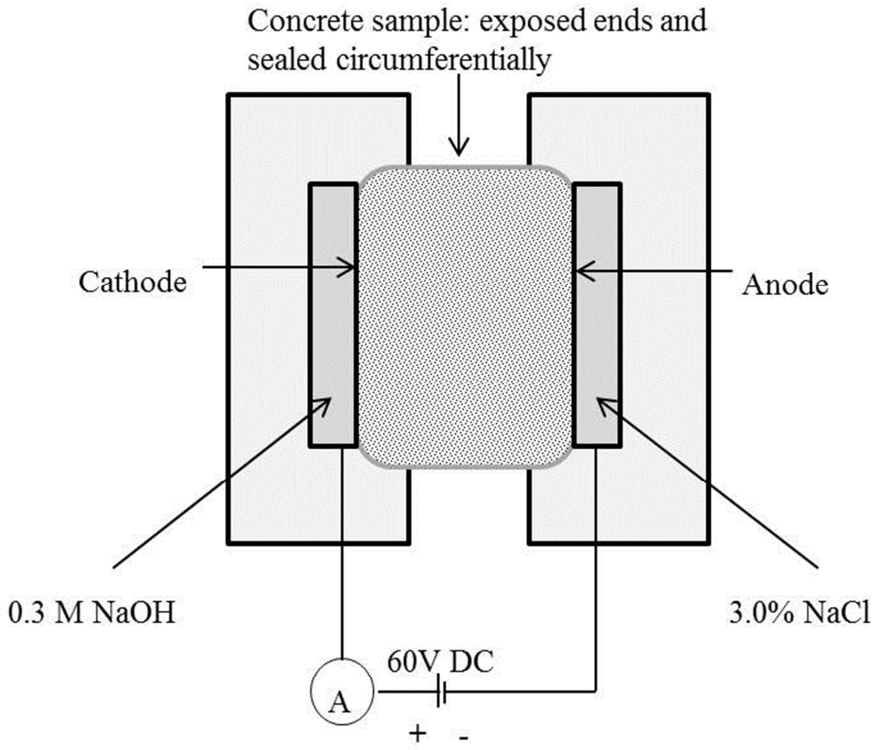

Figure 2-3 Rapid Chloride Test setup after ASTM C1202

The amount of charge passed has been shown to correlate with higher permeability. Concrete is usually less resistive to charge flow through its saturated pore structure because of a high number of interconnected pores that also are responsible for high permeability.

Major critiques with this test arise from three main areas: (1) The total charge passed is related to all of the ions and electrolytes in solution and not just the chlorides. Therefore the measurements will vary based on state of the solution that is saturating the sample. (2) Charge is measured initially before steady state migration is allowed to occur. (3) The high direct current voltage causes an increase in temperature, which for low quality concretes increases the charge flow rate (Stanish, Hooton and Thomas 2001). These criticisms are reflected in ASTM C1202 (2012) statement on precision which states that single operator coefficient of variation for a single operator is 12.3% and two tests performed by the same operator should not differ more than 35%. In practice, usually three specimens are tested and the average of the specimens should not differ by more than 29% between laboratories. This becomes problematic when categorizing acceptance criterion, when 29% of the typical 3500 coulombs is ~1000 coulombs between two different testing facilities.

1.4.5 – AASHTO TP95-ll: Standard Method of Test for Surface Resistivity Indication of Concrete's Ability to Resist Chloride Ion Penetration (Surface Resistivity)

Surface resistivity tests have been gaining acceptance as relative measures of concrete quality and performance. A provisional AASHTO standard has been developed for surface resistivity. The Florida DOT has been using surface resistivity since 2004 in its test specification FM 5-578 (2004). As previously demonstrated, concrete permeability is functionally related to its conductivity/resistivity. Using a direct current to pass charge can create a polarization effect near the ends. This is rectified by passing an alternating current through the sample. A Wenner

probe four-electrode resistivity meter is generally used (Stanish, Hooton and Thomas 2001). The outer most pair of electrodes create an alternating current while the inner probes measure the potential difference created between them (Hamilton III and Boyd 2007). The electric field and Gauss's law is demonstrated in *Figure 2-4.*

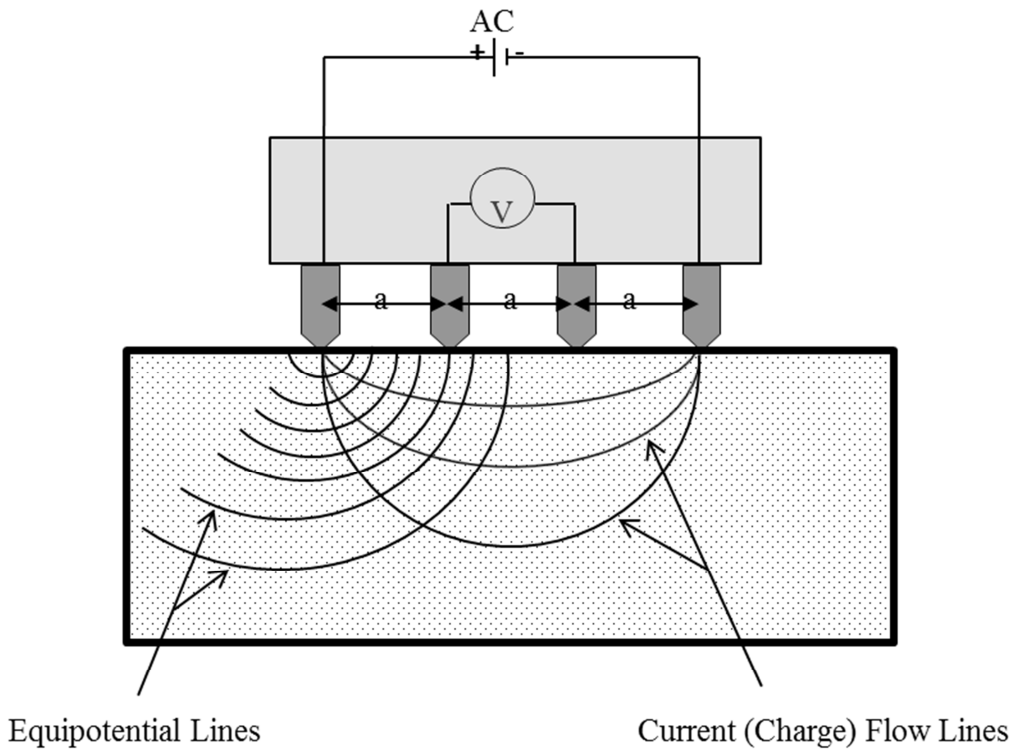

Figure 2-4 Wenner Probe Array after Hamilton III and Boyd (2007)

Results obtained from the Wenner probe are also subject to variance due to the saturation condition in the sample and the conductivity of the solution. Field in-situ tests intensify the importance of the saturation condition in the sample. Drying techniques and then application of known pore solution has been tried, but some drying techniques can induce more micro-cracks than are actually representative of the concrete microstructure. Additionally, the steel reinforcement of the concrete can "short circuit" the result. Some have suggested taking

measurements perpendicular to reinforcement, but for most bridge applications with temperature and shrinkage steel this is not feasible (Hamilton III and Boyd 2007). Thomas and Stanish (2001) have recommended the Wenner probe only be used in the laboratory on laboratory-cast cylinders or core samples containing no structural steel or fibers.

FM 5-578 (2004) testing method by the Florida DOT requires standard 4 x 8 in. cylinders that are cured in a moist room and not in a lime water tank. This is because the lime on the surface will affect the electrical conductivity measurements. The probe is then used to take readings twice on marked quadrants of the cylinder and the results averaged. Typically, three specimens are all tested and the resistivity values averaged at the end. Chini, Muszynski and Hicks (2003) evaluated the relationship between the rapid chloride test (ASTM C1202) and the surface resistivity test. Over 500 samples were tested in Florida and coefficients of determinations (R^2) were determined to be correlated as 0.95 at 28 days and 0.93 at 91 days. Given the precision and bias stated earlier in section *2.4.4* of 29% between laboratories, these tests could be considered to be very well correlated.

2.5 - Curing Environment Effects on Concrete Strength and Hydration

2.5.1 - Maturity of Concrete

Concrete strength means many different things to people in the industry. The strength of interest can vary from when forms may be removed or when the next lift of slip-forming can be done, to when initial set arrives and allows final finishing to take place. Most structural engineers are most concerned with the compressive strength (f'c) measured at 28 days to ensure adequate strength for their design assumptions and compliance with the building code. Project managers

are always ensuring that the schedule can proceed on the project, whether it is a building or opening roads and bridges to traffic. The early-age period of concrete is minuscule compared to its service life, but the initial material interaction influences the behavior of the concrete for the rest of its design life (Monteiro 2006).

The chemical reaction that takes place between cement and water is an exothermic reaction (Mindess, Young and Darwin 2003). The degree of cement hydration depends both on time and temperature. Since hydration is a function of more than one variable equivalent mixtures cured at differing temperatures will have different compressive strengths. Maturity methods have been developed where strength is no longer defined in terms of time, but as a function of temperature and time known as maturity. Normal OPC concrete placed in higher temperatures exhibits higher (accelerated) early strength than concrete placed at colder temperatures. Therefore concrete placed at higher temperatures is more mature at early ages. At later stages, the reverse happens - normal OPC concrete placed at lower temperatures exhibits higher strength, this is known as the crossover effects. *Figure 2-5* illustrates this phenomenon.

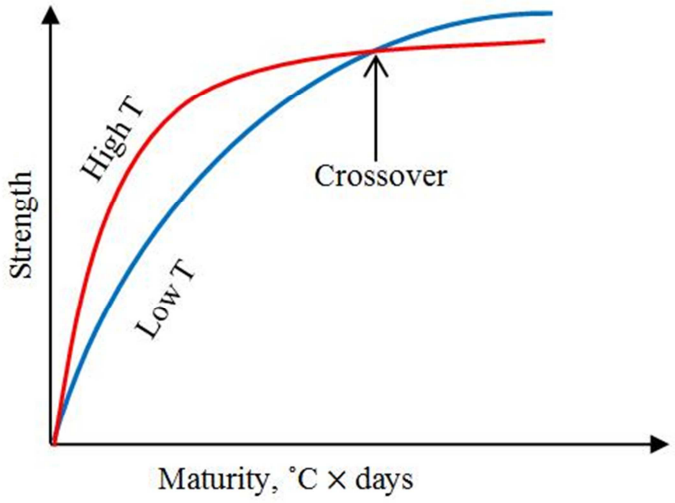

Figure 2-5 Curing temperature crossover effect

When reactions proceed at higher temperatures water can become trapped away from un-hydrated cement grains, keeping them from reacting. This is one factor that allows the concrete cured at the lower temperature to eventually catch up and "crossover" the higher temperature's strength at later ages. The most commonly used maturity method is the Nurse-Saul method, also known as the Time-Temperature method (ASTM C1074 2011). In this method, the maturity is the integral of a time vs. temperature plot. It is assumed that identically proportioned mixtures made from the same constituent materials will attain the same strength when their maturities are equal. This is seen in *Eq. 2.5.1a.*

$$M(t) = \Sigma(T_a - T_0)\Delta t, \qquad \lim_{t \to 0} M(t) = \int_0^t (T_a - T_0)dt \qquad (2.5.1a)$$

Where: M = maturity (˚C x days)

T_a = the average temperature during interval (˚C)

T_0 = is the datum temperature (˚C)

Δt = is the time interval and limits of integration (days)

ASTM C1074: Standard Practice for Estimating Concrete strength by the Maturity Method, recommends datum temperatures of 0 ˚C even though traditionally -10 ˚C is the temperature under which strength gain ceases. There are well documented correlations between maturity and compressive strength using the Nurse-Saul method.

Another model was developed by an Arrhenius relationship rather than a linear time temperature relationship as done in the Nurse-Saul method. This method was named the equivalent age method and is shown in *Eq. 2.5.2* (ASTM C1074 2011).

$$\text{Equivalent Age} = \sum e^{\frac{-E}{R}\left(\frac{1}{273+T_a} - \frac{1}{273+T_s}\right)}\Delta t \qquad (2.5.2)$$

Where: Δt = a time interval in hours

T_a = average concrete temperature (K)

T_s = specified Temperature (20˚C +273) (K)

E = activation energy (J/mol)

R = universal gas constant (J/(mol K))

Many concerns have arisen that show modeling early-age maturity in this manner does not take into account relative humidity and temperature/hydration heat at very early age. Introducing more variables subsequently makes the above relation disproportional with time and strength evolution (Monteiro 2006). Graphing either *Eq. 2.5.1a* or *2.5.2* and compressive strength will create a graph where fairly accurate predictions of the percent of ultimate compressive strength can be determined. The compressive strengths are determined by entering the graph at the corresponding x axis maturity and reading the resulting strength value or percentage, as seen in *Figure 2-6*.

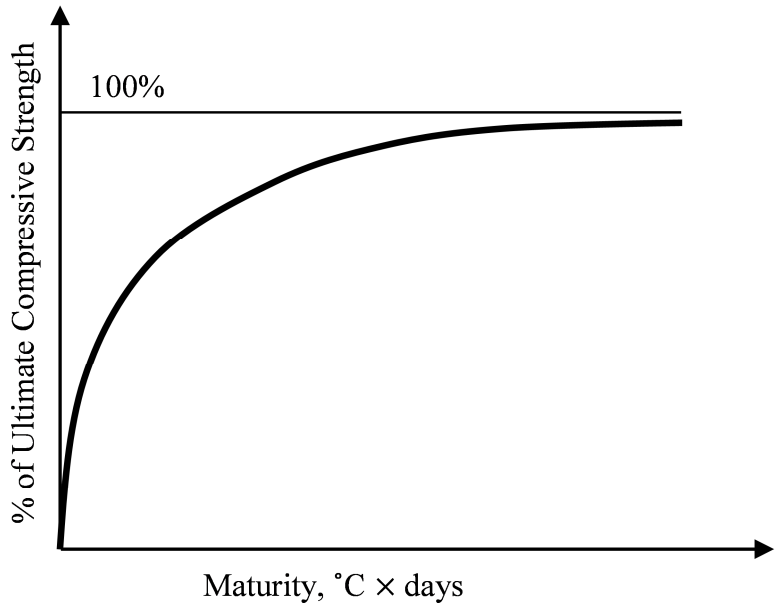

Figure 2-6 Maturity vs. Percent of Ultimate Compressive Strength Reached

Mindess et al. (2003) makes use of the Plowman equation to model the relationship between strength and maturity in *Eq. 2.5.3.*

$$S_m = a + b \log m \qquad (2.5.3)$$

Where: S_m = the compressive strength at maturity m (psi)

a and b = scaling effects that can be derived from mix and from laboratory tests (psi)

2.5.2 - Measures of Strength

The 28 day compressive strength (f'c) is normally the major criteria for concrete acceptance. If statistical data is available from the mix and therefore high confidence in its performance, ACI 318: *Building Code Requirements for Structural Concrete* (2008) allows reduction equations to be used on f'cr. These equations still meet the design f'c; the target strength of f'cr is able to be reduced. f'cr is the mean value of the statistical strength distribution

that allows the design f’c to be at 95% exceedance . ACI 318-5.5 lists requirements as data becomes available from construction that reduces the amount that f’cr must be greater than f’c. Hereafter f’c notation will be used as the required strength. ACI 318 also specifies the curing environment, regimen and how different cured specimens relate to one another.

Standard cured and field cured specimens both follow ASTM C31 (2012). The standard cured specimens are to be stored in an area between 60 and 80 ˚F for a period up to 48 hours after placement- known as initial curing. After initial curing has taken place and within 30 minutes of being de-molded, the lab cured specimens are either placed in a moist room or in a lime water bath. The mix has met its strength requirement if all combinations of three consecutive averages of cylinder breaks are greater than the f’c and no individual cylinder breaks more than 500-psi below the f’c for concretes designed for 5000-psi or below. For concrete greater than 5000-psi, no individual cylinder may fall below by more than 0.10*f’c (ACI 318 2008).

Field cured cylinders, according to ASTM C31 (2012), must be molded at the same time and from the same sample of concrete retrieved. After the specimens are molded they must be moved to the desired location on site that will mimic the curing environment of the structure and sealed after they arrive. Once the required initial curing period has been reached, specimens are de-molded and left in the field exposure area. Field cured cylinders are tested at the same time interval as the lab specimens and they must be at least 85% of a lab companion cylinder. The 85% limitation does not apply if the field cylinder strength exceeds the f’c by 500-psi or more. Field cured cylinders are typically not used for acceptance criterion unless specified by the governing code body (ACI 318 2008).

When low strength results are obtained from either the lab cylinders failing to reach strength criterion or field exhibiting deficiencies or poor curing, actions must be taken to verify structural integrity. Although field cylinders only simulate the in-situ concrete properties because of differences in heat transfer and moisture retention, if the field strengths are low, further investigation of the structure must be done to ensure the material will perform properly. To verify the performance of the in-situ concrete when poor lab results have occurred or field specimens show deficiencies, cores samples shall be obtained according to ASTM C42 (2006) and three core specimens shall be taken per each material property to be evaluated. ACI 318-R5.6.5.4 stipulates the average of three core specimens must be a minimum 0.85*f'c and no individual test can be below 0.75*f'c. It is also of great importance to follow ASCTM C42 when using a wet coring process. If the samples are not properly moisture conditioned, large variances and non-representative values are obtained. Ultimately, the adequacy of the structure remains on the responsible code authority and designer. Other non-destructive tests and strengthening methods can be employed (ACI 318 2008).

2.5.3 - Moisture and Relative Humidity Effects on Portland Cement Hydration

Modern hydraulic cement gains strength through hydration and the mechanical properties of the mix are dependent on it. Hydration, although being studied for many years, is still not completely understood because of complexities of the reactions. In most studies, the reaction mechanism of individual compounds is done separately. Assuming no interaction occurs between compounds allows good insight, but is not entirely true. The flaws in this assumption are made evident by all of the hydration products consuming CaO and some competition for the Ca^{2+} cation. C_3A and C_4AF also compete for sulfur ions which in turn fluctuates the reaction rate and the degree of reactivity. Perhaps the best example of the combined constituent reactions is found

in the formation of C-S-H incorporating varying levels of sulfate, alumina and iron. With these compounds being bound up in hydration, there are less calcium sulfoaluminates (ettringite) in the hydration of normal cement compared to pure compounds (Li 2011). With the complexity of the hydration mechanisms and kinetics, understanding the role of moisture and humidity which drive the reaction is of great importance.

The reaction between cement and water is a combined physical and chemical process. As the process continues, the interparticle bonding strengthens and the porosity decreases. For a unit mass of cement, a mass fraction of 0.21 to 0.28 of chemically bound (or hydrate) water is needed for hydration. In addition to the hydrate water, water is also adsorbed to surfaces and interlayer spaces (or gel spaces). This water is physically bond in the gel structure and referred to as bound water or gel water. Most concretes in service have gel water present because of the adhesion forces that require high excitation energies of around 105˚C to overcome (ACI 308 2008). Cement paste structure and morphology can be characterized as poorly crystallized clay, wherein (like clay) it retains water in its interlayer region (Mindess, Young and Darwin 2003). The gel water forming on the hydration surfaces has been found to be equal to the amount of chemically bound water. Continued hydration is only possible when enough water is available for reacting chemically and for filling the interlayer pores. Therefore the total water consumed by the hydration reaction is the sum of the chemical and gel pore water. Thus the water requirement for hydration is around 0.42 mass fraction of cement (ACI 308 2008).

Even with the concrete containing the required mass fraction of water, cement hydration will not proceed unless the relative humidity is above 80%. The cement will cease hydration if C_3S, C-S-H and CH are all in equilibrium. The only condition that would allow this is if no excess water was available in the system; but as the relative humidity is reduced, the

corresponding decrease in water activity does allow an equilibrium condition to exist when excess water is available. When the relative humidity is at 80%, the capillary pressure resulting at that humidity alters the solubility of C_3S enabling it to be in equilibrium with water. This is resolved thermodynamically by Le Chatelier's principle and the chemical shrinkage of the system. Le Chatelier's shows there exists a difference in the volume of products compared to the volume of reactants. Since the volume of products is less than the reactants, a negative pressure must be acting upon the reaction. The negative pressure resisting the reaction is the capillary pressure which is derived from the change in relative humidity (Flatt, Scherer and Bullard 2011). When dealing with relative humidity it is important to recognize that relative humidity is not the percent of moisture in the air, rather it is the ratio of partial vapor pressures to that of a saturated state (e.g. relative humidity can be measured in a vacuum). Clearly, if the rate of hydration is dependent on the relative humidity, then concrete cured at higher relative humidity will hydrate at a much faster rate. Since degree of hydration directly correlates with strength, concretes cured at a higher relative humidity will have higher strength and therefore lower permeability.

2.5.4 - Temperature Effects on Supplementary Cementitious Materials

Bamforth (1980) looked at the effects of SCMs on concrete long term strength under different curing conditions by measuring the concrete mechanical properties of three different mixtures: (1) portland cement only, (2) blended portland cement and fly ash, (3) blended portland cement and slag. One of the first notable contributions from this work is the behavior of thermals stresses and the increase of the concrete modulus. Blended cement concretes do produce higher modulus concrete; however, low modulus and high strength at early ages in order to encourage creep is usually desired. If the concrete can be viscoelastic and allows stresses to be relieved by creep, instead of cracking, it will have longer service life – less chloride ingress

and section loss. With concrete placements less than two meters in thickness, the benefit of temperature reduction is more desirable than the ill effects of the increased stiffness. When the lifts of concrete are to exceed 2.5 meters, the benefit of the lower temperature no longer outweighs the ill effects of a stiffened modulus; however, fly ash used in these placements provides other benefits.

When concretes undergo cyclical temperatures experienced during hydration (modeled as emanating from its centroid), accelerated hydration occurs with the increased heat of hydration. This fact cannot be witnessed under standard curing methods, but is significantly different when compared with matched temperature curing cycles. Ordinary portland cement concrete (OPC) strength decreases 30% and fly ash increases 20% from standard cured. While using fly ash does not decrease the thermal cracking of mass concrete, its increase in mechanical properties is desirable compared to OPC (Bamforth 1980). The difference and importance between standard curing and matched temperature curing is further illustrated in *Figure 2-7.*

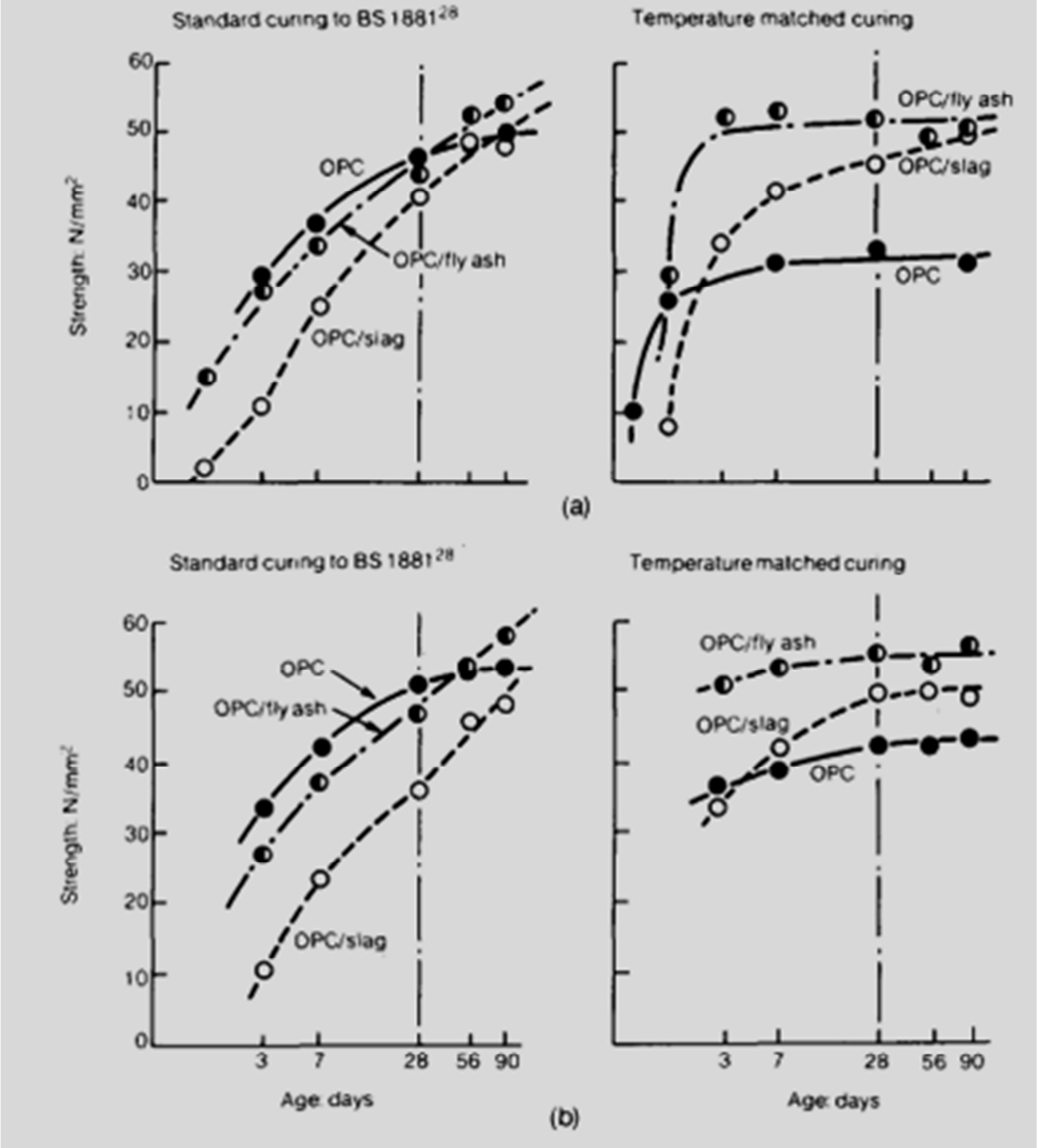

Figure 2-7 Compressive Strength of Standard and Matched Temperature Curing of Concrete: (a) cubes cast in-situ, (b) cubes cast in laboratory.

Reprinted from Bamforth (1980) with permission

Haque, Day and Langan (1988) reported in a study of fly ash replacement at levels of 20, 35 and 50 percent and under different curing environments of 50 and 100 percent relative humidity and a field cured regimen confirming that field cured specimens were not

representative of in situ concrete. They also determined for high cementitious material concretes incorporating fly ash had no more detrimental effects when exposed to the elements than plain cement only mixes. Curing specimens at lab temperatures and 50% relative humidity also does not represent in-situ moisture conditions or strength gain. Since field cylinders often dry out and are kept in a relative humidity environments lower than 80 percent, and lab cylinders being kept at 50% RH do not allow cement hydration to proceed as it would in-situ and unimpeded as in moist cured specimen, they are poor indicators of the concrete properties.

2.6 - Conclusions Drawn From Literature

Given the complexities of the ingress mechanisms and the interactions between them, it is very important the performance evaluations are able to reflect the complexities of the phenomena. Normal OPC is complex enough on its own to model with differing temperatures and moisture conditions. This is further exacerbated when SCMs are used. Now conditions based on reaction rates and pozzolanic reactions have to be considered. Many good methods have been developed in the past for OPC; it will be of much importance to confirm the accuracy of these tests when SCMs are used. Additionally, economic, efficient and accurate tests are needed - as much of the U.S. infrastructure is beyond its design life and must be maintained, rebuilt or repaired.

Chapter 3 - Materials

3.1 - Cementitious Materials

All of the mixture proportions and materials were kept constant (not considering the use of add mixtures used to meet air and slump specifications) except for the cementitious materials. Class F fly ash and Class C fly ash are categorized according to ASTM C618. Mix 1 used only portland cement, Mix 2 replaced 25% by mass of the cementitious material with Class F fly ash, and Mix 3 replaced 25% by mass of the cementitious material with Class C fly ash. The cementitious material composition and properties are shown in *Tables 3-1 – 3-3* for the cementitious materials used in the concrete placed in different seasons.

Table 3-1 Cement Composition and Properties by Placement Season, Sugar Creek, MO Plant

Item	Spec Limit	Test Result		
		Season 1	Season 2	Season 3
Oxide Analysis				
SiO_2 (%)	xxx	19.8	19.7	19.8
Al_2O_3 (%)	6.0 max	4.9	4.9	4.9
Fe_2O_3 (%)	6.0 max	3.1	3.1	3.1
CaO (%)	xxx	63.4	63.5	63.5
MgO (%)	6.0 max	1.4	1.5	1.5
SO_3 (%)	3.0 max*	3	3	2.8
Loss on Ignition (%)	3.0 max	2.5	2.6	2.7
Insoluble residue (%)	0.75 max	0.43	0.37	0.22
Limestone (%)	5.0 max	4.4	4.5	4.5
Adjusted Potential Phase Composition (ASTM C150)				
C_3S (%)	xxx	54	55	55
C_2S (%)	xxx	16	15	15
C_3A (%)	8 max	8	8	8
C_4AF (%)	xxx	9	10	10
$C_3S + 4.75*C_3A$ (%)	100 max	90	91	91
Blaine Fineness (m^2/kg) (ASTM C204)	280-430	373	372	362

* May exceed 3.0% SO_3 maximum based on C-1038 results of < 0.02% expansion at 14 days

Table 3-2 Class F Fly Ash Mill Sheets per Placement Season, Chanute, KS Plant

Item (ASTM C618)	Spec. Limit	Test Result		
		Season 1	Season 2 **	Season 3
SiO_2 (%)	xxx	52.44	52.44	52.17
$A_{l2}O_3$ (%)	xxx	18.8	18.8	17.45
Fe_2O_3 (%)	xxx	6.65	6.65	6.42
Σ SiO_2, Al_2O_3, Fe_2O_3 (%)	70.0 min.	77.89	77.89	76.04
CaO (%)	xxx	14.15	14.15	14.21
MgO (%)	xxx	3.14	3.14	2.66
SO_3 (%)	5.0 max	2.00	2.00	1.95
Na_2O (%)	xxx	0.83	0.83	0.85
K_2O (%)	xxx	0.82	0.82	1.04
Total Alkalies as Na_2O %	xxx	1.37	1.37	1.54
Loss on Ignition (%)	6.0 max	0.58	0.58	0.73
Specific Gravity	xxx	2.49	2.49	2.49

* Meeting 7 or 28 day strength activity index indicates specification compliance

** Same supply of fly ash used by batching company

Table 3-3 Class C Fly Ash Mill Sheets per Placement Season, Jeffery Energy Center, St. Marys, KS Plant

Item (ASTM C618)	Spec. Limit	Test Result		
		Season 1	Season 2	Season 3
SiO_2 (%)	xxx	29.16	29.72	29.27
Al_2O_3 (%)	xxx	19.26	19	18.14
Fe_2O_3 (%)	xxx	6.29	6.15	6.86
Σ SiO_2, Al_2O_3, Fe_2O_3 (%)	50.0 min.	54.71	54.87	54.27
CaO (%)	xxx	29.89	30.32	30.32
MgO (%)	xxx	7.29	7.38	7.96
SO_3 (%)	5.0 max	2.62	2.59	2.51
Loss on Ignition (%)	6.0 max	0.25	0.23	0.23
Specifiac Gravity	xxx	2.79	2.79	2.78

3.2 - Aggregate Selection

Three aggregates were blended in the mixtures used in this study. The three aggregates chosen where: (1) normal Kansas River sand (KPSAND), (2) coarser sand meeting ASTM C33 size 89 requirements (KPSA1), and (3) pea gravel (KPCA4). Optimized aggregate gradations were designed by KDOT and the concrete supplier using the Shilstone Method and “haystack” gradations. All of the mixtures used the same percentages of each aggregate, 50% KPSAND, 15% KPSA1 and 35% KPCA4. Because of the difference in the specific gravity between the cement and SCMs used, all aggregate content was adjusted in batches containing SCMs to maintain design percentages and was not anticipated to be a significant factor. The percent passing of each aggregate type and a combined gradation plot is shown in *Figure 3-1*.

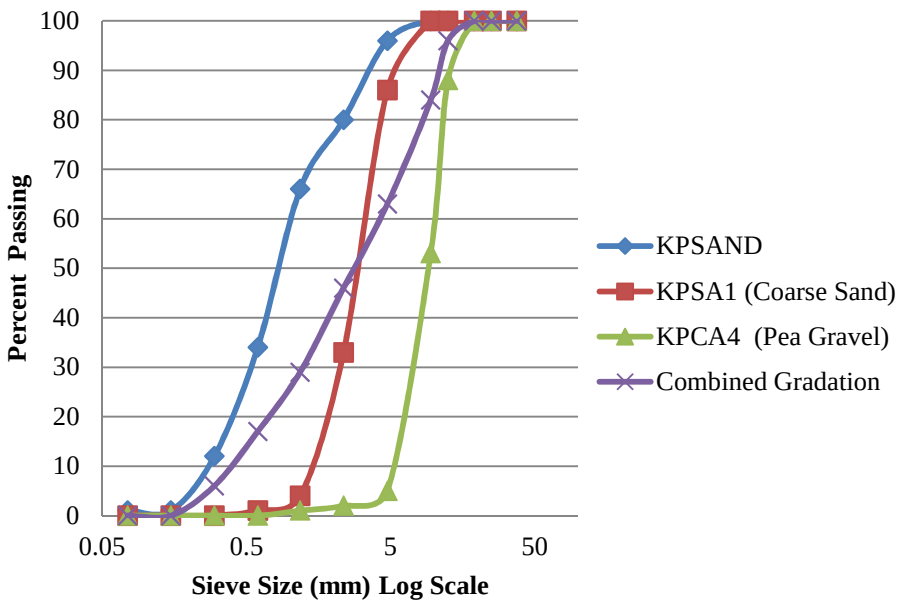

Figure 3-1 Aggregate Gradation Plot

3.3 - Complete Concrete Mix Designs

Table 3-4 shows the complete mix designs as given by the concrete producer. KSU Mix 1, is the control mix with no SCM's used for cementitious materials; KSU Mix 2, utilizes 25% of its cementitious material as class F fly ash; KSU Mix 3, utilizes 25% of its cementitious material as class C fly ash.

Table 3-4 Concrete Mix Designs

	Mix Design		
	KSU Mix 1	**KSU Mix 2**	**KSU Mix 3**
	OPC	**F-ash**	**C-ash**
w/c	0.42	0.42	0.42
Lafarge Cement (lbs/yd^3)	564	423	423
Class F fly ash (lbs/yd^3)	0	141	0
Class C fly ash (lbs/yd^3)	0		141
Water (lbs/yd^3)	237	237	237
Air Entrainer (oz/cw)	0.53	0.53	0.53
Mid-Range Water Reducer (oz/cw)	6	6	6
Fine Agg. 1 KPSAND (Sand) (lbs/yd^3)	1522	1510	1513
Fine Agg. 2 KPSA1 (Coarse Sand) (lbs/yd^3)	457	453	454
Coarse Agg. KPCA4 (Pea Gravel) (lbs/yd^3)	1045	1037	1039
Design Air Content (%)	6.5	6.5	6.5

Chapter 4 - Methods

4.1 - Introduction

Much interest in quantifying and qualifying concrete performance has arisen, particularly in the interest of casting season effects and correlations between in-situ performance and that of field and lab cured specimens. These relations become further complicated by the use of supplementary cementitious materials.

Concrete slabs placed have dimensions of 10 ft. x 8 ft. by 10 in. An extra row of 9 cylinders was added for redundancy should cores be damaged in extraction or testing errors occur. Concrete was delivered in 4 yd^3 quantities by Midwest Concrete Materials. The slab as specified plus the 108 cylinders required for lab and field cured testing left more than 10% of the concrete leftover for waste and quality control field testing. Strength and boil tests for the summer, fall, and spring slabs were conducted by KSU. Rapid chloride permeability testing (RCPT) of companion samples was performed by the KDOT materials laboratory. Thermocouple temperature sensors were embedded in each slab cast and in two field cured cylinders for each mixture.

4.2 - Site Preparation

Coordination between The University of Kansas and Kansas State University helped to ensure similar practices and site conditions. Kansas State University placed the concrete slabs used in this project at the Civil Infrastructure Systems Laboratory (CISL). The field cylinders were placed outside adjacent to the slabs. The laboratory cured cylinders were kept inside an air conditioned room at CISL in a lime-saturated water bath kept at 73° ±3°F.

Cut and fill was done on a 1600ft.^{2} site west of the main CISL building using a skid loader. The soil was compacted using a roller compactor. A 4 in. thick layer of AB-3 base material was placed and compacted with a skid loader, roller compactor and a plate vibrator. Forms were than erected having finished slab dimensions of 10 ft. x 8 ft. by 10 in. deep. *Figure 4-1a* and *Figure 4-1b* show the finished site layout and the typical form layout used for each placement respectively. A subgrade pad was also made with AB-3 base materials to mimic the curing environment of the concrete slabs for the field cylinders after they had been de-molded.

(a)

(b)

Figure 4-1 (a) Finished Site Layout, (b) Typical Forming Layout

4.3 - Placement of Slabs

Each slab was placed according to KDOT Standard Specification 501: Portland Cement Concrete Pavement (QC/QA) (2007). The subgrade, formwork, and transit mixer chute were moistened prior to discharge of concrete from the truck. Initial samples of air content and slump were taken. If the slump was initially above 4 in., concrete would continue to be worked in the truck and slump would be taken approximately on ten minute intervals until it was reduced to 4 in. or less. Once testing showed that the concrete met placement specifications, placement of the slabs began immediately.

Following the placement of the first half of the slab, the chute was completely diverted into a moistened skid-loader bucket (8 $ft.^3$ volume). The sample was then transported to where the test cylinders were to be made, after which the sample was remixed. Standard fresh concrete

quality control tests were then performed. Insertion (spud) vibrators were used to consolidate the slabs and used at intervals of 1.5 the vibrators radius of influence. Care was taken during vibration to not cause segregation. The Slabs were then screeded utilizing a sawing motion and then surface finished with a bull float. WR Meadows Seal Tight 1610 curing compound was then applied to the slabs. Light rain occurred just after finishing season 1, slab 2. The rain was not intense enough to cause surface impressions in the slab and plastic was placed over the slab within minutes of the precipitation starting to prevent any damage to the concrete surface or any dimpling to the surface. The plastic sheeting was removed within the hour of the precipitation ceasing, which was about an hour after the rain began. For the winter placements, standard KDOT required cold weather precautions were taken during winter placements by placing cure over the concrete surface and then adding plastic, burlap, blankets and sheets of plywood on top to keep insulating materials from blowing away in the wind and also to add another layer of insulation.

4.4 - Casting of Test Cylinders

Once the sample of concrete was retrieved from the concrete truck, it was transported to where the test cylinders were made on the level shop of CISL. All test cylinders were made using 4 in. by 8 in. molds and followed ASTM C31. A total of 120 cylinders were made for each slab, with each cylinder numbered 1-60 (lab) or 1-60 (field). The cylinders were consolidated using internal vibration following ASTM C31. The cylinders were placed in two approximately equal volume layers and the vibrator was inserted once per layer. After each layer had been vibrated, the vibrator was removed slowly as to not cause a void during its retraction. The cylinder walls were tapped between 10 and 15 times to release entrapped air voids in the concrete and along the mold-concrete interface. The cylinders were finished using a flat bar or a magnesium/wood float

(ASTM C31 2012). Cylinders were made in an alternating fashion between field and lab to ensure an even distribution of each portion of the test sample in the field and lab cured conditions. Field cured cylinders were placed on a 4 in. AB-3 layout pad and Lab cured cylinders were placed in an air conditioned lab at room temperature in CISL immediately after creation. Field cured cylinders were de-molded the next day and placed back on the 4 in. AB-3 layout pad. Lab cured cylinders were also de-molded the next day and placed in a lime-saturated tank with a heating element, thermostat, and water circulator to ensure the cylinders were maintained at the proper temperature.

4.5 - Core Sampling of Slabs

ASTM C42 (2010) was followed in taking core samples from the slabs with the exception of ASTM C42 7.3.3, which states that the cores are to be placed in non-absorbent containers after they were last in contact with water (e.g. cutting cylinders to length with a wet saw) for a minimum of five days. For the intent of this research, cores were to remain in place until one week of the specified testing date in order to minimize the effects of the cores experiencing differing temperature and moisture conditions than the in-situ concrete. This did not always allow adequate time for five days of conditioning; however, cores were always wiped clean and allowed to surface dry and then placed in non-absorbent containers.

Cores were sampled on 1 ft. centers, which translate to 8 in. clear spacing for cores not directly adjacent to the edge of the slab and clear spacing of 10 in. for cores directly adjacent to the edge of the slabs. Coring takes a lot of cutting force, and this force only increases as the concrete gains strength. It is important to keep the coring rig deck flush to the surface of the concrete. If the coring rig is not kept flush with the surface, it will begin to rise up as more force is placed downward on the cutting head. If the deck deviates too far from flush with the concrete

surface, skin friction develops between the concrete and the coring bit. The core sample then becomes much less uniform and shows “wobble.” Female concrete anchors were embedded in the surface of the slab to clamp the coring rig to the concrete surface using bolts and a guide beam. The cores were removed afterward by using a piece of tie wire, looping around the hoop direction, and pulling vertically upward. This process and result is shown in *Figure 4-2*.

(a)

(b)

(c)

Figure 4-2 (a) Typical Wet Coring, (b) Coring Rig Fastened with Guide Beam, (c) Amount of "Wobble" Compared to Straight Edge

Cores were taken transverse to how the slab was poured with coring done in such a manner not to have the same material tests being performed on consecutive rows of concrete placed. This reduced bias in the core properties measured that could stem from variability from the first portion of the concrete discharged from the truck and the last portion. The slab was poured by discharging the concrete in two passes for approximately every 1.5 ft. of the slab dimension. As long as coring was done transverse to the chute discharge direction, there should be approximately 3.5 ft^3 in between successive cores. The concrete placement sequence and coring direction were perpendicular, as shown in *Figure 4-3*.

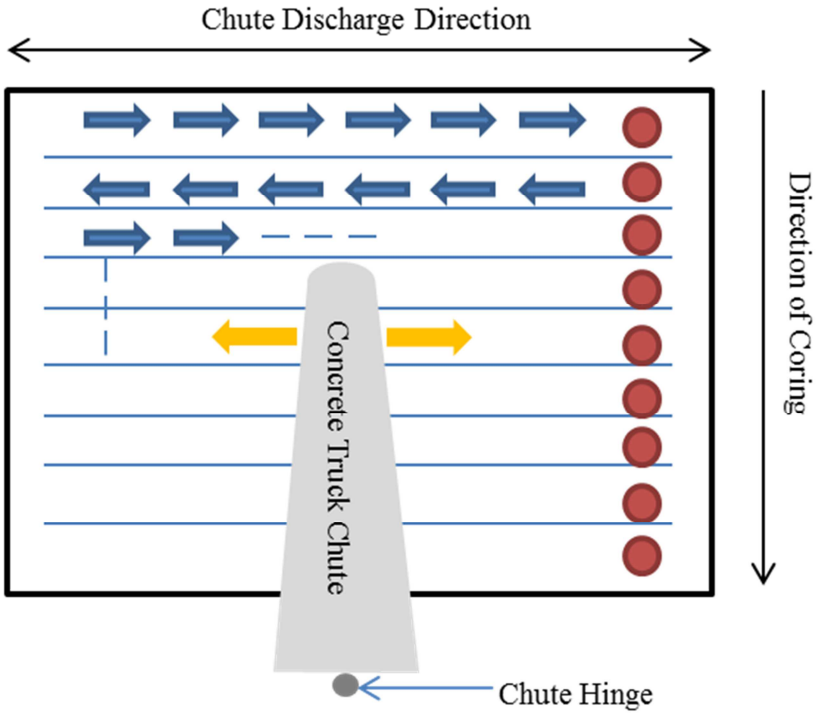

Figure 4-3 Placement Sequence Diagram

4.6 - Material Testing and Evaluation Methods

4.6.1 - Compressive Strength Testing

Compressive strength tests were performed by Kansas State University and followed ASTM C39 (2012). For the core specimens the top 3/8 in. of the core was saw cut with a wet lubricated saw and the other end was then cut off to have the sides perpendicular to the ends. KDOT's length to diameter corrections were used and are seen in *Eq. 4.6.1a,b.*

$$\text{If } \frac{L}{D} > 2; \quad P = \frac{P_u * 100}{110 - 5\left(\frac{L}{D}\right)} \tag{4.6.1a}$$

$$\text{If } \frac{L}{D} < 2; \quad P = \frac{P_u * 100}{95 + 0.2\left(\frac{D}{L}\right) + 19.5\left(\frac{D}{L}\right)^2} \tag{4.6.1b}$$

Where: *Pu* = ultimate compressive strength per test (psi)

L/D = corresponding length to diameter ratio of the specimen

All specimens were sulfur capped according to ASTM C617 (2010) to maintain uniformity. The process of taking diameters, lengths and then sulfur capping is shown in *Figure 4-4*.

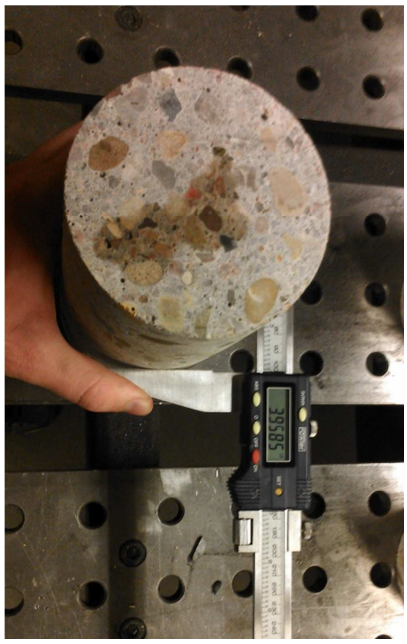

(a)

(b)

(c)

(d)

Figure 4-4 (a) Diameter, (b) Length, (c) Sulfur Capping, (d) Compressive Strength

4.6.2 - Volume of Permeable Voids Testing

Volume of permeable voids analysis (boil test) was performed by Kansas State University and followed the specifications outlined by ASTM C642 (2006). After the completion of the coring process and moisture conditioning of other field samples and lab samples, all samples were transported back to Kansas State University's main concrete lab in Fiedler Hall. The specimens for both the volume of permeable voids test and compressive strength tests were cut to specified dimensions using a wet saw as seen in *Figure 4-5* – 2 in. for the boil test and 8 in. for compressive strength.

Figure 4-5 Sample Wet Sawing

Once the specimens were cut, they were cleaned and allowed to surface dry (except for the labs specimens) and placed in the corresponding moisture condition.

Once the compressive strength specimens were tested on the appropriate day, the 2 in. boil test samples were placed in the oven. Oven dry weights were obtained and no samples were in the oven less than 48 hrs. in order to maintain consistency. They were then removed from the oven and allowed to cool to room temperature; they were weighed and then submersed in tap water for a minimum of 48 hrs. The specimens were than surface dried to a saturated surface dry (SSD) condition, weighed and continued to be placed in boiling water for a minimum time of 5 hrs. The specimens were boiled in a five gallon container with ¼ in. rods at the bottom with expanded metal placed on top to allow the specimens not to be in contact with the hot bottom of the container, which sat on a hot plate. The specimens were stacked on each other for a total height of three specimens. When the boiling time duration was met, the specimens were removed and submersed to find an apparent mass. After the apparent mass was found, the specimens were then surface dried to saturated surface dry conditions and weighed. The process is summarized in *Figure 4-6.*

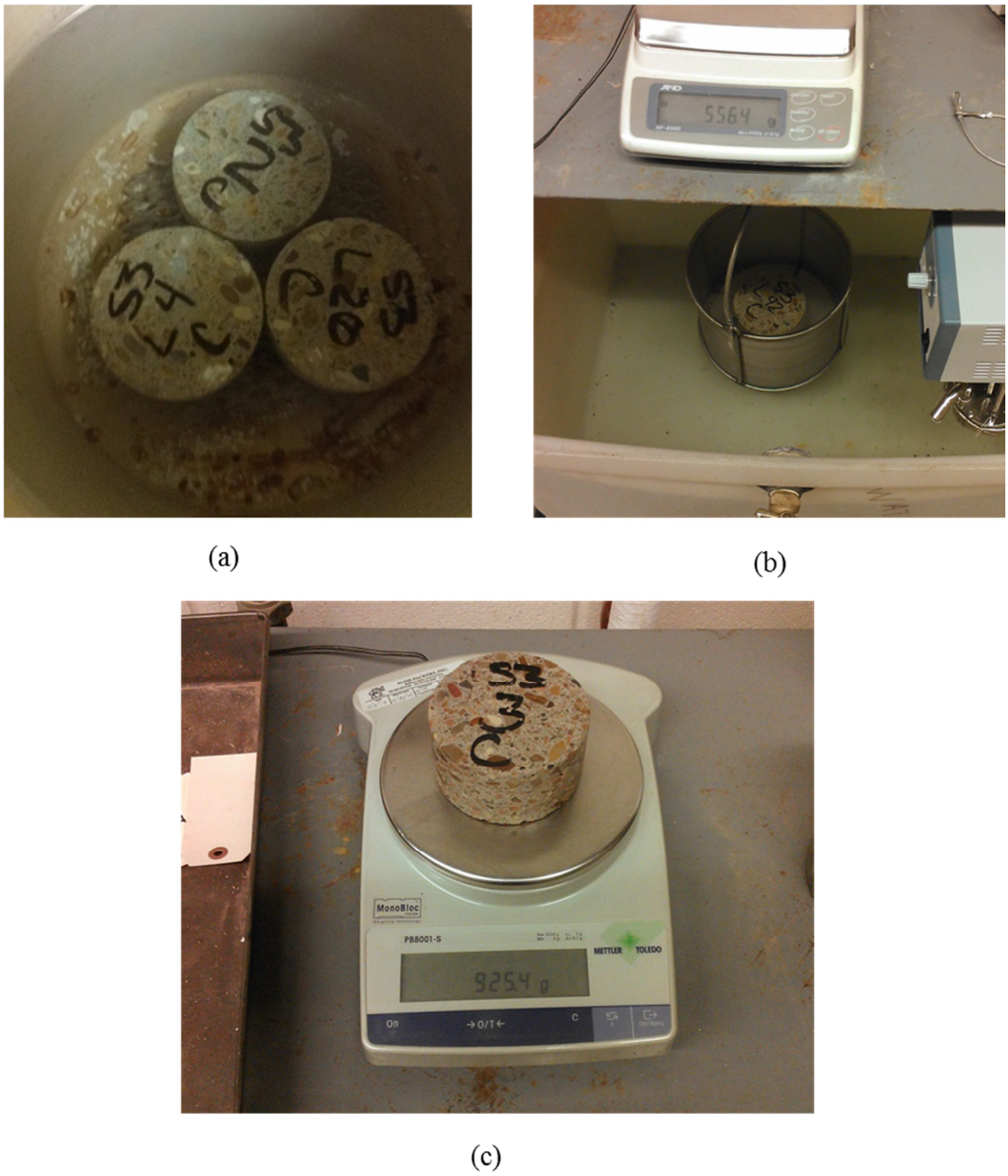

(a) (b)

(c)

Figure 4-6 (a) Boiling Stack Setup, (b) Apparent Mass in Water, (c) SSD Mass

The determination of the volume of the pore space has been given earlier in *Eq. 2.4.*3.

4.6.3 - Rapid Chloride Permeability Testing

Rapid chloride permeability testing was conducted by KDOT's materials laboratory according to ASTM C1202 (2012) as described in section *2.4.4.* The samples were transported from Kansas State University's Fiedler Hall to KDOT's materials and testing laboratory in Topeka, KS. The samples were than cut to the proper dimension, placed in a desiccator and a vacuum was created in the desiccator for 3 hrs. De-aired water was then introduced to vacuum saturate the specimen and the vacuum pump was run for an additional hour with the specimens under the water. Air was then allowed to re-enter the desiccator and samples were maintained submersed for an additional 18 ± 2 hrs.

Post vacuum saturation, the specimens were then removed from the water and transferred to a suitable container to maintain a RH of 95% or higher. Specimens were then placed in the receiving cell block and sealed to ensure no draining of the cell solution down the side of the specimen. The specimen receiving cell corresponding to the top of the specimen was than filled with 3.0% NaCl solution. This would be the negative terminal when connected to the power supply. The other cell that receives the bottom of the sample was then filled with 0.3 N NaOH (where the N for NaOH means normality and is equivalent to molarity) and becomes the positive terminal when connected to power supply. The electrical connection was made to the proper receiving cells and measurement equipment. The power supply of 60V ± 0.1V could then be switched on as long as the specimen, receiving cells and chemical solutions are in the temperature range of 20-25 ˚C. The ambient temperature range around the specimen was maintained throughout the test as 20-25 ˚C, and the solution temperatures remained under 90 ˚C to avoid damages to receiving cells and flawed measurements. Readings were taken at a minimum of every 30-min. and concluded at 6 hrs. A plot was then developed for current

(amperes) versus time (seconds) and is integrated giving units of coulombs. The integral over the whole test yields the total charge passed. Correction factors were applied for differing diameters by normalizing the charges past by multiplying the case specific charges passed by the square of the ratio of the idealized diameter to the actual diameter of the specimen, as shown in *Eq. 4.6.3*.

$$Q_s = Q_X \times \left[\frac{95\text{mm}}{\text{x}}\right]^2 \quad (4.6.3)$$

Where: Q_s = Total charge passed (coulombs) for 95 mm. sample diameter

Q_x = Total charge passed (coulombs) for x mm. sample diameter

x = Diameter of specimen

4.6.4 - Temperature Evaluation

The hydration temperature and long term hydration and specimen temperatures of the slab and field cured specimens were recorded by type T thermocouple sensors. The sensors were placed 4 to 5 in. vertically from the aggregate sub-base in the center of the slab and approximately 4 in. deep into the center of two 4 x 8 in. field cylinders. Data was sampled every five minutes and averaged over a duration of one hour. The data acquisition setup is shown in *Figure 4-7.*

(a) (b)

Figure 4-7 (a) Data acquisition housing, (b) Data logger and multiplexor

The lab cured specimens were stored at 73 ± 3°F in a lime saturated tank, and is assumed to be their temperature state.

Chapter 5 - Results

5.1 - Fresh Concrete Properties

The fresh concrete properties of slump, entrained air, concrete temperature, unit weight and the ambient air temperature for each placement season is shown in *Table 5-1*.

Table 5-1 Fresh Concrete Properties Obtained at Placement

Mix.	Cementitious Material	Date	Slump (in.)	Air Temp. (˚C)	Concrete Temp. (˚C)	Unit Wt. (lb./ft^3)	Air (%)
Season 1 (Summer)							
OPC	100% Portland Cement	8/3/2011	4	27.2	30.0	140.8	6.4
F-ash	25% F Ash, 75% Portland Cement	8/12/2011	3.5	24.4	27.2	NA	5.5
C-ash	25% C Ash, 75% Portland Cement	8/19/2011	2.25	26.7	28.9	142.5	5.8
Season 2 (Fall)							
OPC	100% Portland Cement	10/19/2011	2.75	4.0	10.8	141.88	6
F-ash	25% F Ash, 75% Portland Cement	10/28/2011	4	2.0	8.7	139.6	7.3
C-ash	25% C Ash, 75% Portland Cement	11/11/2011	1.5	4.1	8.2	143.92	5.2
Season 3 (Spring)							
OPC	100% Portland Cement	3/28/2012	1.75	16.2	22.2	143.72	5.3
F-ash	25% F Ash, 75% Portland Cement	4/6/2012	4	12.9	19.1	140.68	6.1
C-ash	25% C Ash, 75% Portland Cement	4/13/2012	0.75	19.6	22.6	144.88	5

5.2 - Results of Season 1, 2 and 3

Figures 5-1a -5-1c summarize Season 1, 100% OPC compressive strength, volume of permeable voids and Rapid Chloride Permeability Test for all curing environments respectively. All error bars shown on compressive strength figures represent two standard deviations of the sample.

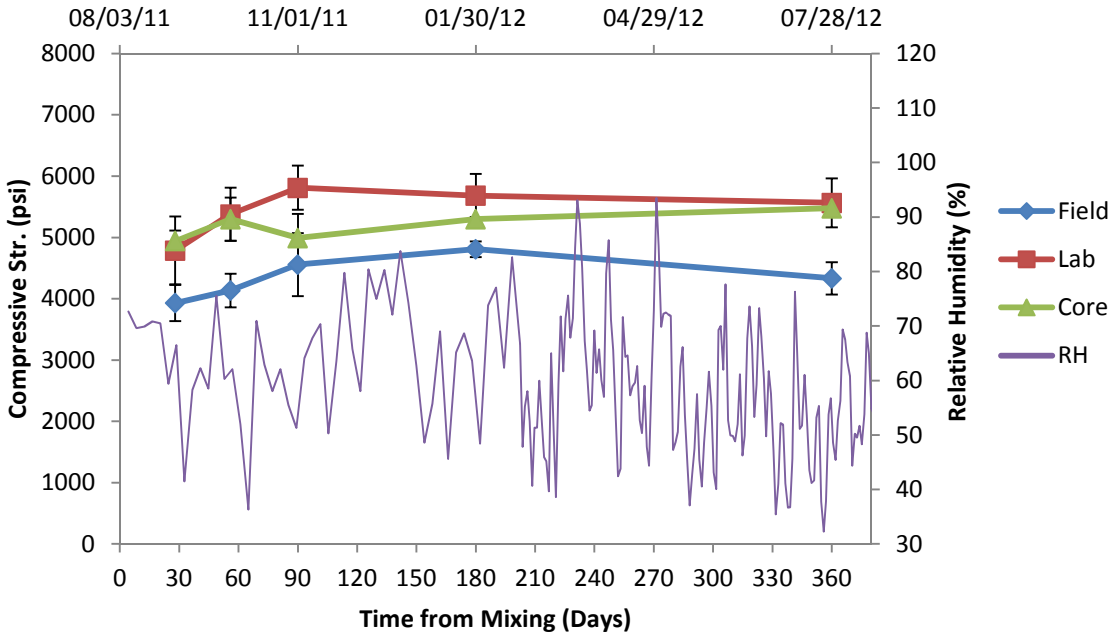

(a)

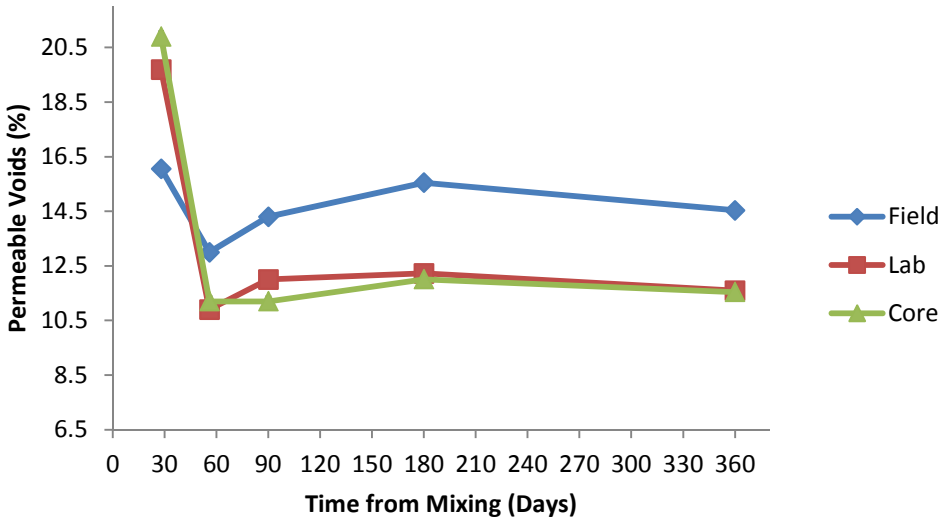

(b)

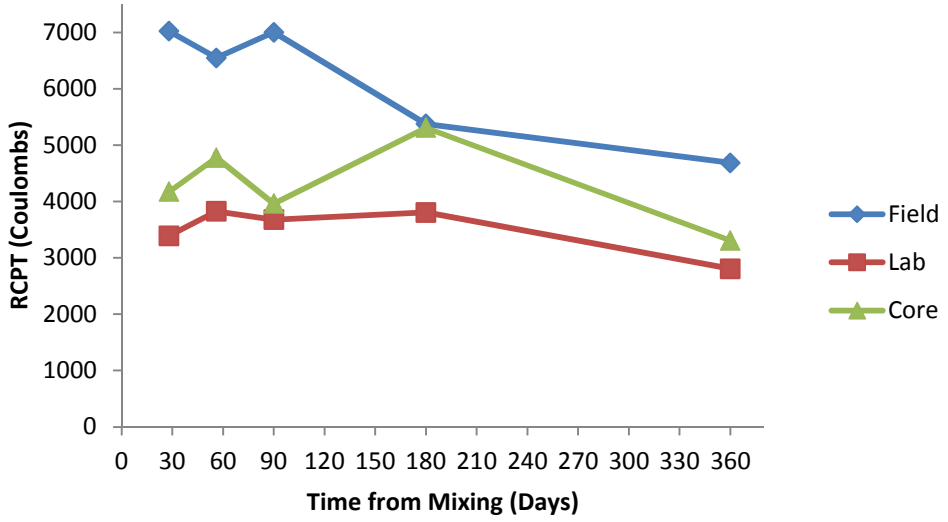

(c)

Figure 5-1 Season 1, 100% OPC (a) Compressive Strength, (b) Volume of Permeable Voids and (c) RCPT

Figures 5-2a -5-2c summarize Season 1, 25% F-ash compressive strength, volume of permeable voids and Rapid Chloride Permeability Test for all curing environments respectively.

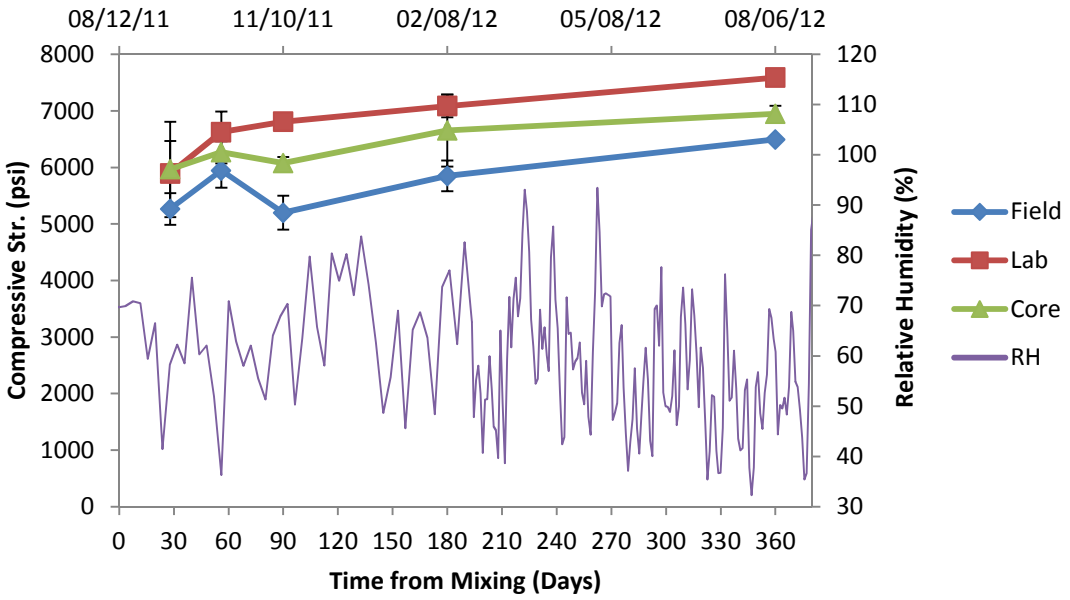
08/12/11
11/10/11
02/08/12
05/08/12
08/06/12
Compressive Str. (psi)
Relative Humidity (%)
Time from Mixing (Days)
Field
Lab
Core
RH

(a)

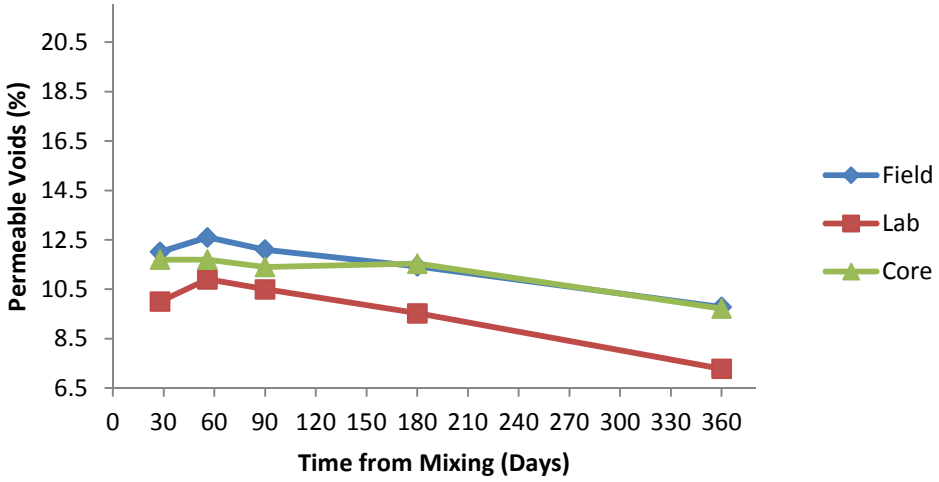
Permeable Voids (%)
Time from Mixing (Days)
Field
Lab
Core

(b)

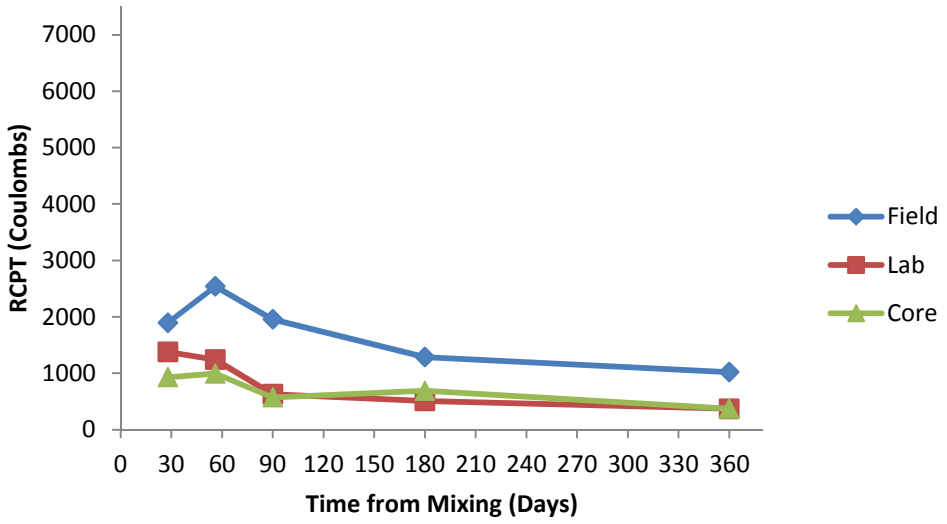

(c)

Figure 5-2 Season 1, 25% F-ash (a) Compressive Strength, (b) Volume of Permeable Voids and (c) RCPT

Figures 5-3a -5-3c summarize Season 1, 25% C-ash compressive strength, volume of permeable voids and Rapid Chloride Permeability Test for all curing environments respectively.

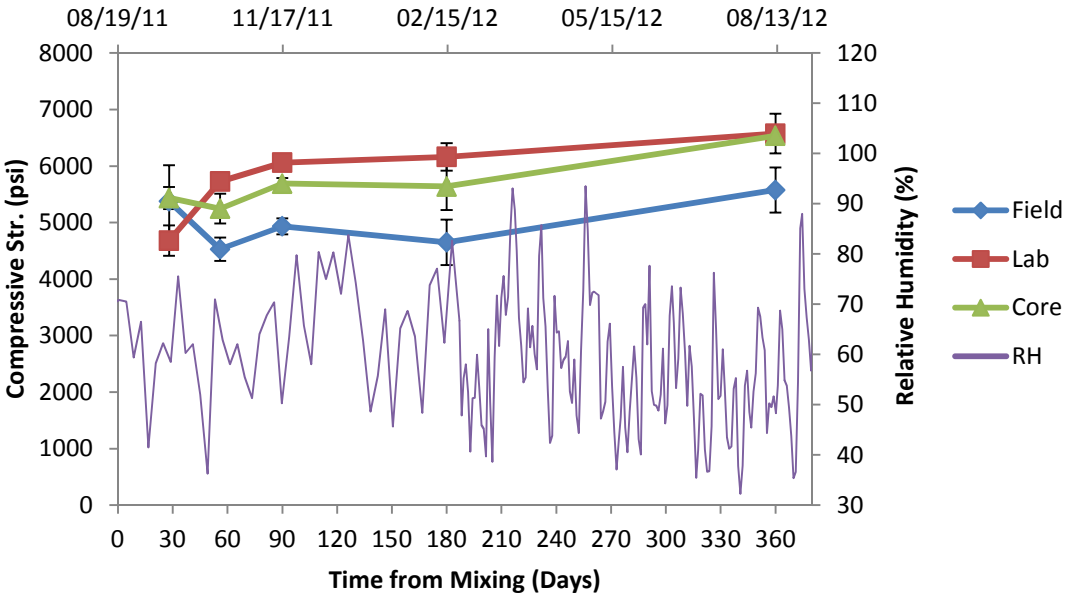
08/19/11
11/17/11
02/15/12
05/15/12
08/13/12
Compressive Str. (psi)
Relative Humidity (%)
Time from Mixing (Days)
Field
Lab
Core
RH

(a)

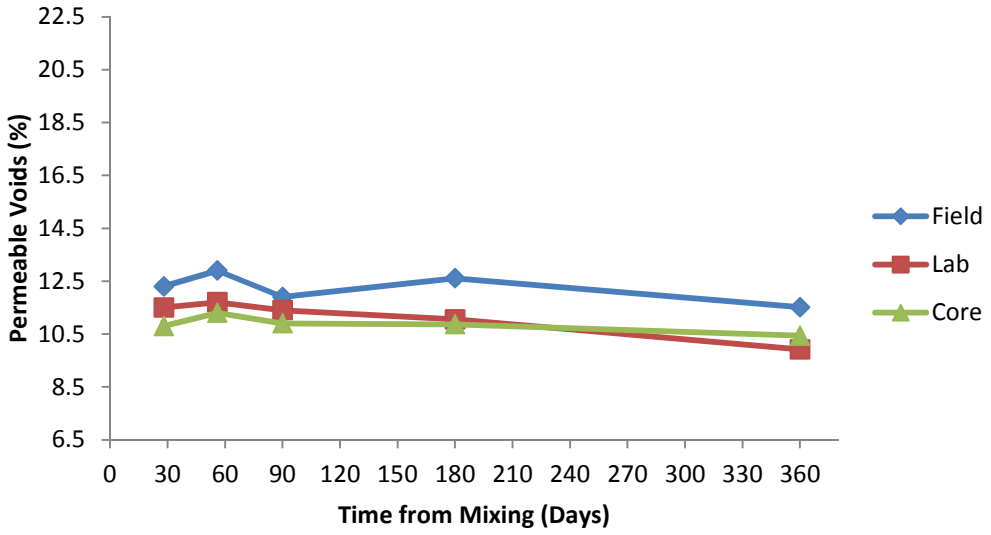
Permeable Voids (%)
Time from Mixing (Days)
Field
Lab
Core

(b)

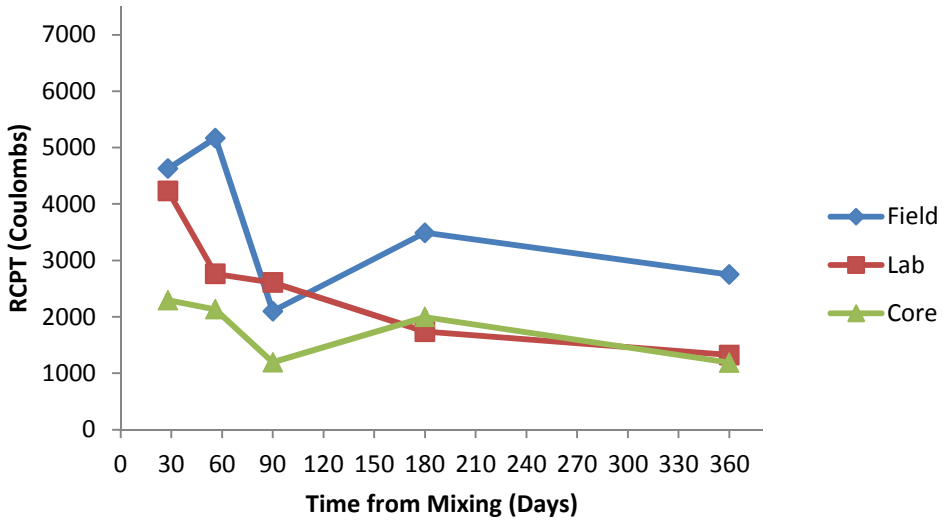

(c)

Figure 5-3 Season 1, 25% C-ash (a) Compressive Strength, (b) Volume of Permeable Voids and (c) RCPT

Figures 5-4a -5-4c summarize Season 2, 100% OPC compressive strength, volume of permeable voids and Rapid Chloride Permeability Test for all curing environments respectively.

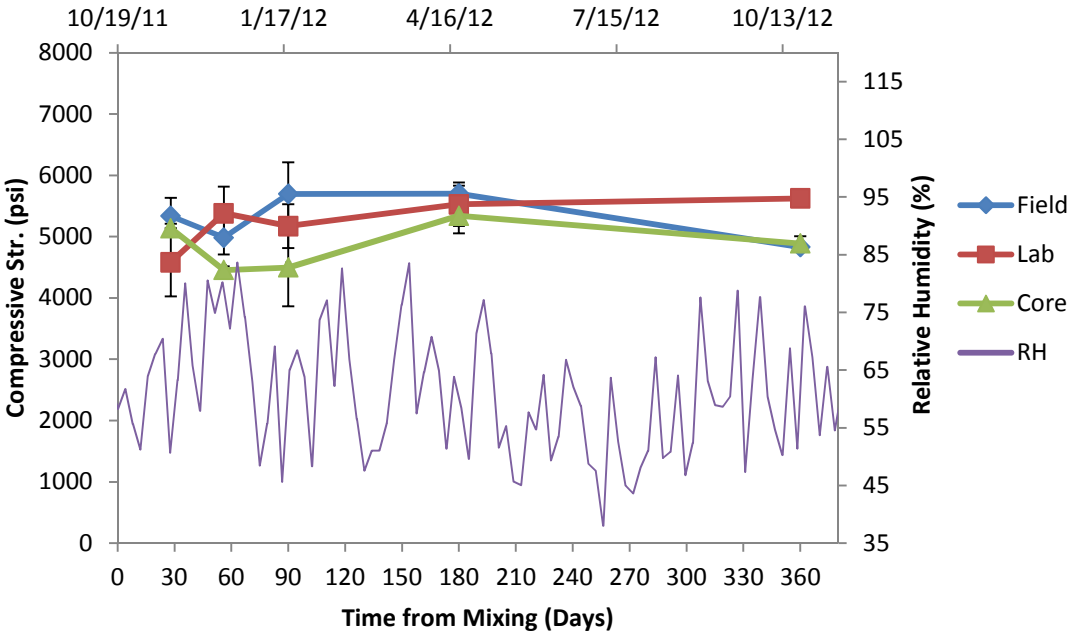
10/19/11
1/17/12
4/16/12
7/15/12
10/13/12
8000
7000
6000
5000
4000
3000
2000
1000
0
Compressive Str. (psi)
115
105
95
85
75
65
55
45
35
Relative Humidity (%)
0 30 60 90 120 150 180 210 240 270 300 330 360
Time from Mixing (Days)
Field
Lab
Core
RH

(a)

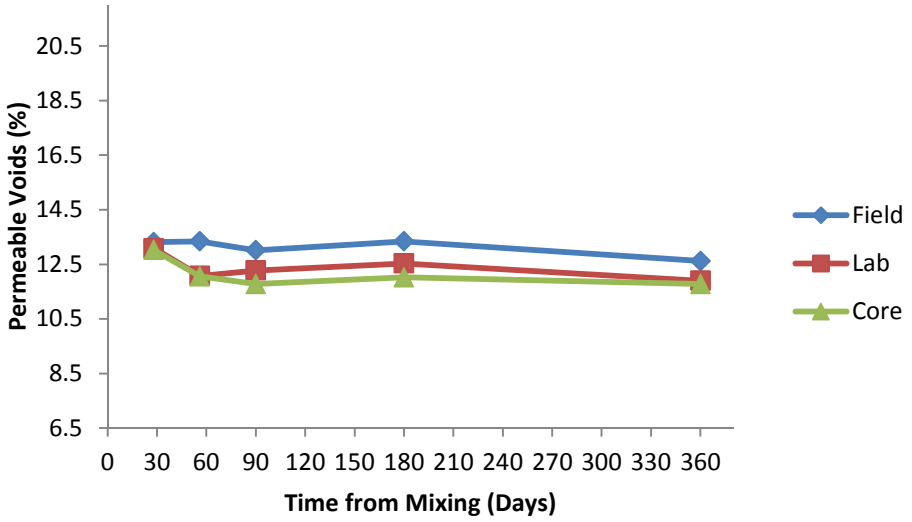
20.5
18.5
16.5
14.5
12.5
10.5
8.5
6.5
Permeable Voids (%)
0 30 60 90 120 150 180 210 240 270 300 330 360
Time from Mixing (Days)
Field
Lab
Core

(b)

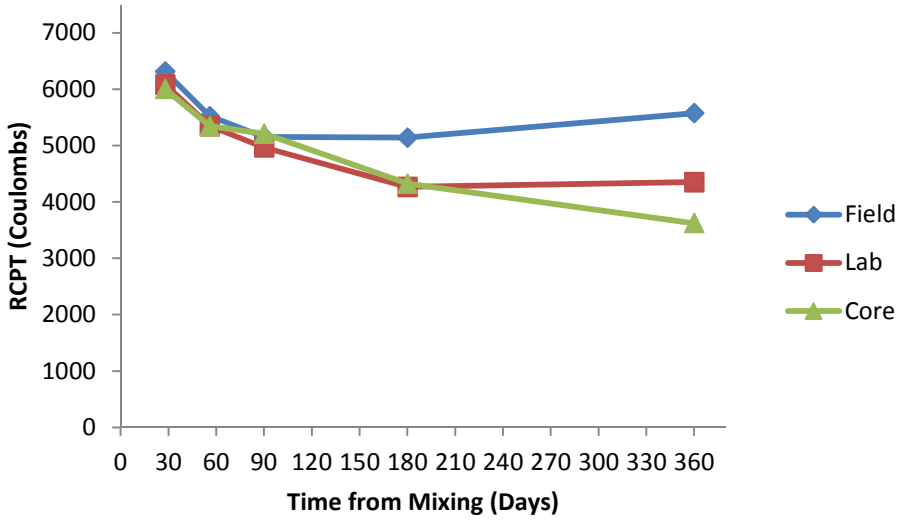

(c)

Figure 5-4 Season 2, 100% OPC (a) Compressive Strength, (b) Volume of Permeable Voids and (c) RCPT

Figures 5-5a -5-5c summarize Season 2, 25% F-ash compressive strength, volume of permeable voids and Rapid Chloride Permeability Test for all curing environments respectively.

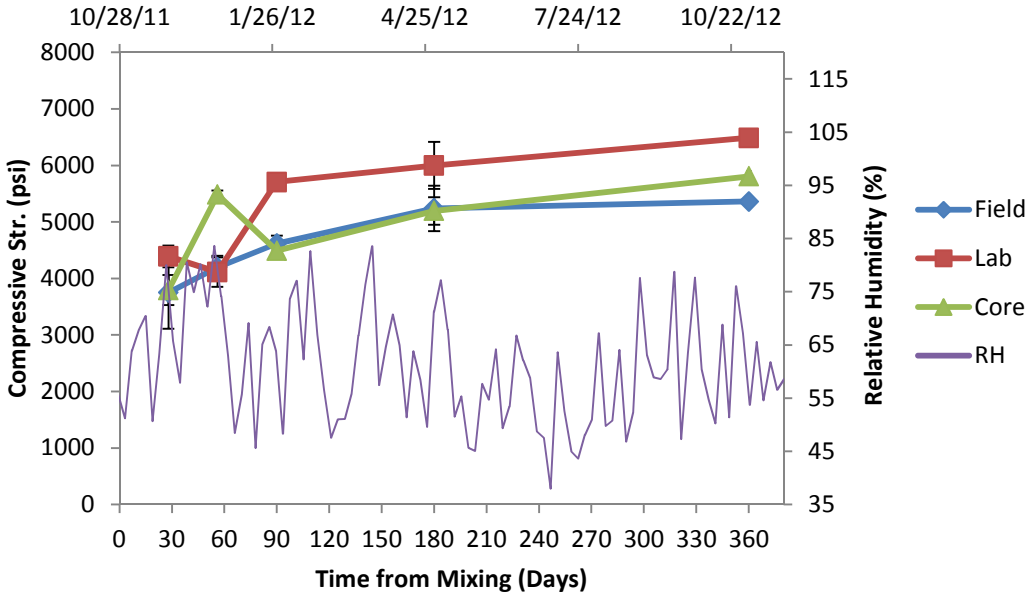
10/28/11
1/26/12
4/25/12
7/24/12
10/22/12
8000
7000
6000
5000
4000
3000
2000
1000
0
Compressive Str. (psi)
115
105
95
85
75
65
55
45
35
Relative Humidity (%)
0 30 60 90 120 150 180 210 240 270 300 330 360
Time from Mixing (Days)
Field
Lab
Core
RH

(a)

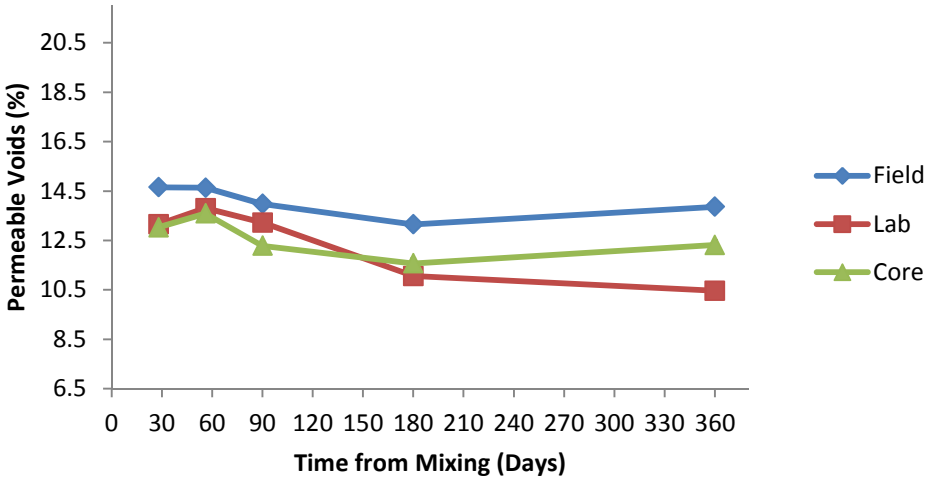
20.5
18.5
16.5
14.5
12.5
10.5
8.5
6.5
Permeable Voids (%)
0 30 60 90 120 150 180 210 240 270 300 330 360
Time from Mixing (Days)
Field
Lab
Core

(b)

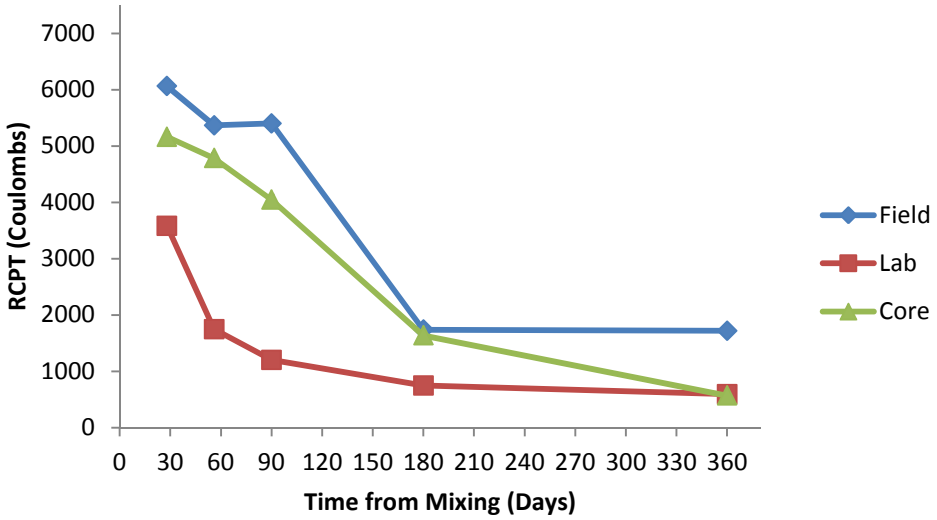

(c)

Figure 5-5 Season 2, 25% F-ash (a) Compressive Strength, (b) Volume of Permeable Voids and (c) RCPT

Figures 5-6a -5-6c summarize Season 2, 25% C-ash compressive strength, volume of permeable voids and Rapid Chloride Permeability Test for all curing environments respectively.

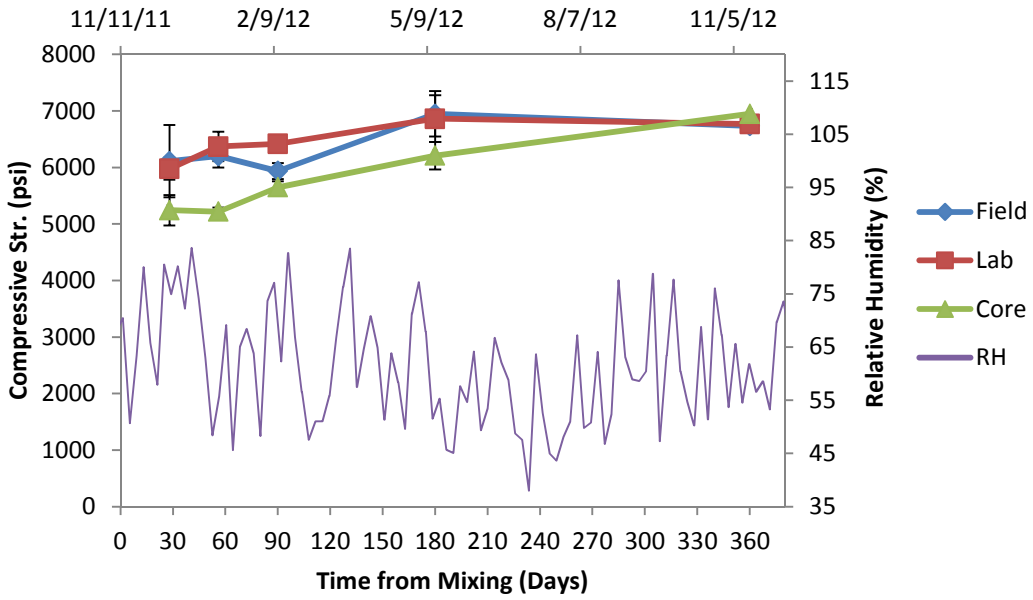
11/11/11
2/9/12
5/9/12
8/7/12
11/5/12
8000
7000
6000
5000
4000
3000
2000
1000
0
Compressive Str. (psi)
115
105
95
85
75
65
55
45
35
Relative Humidity (%)
0 30 60 90 120 150 180 210 240 270 300 330 360
Time from Mixing (Days)
Field
Lab
Core
RH

(a)

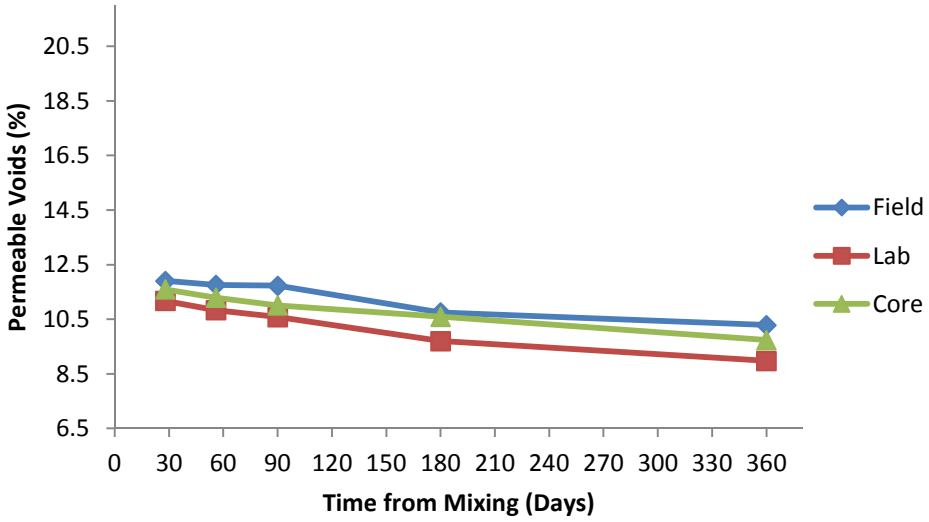
20.5
18.5
16.5
14.5
12.5
10.5
8.5
6.5
Permeable Voids (%)
0 30 60 90 120 150 180 210 240 270 300 330 360
Time from Mixing (Days)
Field
Lab
Core

(b)

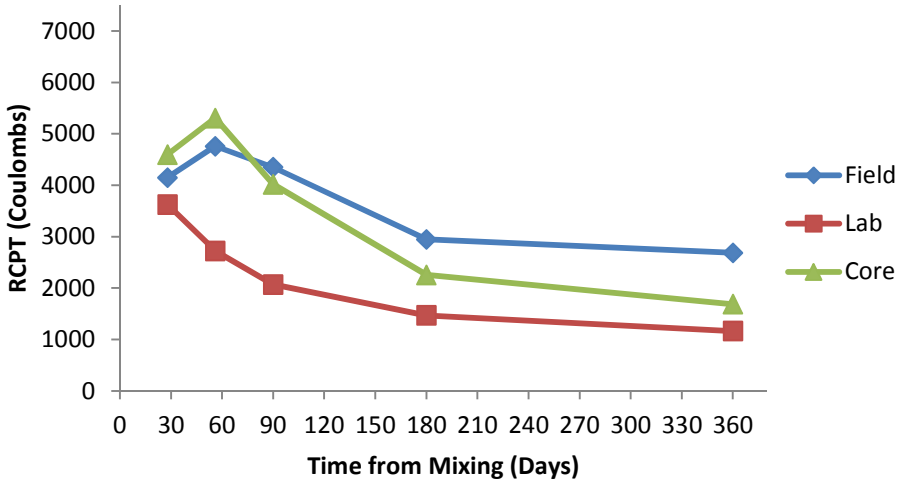

(c)

Figure 5-6 Season 2, 25% C-ash (a) Compressive Strength, (b) Volume of Permeable Voids and (c) RCPT

Figures 5-7a -5-7c summarize Season 3, 100% OPC compressive strength, volume of permeable voids and Rapid Chloride Permeability Test for all curing environments respectively.

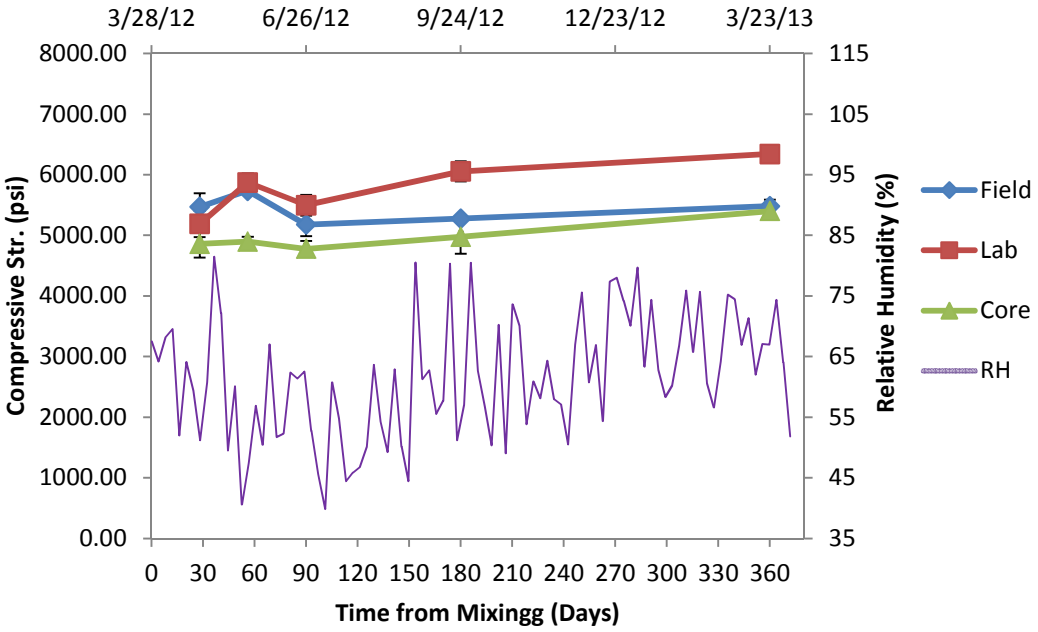
3/28/12
6/26/12
9/24/12
12/23/12
3/23/13
8000.00
7000.00
6000.00
5000.00
4000.00
3000.00
2000.00
1000.00
0.00
115
105
95
85
75
65
55
45
35
0 30 60 90 120 150 180 210 240 270 300 330 360
Time from Mixingg (Days)
Compressive Str. (psi)
Relative Humidity (%)
Field
Lab
Core
RH

(a)

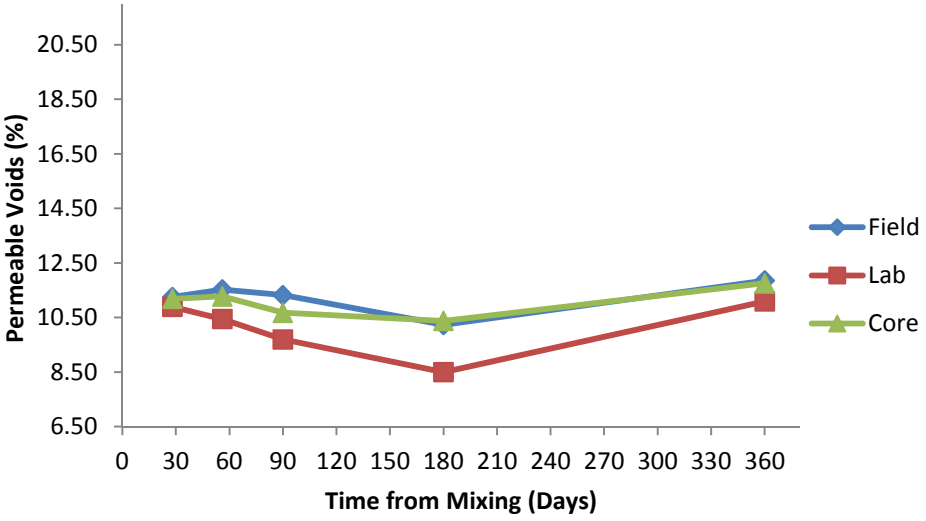
20.50
18.50
16.50
14.50
12.50
10.50
8.50
6.50
0 30 60 90 120 150 180 210 240 270 300 330 360
Time from Mixing (Days)
Permeable Voids (%)
Field
Lab
Core

(b)

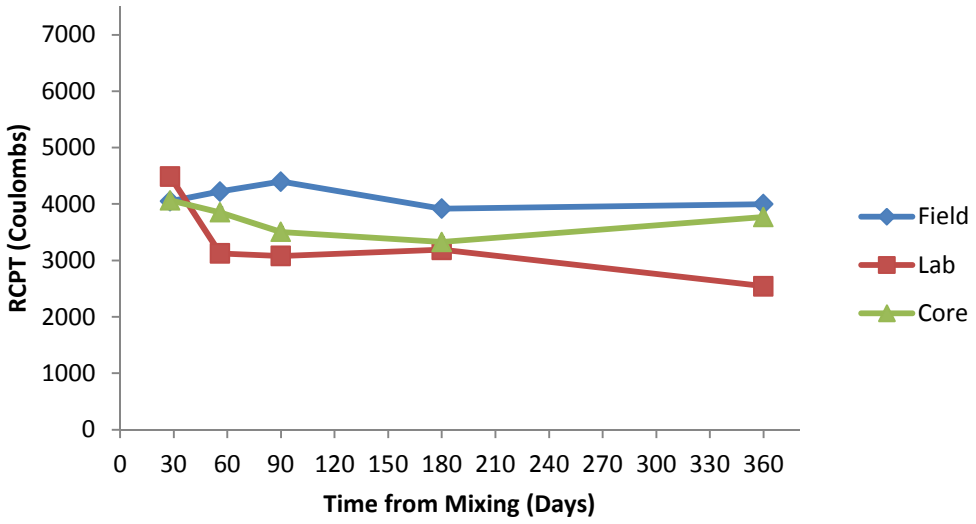

(c)

Figure 5-7 Season 3, 100% OPC (a) Compressive Strength, (b) Volume of Permeable Voids and (c) RCPT

Figures 5-8a -5-8c summarize Season 3, 25% F-ash compressive strength, volume of permeable voids and Rapid Chloride Permeability Test for all curing environments respectively.

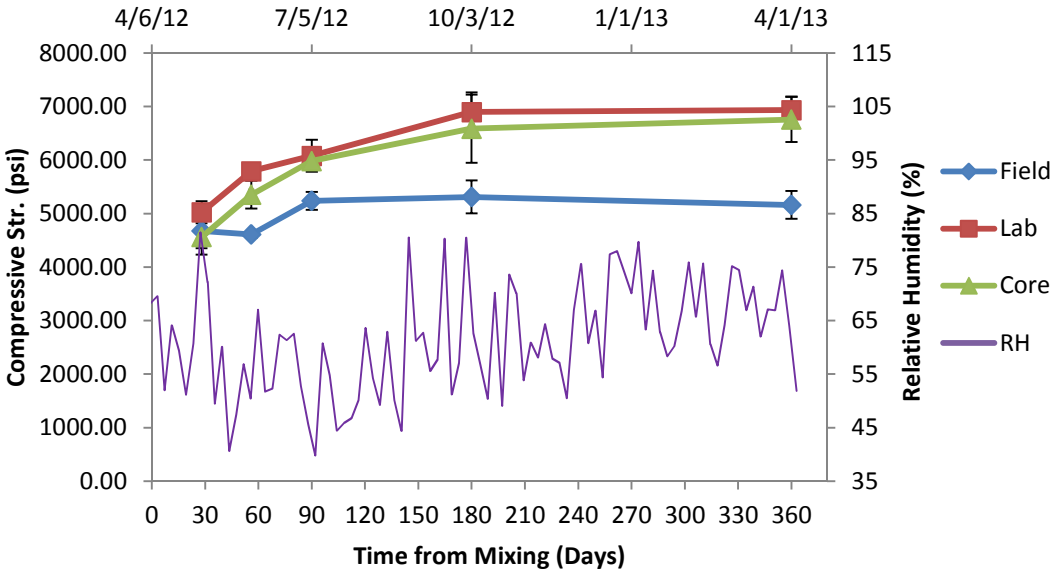
4/6/12
7/5/12
10/3/12
1/1/13
4/1/13
8000.00
7000.00
6000.00
5000.00
4000.00
3000.00
2000.00
1000.00
0.00
Compressive Str. (psi)
115
105
95
85
75
65
55
45
35
Relative Humidity (%)
0 30 60 90 120 150 180 210 240 270 300 330 360
Time from Mixing (Days)
Field
Lab
Core
RH

(a)

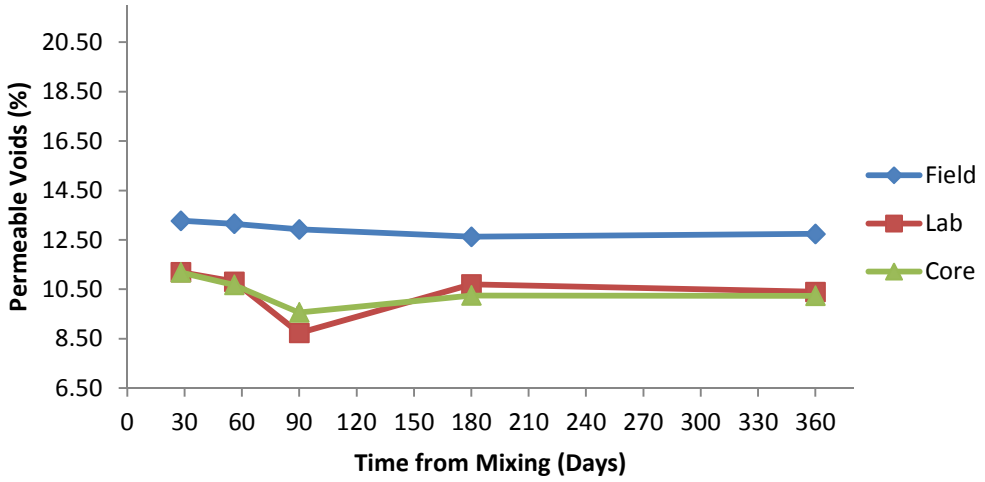
20.50
18.50
16.50
14.50
12.50
10.50
8.50
6.50
Permeable Voids (%)
0 30 60 90 120 150 180 210 240 270 300 330 360
Time from Mixing (Days)
Field
Lab
Core

(b)

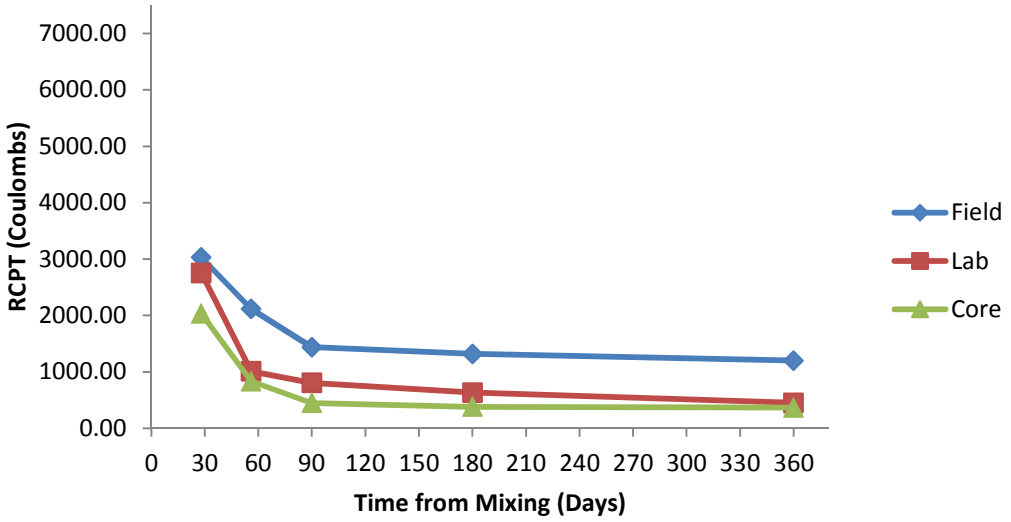

(c)

Figure 5-8 Season 3, 25% F-ash (a) Compressive Strength, (b) Volume of Permeable Voids and (c) RCPT

Figures 5-9a - 5-9c summarize Season 3, 25% C-ash compressive strength, volume of permeable voids and Rapid Chloride Permeability Test for all curing environments respectively.

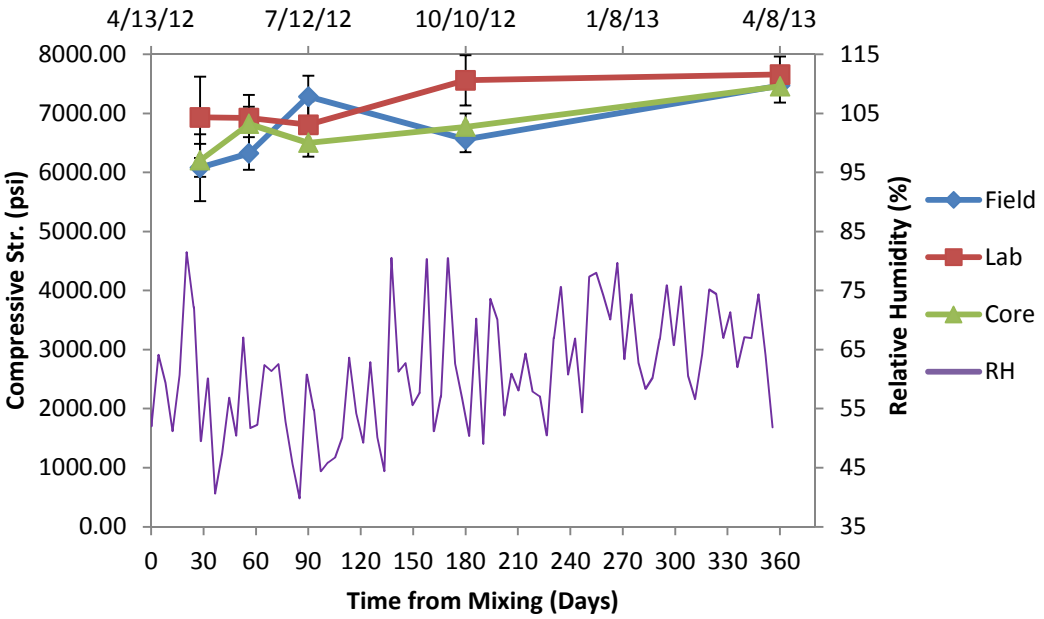
4/13/12
7/12/12
10/10/12
1/8/13
4/8/13
8000.00
7000.00
6000.00
5000.00
4000.00
3000.00
2000.00
1000.00
0.00
Compressive Str. (psi)
115
105
95
85
75
65
55
45
35
Relative Humidity (%)
0 30 60 90 120 150 180 210 240 270 300 330 360
Time from Mixing (Days)
Field
Lab
Core
RH

(a)

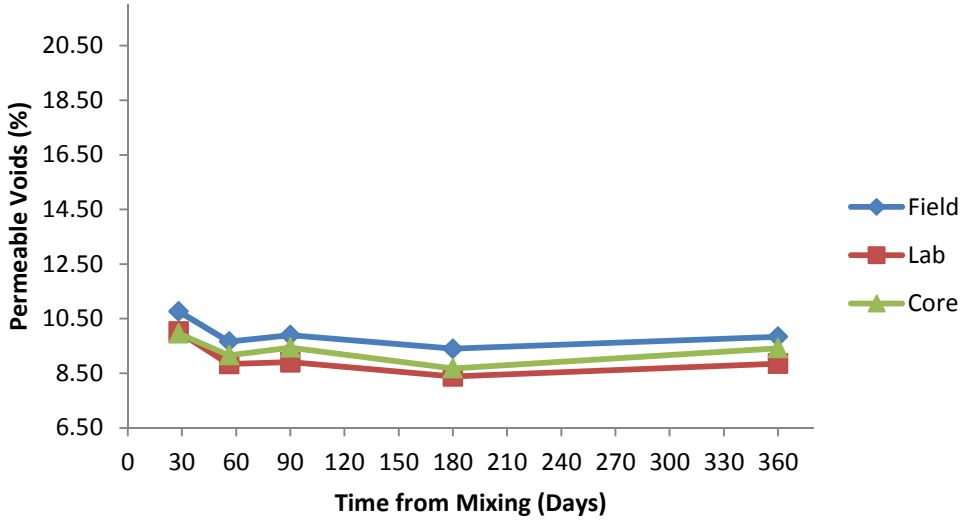
20.50
18.50
16.50
14.50
12.50
10.50
8.50
6.50
Permeable Voids (%)
0 30 60 90 120 150 180 210 240 270 300 330 360
Time from Mixing (Days)
Field
Lab
Core

(b)

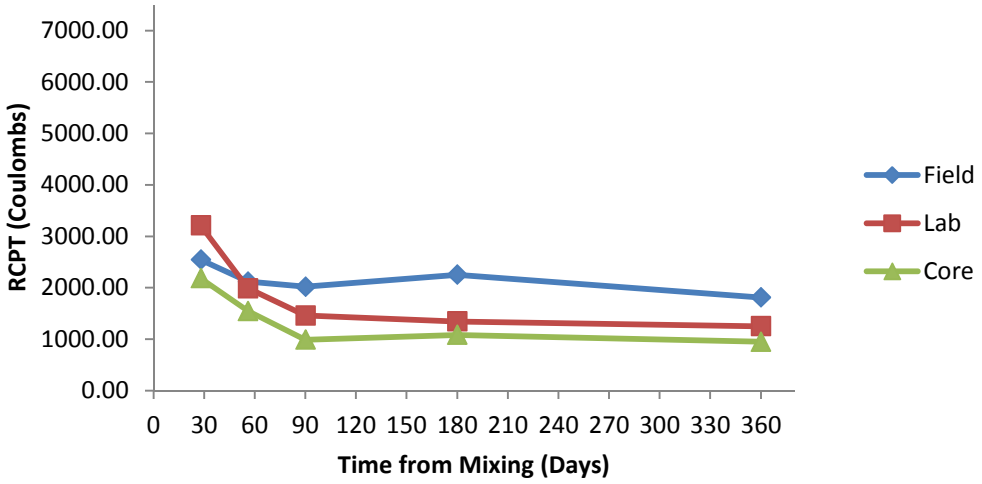

(c)

Figure 5-9 Season 3, 25% C-ash (a) Compressive Strength, (b) Volume of Permeable Voids and (c) RCPT

Chapter 6 - Discussion

6.1 - Mixture Variance with Placement Season

The standard deviations for each concrete mixture for each corresponding testing day (28, 56, 90, 180 and 360) were done across all three seasons for strength, permeable voids and RCPT. These values were than normalized by the summation of each corresponding, longitudinal testing magnitudes. The normalized percent values for 28, 56, 90, 180 and 360 day tests were than summed to get a total variance across all three seasons. An example calculation done for field cured OPC strength is done as follows.

Example Calculation *6.1*:

	Field Comp. Str. (psi)
28 day Season 1	3928.28
28 day Season 2	5336.23
28 day Season 3	5468.70

Standard Deviation (3928.28, 5336.23, 5468.70) = 853.7

Normalizing over combined comp. str. = (853.7 / (3928.28 + 5336.23 + 5468.70)) = 5.79%

This process was done longitudinally for each testing day

	Normalized %
28 day	5.79
56 day	5.39
90 day	3.69
180 day	2.83
360 day	3.94
Sum	21.64

The sum of 21.64% can be seen as the first column in *Figure 6-1*.

Figure 6-1 is the graph of the result of this process and illustrates the effects of the placement season on the concrete mixtures. Note, showing a high cumulative percent does not equate directly to poor performance. For example, RCPT data could range from 100 to 3000 coulombs and show a very high value for the cumulative normalized standard deviation, but in reality be very good quality concrete because the RCPT value is well below 3500 coulombs. This is opposed to a data range from 4500 to 5000 coulombs which would show a lower value for the cumulative normalized standard deviation, but be of poor performance because the values are well above 3500 coulombs.

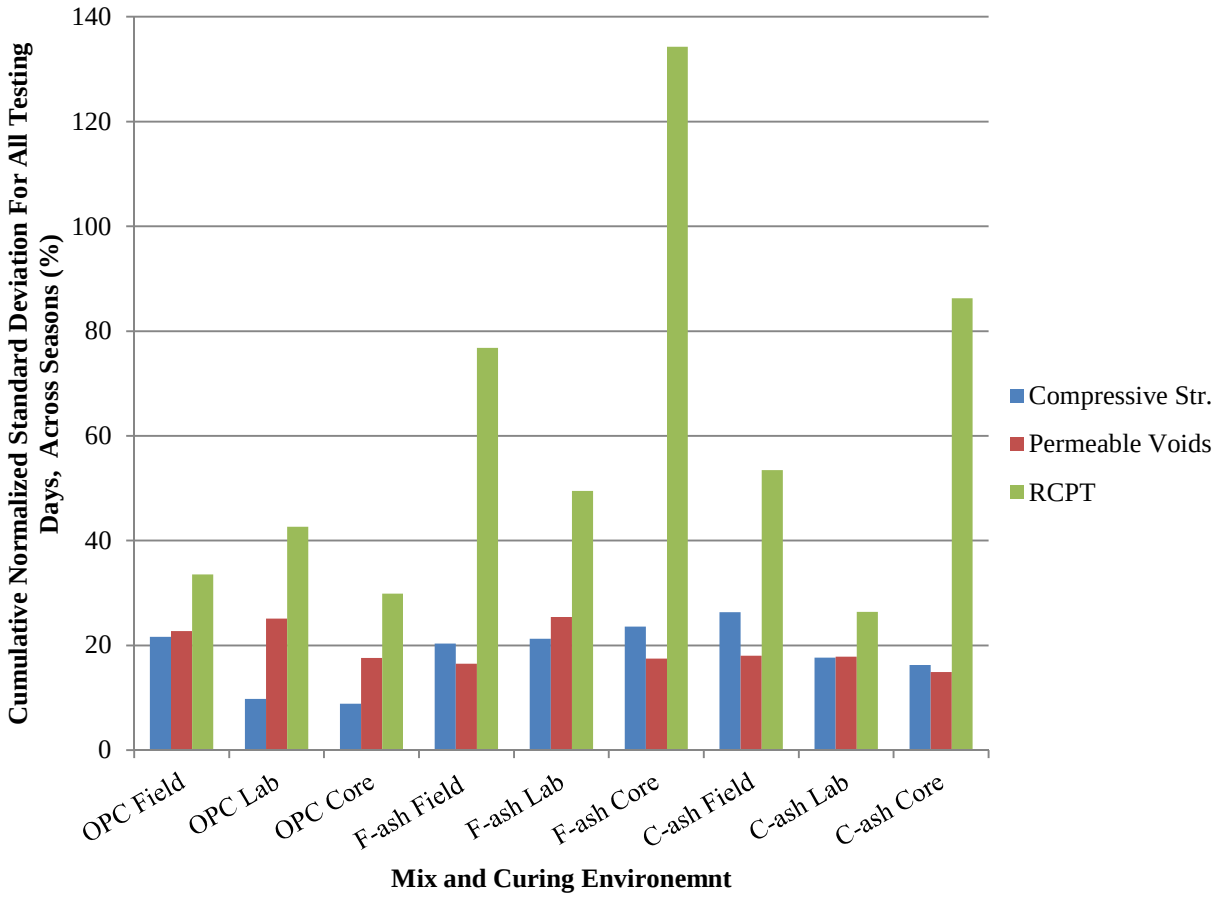

Figure 6-1 Cumulative Normalized Variance across All Placement Seasons

The F-ash cores showed the highest percent variance. F-ash (with its lower calcium content) has been known to increase strength and lower permeability at high temperatures because the temperature accelerates the pozzolanic reaction (Monteiro 2006). This accelerated pozzolanic reaction is shown in the 28 day RCPT value for Season 1 (summer) F-ash as 928 coulombs, which is very low. Conversely, F-ash also is known for having slower strength gain during normal and colder temperatures, the 28 day RCPT for Season 2 (winter) was 5161 coulombs and 28 day Season 3 (spring) was 2035 coulombs. Regardless of the placement season, all RCPT values of F-ash cores at 360 day tests were less than 600 coulombs. For each of the three curing environments, the F-ash exhibited the highest percent variance for the RCPT in the curing environment.

The OPC showed the least change with the lab and core curing environments with respect to strength and showed similar percent change compared to the other mixtures in the field curing environment. The similar percent changes in the field would suggest that all field cylinders go through similar thermal stresses and freeze-thaw degradation and respond in a like manner to the field exposure. The OPC mixture showed the lowest strength, highest value of RCPT and the highest volume of permeable voids from core and lab curing environments across all seasons at 360 day tests. It also had the highest RCPT values among the field curing conditions, but outperformed the F-ash mixture in volume of permeable voids and strength at 360 days for Season 2 and 3 – most likely because of the slow strength gain of F-ash at low and moderate temperatures. The OPC mixture did not outperform the C-ash mixture for any 360 day test.

6.2 - Impacts of Curing Environment

The impacts of the curing environment can be seen in *Table 6-1* and the corresponding percent changes based on lab results in *Table 6-2*. The differences have been averaged over all of the testing dates.

Table 6-1 Curing Effects Compared to Lab Cure

	Field to Lab cured difference			**Core to Lab cured difference**		
	Compressive Str. (psi)	% Permeable Voids	RCPT Coulombs	Compressive Str. (psi)	% Permeable Voids	RCPT Coulombs
	Season 1					
OPC	-1093	1.4	2625	-244	0.1	803
F-ash	-1050	1.9	914	-420	1.6	-114
C-ash	-828	1.1	1096	-271	-0.3	-772
	Season 2					
OPC	53	0.8	539	-394	-0.2	-102
F-ash	-706	1.7	2481	-386	0.2	1664
C-ash	-93	1.0	1569	-653	0.6	1363
	Season 3					
OPC	-363	1.1	1007	-809	0.9	505
F-ash	-1146	2.6	690	-297	0.0	-319
C-ash	-432	0.9	298	-253	0.3	-500

Table 6-2 Curing Effects Compared to Percent of Lab Cure Value

	Field Percent of Lab			Core Percent of Lab		
	Compressive Str. (psi)	% Permeable Voids	RCPT Coulombs	Compressive Str. (psi)	% Permeable Voids	RCPT Coulombs
	Season 1					
OPC	80	114.5	175	96	100.0	123
F-ash	85	121.1	236	94	117.5	95
C-ash	87	110.4	157	96	97.9	76
	Season 2					
OPC	102	106.2	112	93	98.0	98
F-ash	88	114.9	289	95	102.5	214
C-ash	99	110.3	186	90	105.9	163
	Season 3					
OPC	94	111.5	134	86	109.8	118
F-ash	82	125.7	194	95	100.4	71
C-ash	94	110.2	127	97	103.8	74

As seen in *Table 6-2,* the cores containing fly ash outperform the lab cylinders at high temperatures for RCPT and have very comparable compressive strengths and permeable voids.

5.2 - Regression Analysis

Regression analysis was performed to investigate the correlations between strength, RCPT and permeable voids. The first analysis did not designate between mixture types and purely correlated the results to each performance test. This is shown in *Figures 6-2a - 6-2c*, with relations between RCPT and strength, RCPT and permeable voids, and permeable voids and strength respectively.

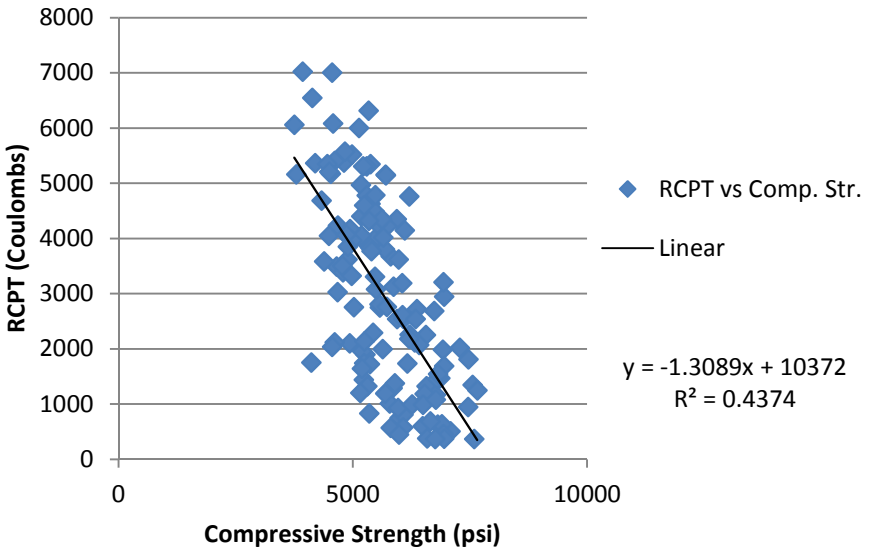
8000
7000
6000
5000
4000
3000
2000
1000
0
RCPT (Coulombs)
0
5000
10000
Compressive Strength (psi)
RCPT vs Comp. Str.
Linear
y = -1.3089x + 10372
R² = 0.4374

(a)

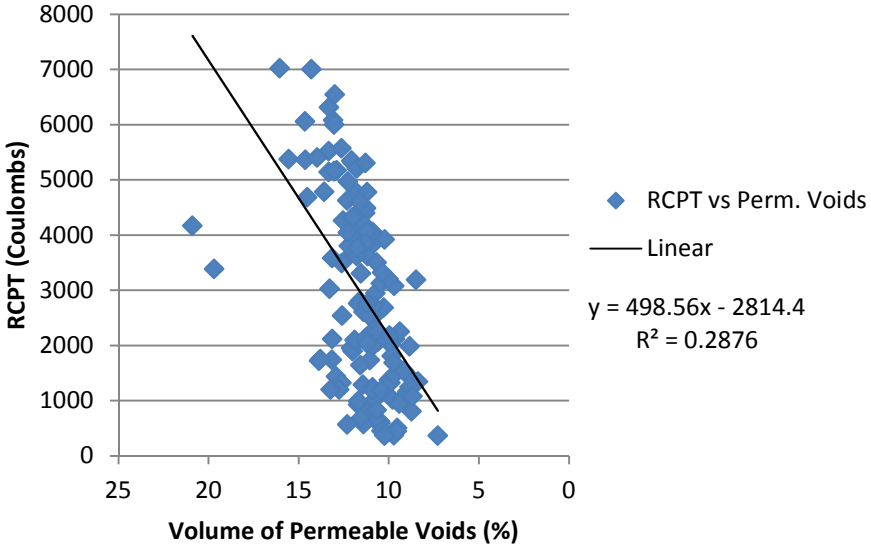
8000
7000
6000
5000
4000
3000
2000
1000
0
RCPT (Coulombs)
25
20
15
10
5
0
Volume of Permeable Voids (%)
RCPT vs Perm. Voids
Linear
y = 498.56x - 2814.4
R² = 0.2876

(b)

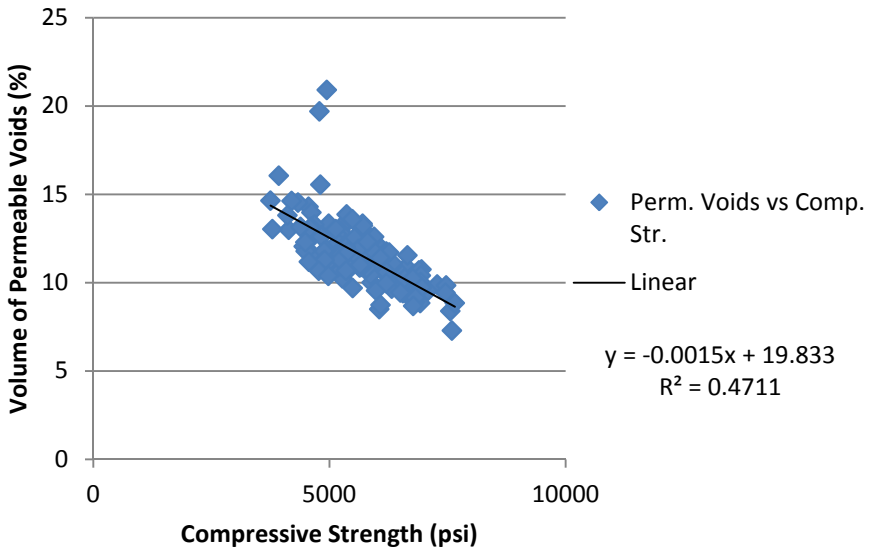

(c)

Figure 6-2 Bulk Regression for (a) RCPT to Compressive Strength, (b) RPCT to Permeable Voids, (c) Permeable Voids to Compressive Strength

As seen from the permeability tests compared to strength, there is the traditional correlation between less permeable concrete and higher compressive strength. This is very much expected, but there is a large amount of variance in the data, as a result the R^2 coefficient of determination is also small. In the comparison of the RCPT and permeable voids analysis, there still exists the trend of the concrete gaining strength with time and also lowering in permeability, but the RCPT and permeable voids cannot be compared directly with a high degree of accuracy as justified by the low R^2 value of 0.29. An important factor to also consider is at high compressive strengths, the concrete does not fail from the cement paste crushing or the bond between the aggregates being sheared, but the aggregates themselves can shear and cause failure.

Further regression analysis was done that differentiated between the cementitious blend used. Since the microstructure of the concrete is highly dependent on the cementitious materials used and the effects of particle packing, pozzolanic reactions, and reaction rates etc. the

correlations were higher. *Figures 6-3a – 6-3c* represent the relations between RCPT and strength, RCPT and permeable voids, and permeable voids and strength respectively for the OPC mixture.

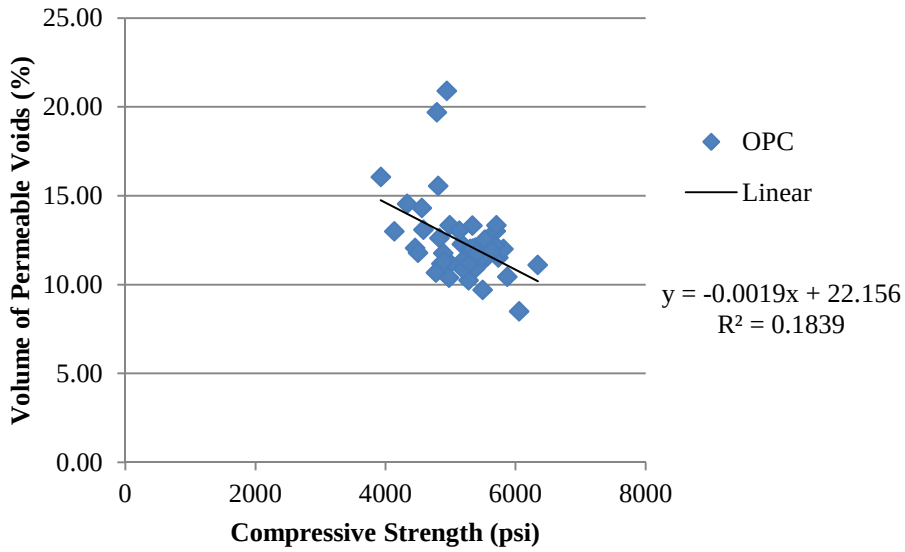

(a)

Red limit lines were also inserted in *Figure 6-3b* based on KDOT Design Specification 401, Table 401-3: The maximum value of permeable voids at 28 days is given as 12.50% and the maximum RCPT coulombs as 3500 at 56 day (KDOT 401 2007). The time requirement of this specification is not reflected in the figure.

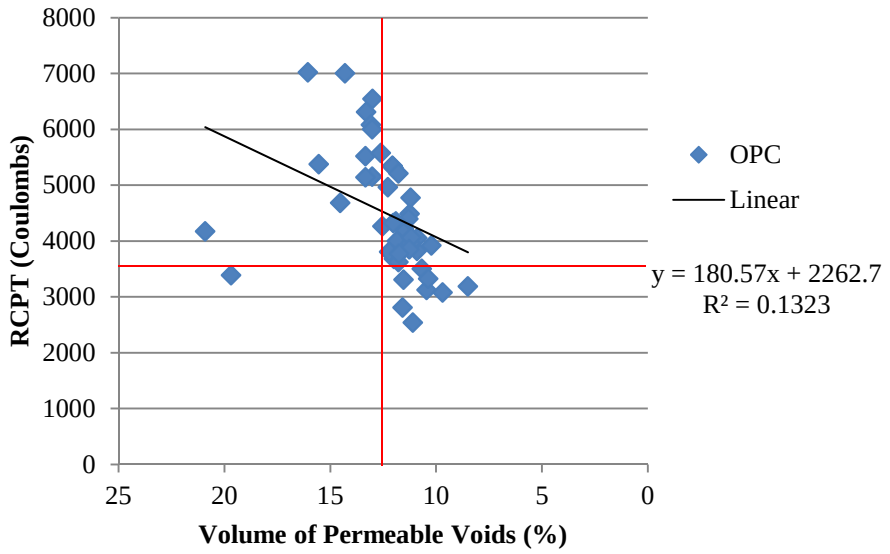

(b)

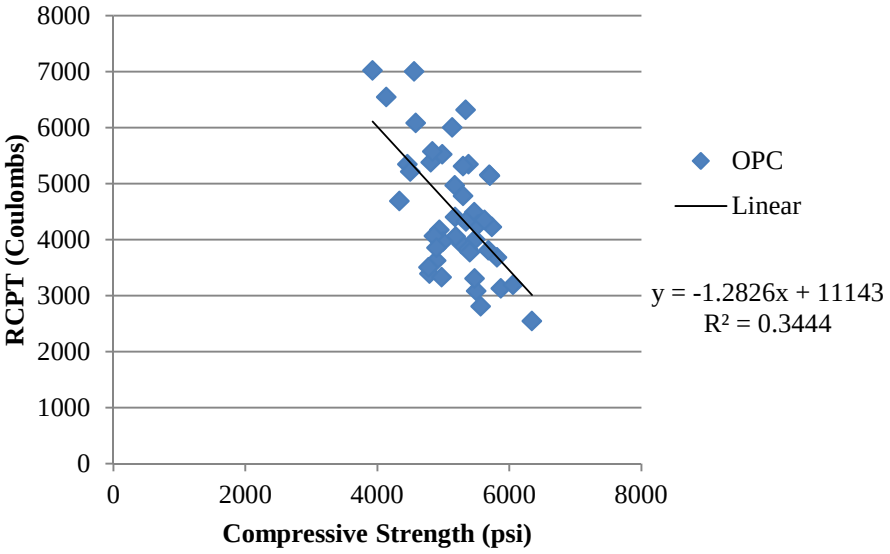

(c)

Figure 6-3 OPC Regression for (a) RCPT to Compressive Strength, (b) RPCT to Permeable Voids, (c) Permeable Voids to Compressive Strength

Figures 6-4a – 6-4c represent the relations between RCPT and strength, RCPT and permeable voids, and permeable voids and strength respectively for the F-ash mixture. Limit lines were also inserted as done for the previous regression.

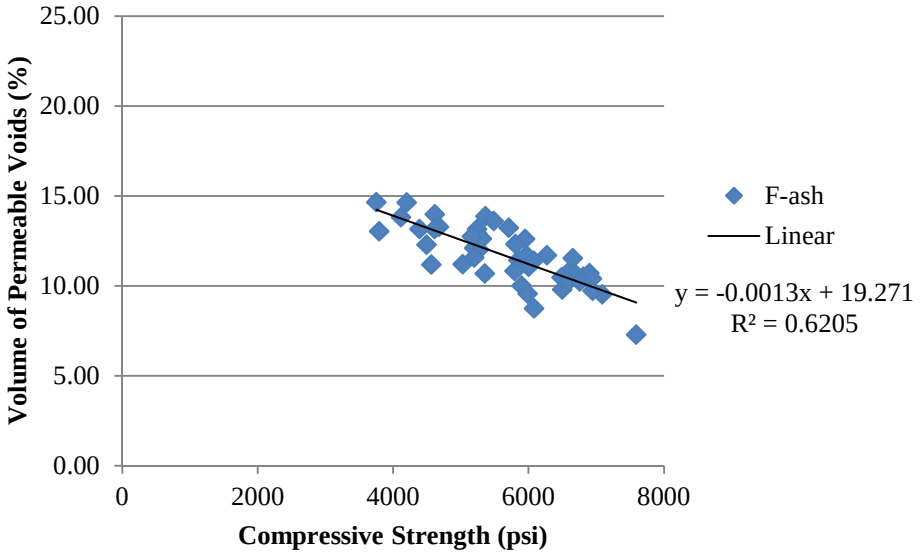

(a)

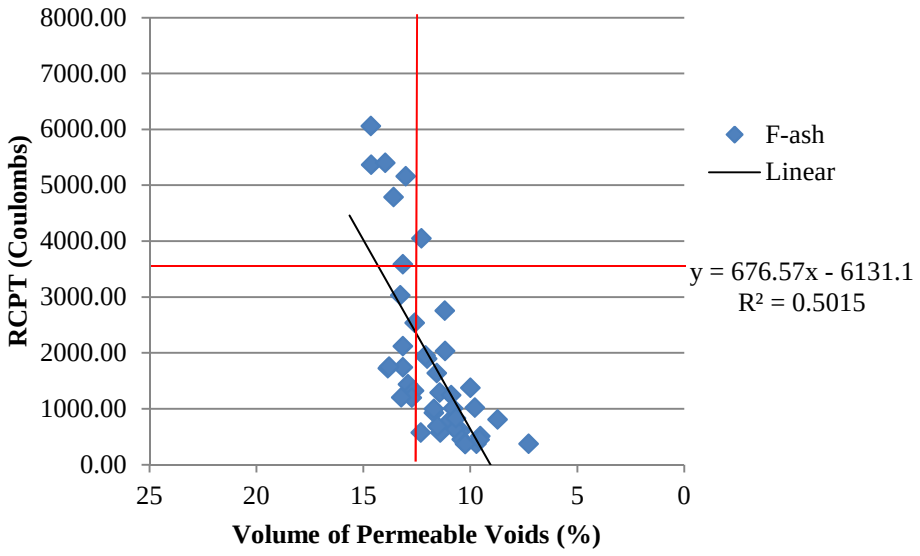

(b)

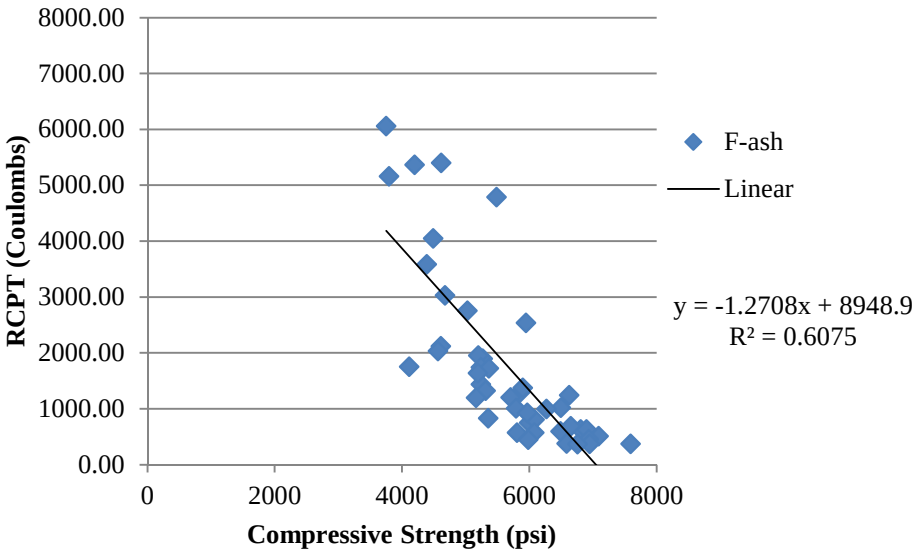

(c)

Table 6-4 F-ash Regression for (a) RCPT to Compressive Strength, (b) RPCT to Permeable Voids, (c) Permeable Voids to Compressive Strength

The F-ash demonstrated higher exponential R^2 values of 0.60 and 0.74 for *Figures 6-4b,c* respectively. Deviating from the OPC and only the RCPT values introduced exponential behavior.

Figures 6-5a – 6-5c represent the relations between RCPT and strength, RCPT and permeable voids, and permeable voids and strength respectively for the C-ash mixture. Limit lines were also inserted as done for the previous regressions.

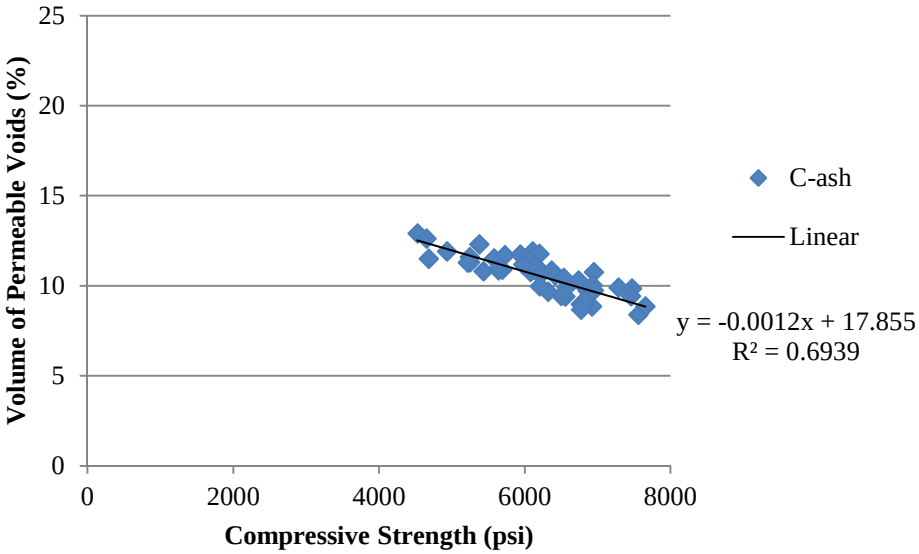
25
20
15
10
5
0
0
2000
4000
6000
8000
Volume of Permeable Voids (%)
Compressive Strength (psi)
C-ash
Linear
y = -0.0012x + 17.855
R² = 0.6939

(a)

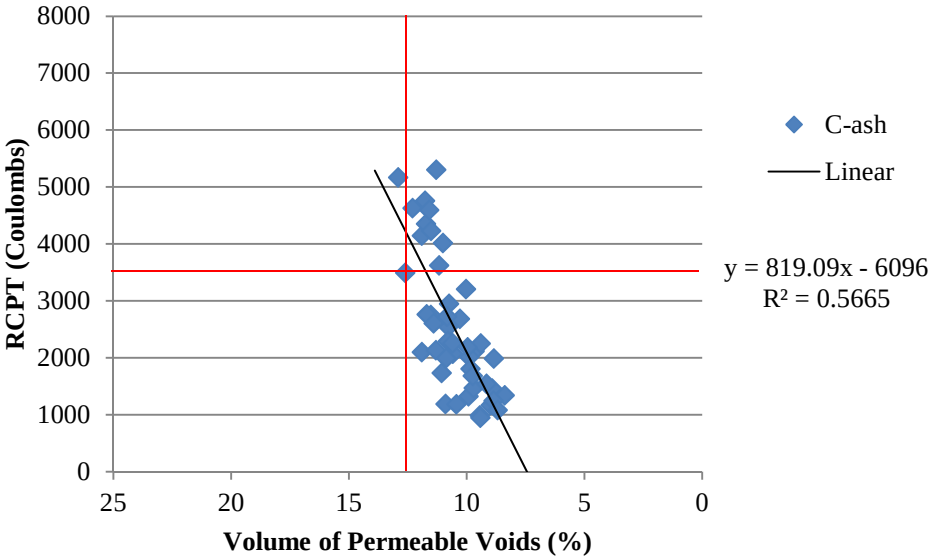
8000
7000
6000
5000
4000
3000
2000
1000
0
25
20
15
10
5
0
RCPT (Coulombs)
Volume of Permeable Voids (%)
C-ash
Linear
y = 819.09x - 6096
R² = 0.5665

(b)

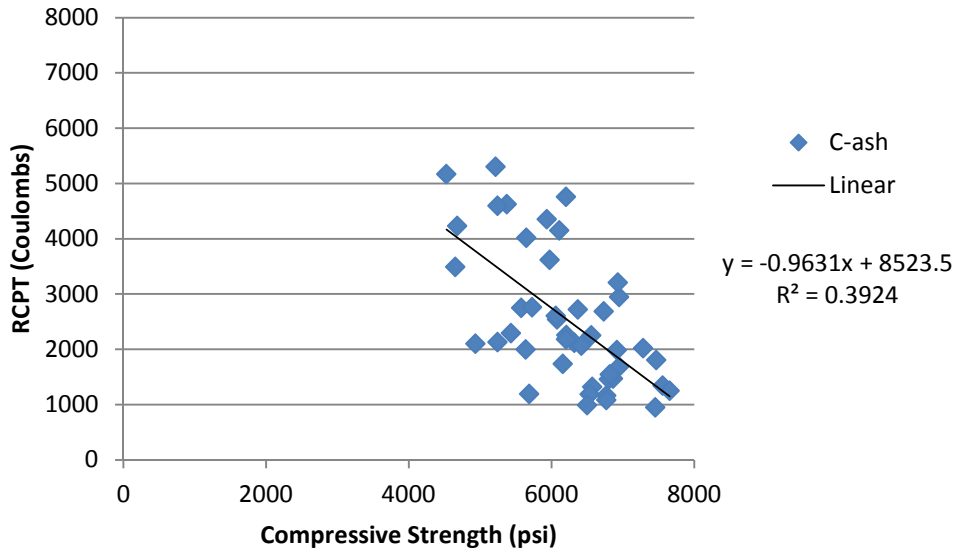

(c)

Figure 6-5 C-ash Regression for (a) RCPT to Compressive Strength, (b) RPCT to Permeable Voids, (c) Permeable Voids to Compressive Strength

The C-ash also demonstrated a higher exponential R^2 value of 0.58 and 0.74 for *Figure 6-5b.* Therefore both fly ash blends cause exponential relations.

The OPC mixture had the lowest R^2 values for every correlation run. The C-ash mixture had the highest correlations except for the relationship between permeable voids and compressive strength. These results are summarized in *Table 6-3.*

Table 6-3 Summary of Correlations

	Linear R^2			
	Combined	**OPC**	**F-ash**	**C-ash**
RCPT to Compressive Str.	0.44	0.18	0.62	0.69
RCPT to Permeable Voids	0.29	0.13	0.5	0.57
Permeable Voids to Compressive Str.	0.47	0.34	0.61	0.69

Perhaps more important than the correlations between the material properties is the actual value of each property. KDOT Standard Specification 401 was again used to evaluate the permeability across all of the cementations blends (KDOT 401 2007). The time parameters of 28 day permeable voids testing and 56 day RCPT results are not reflected in the summary table. The total percentage of each blend meeting this requirement is shown in *Table 6-4*.

Table 6-4 Summary of Permeability by Cement Blend

Permeable Voids < 12.50%			RCPT < 3500 Coulombs			Meeting Both		
OPC	**F-ash**	**C-ash**	**OPC**	**F-ash**	**C-ash**	**OPC**	**F-ash**	**C-ash**
67%	64%	96%	18%	84%	78%	16%	62%	76%

As demonstrated in Table 5-5 only16% of the entire OPC sample met both quality control measures, while the F-ash had 62% of its tests meeting both and the C-ash had the highest percentage meeting both at 76%. This table was independent of the curing environment, but it does strongly show the positive effects of using SCMs. It also shows, regardless of the curing environment, the long term permeability and therefore durability performance of the concrete was much higher.

5.3 - Maturity Analysis

The thermocouple temperature data was taken and corresponding testing day maturity data was then calculated. Season1 maturity curves are shown in *Table 6-5,* Season 2 maturity curves are shown in *Table 6-6* and Season 3 maturity curves are shown in *Table 6-7.*

Table 6-5 Season 1 Maturity Curves

	Nurse-Saul	Equivalent Age
OPC	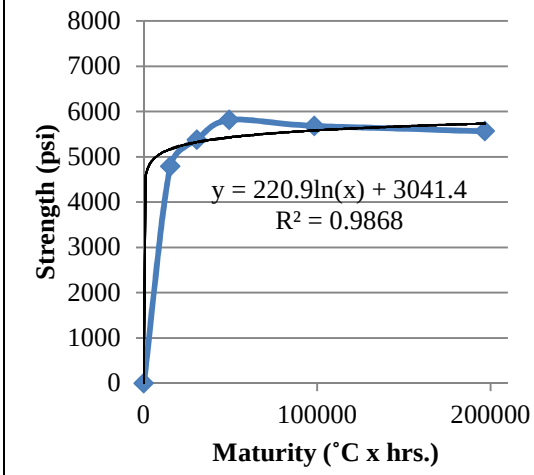	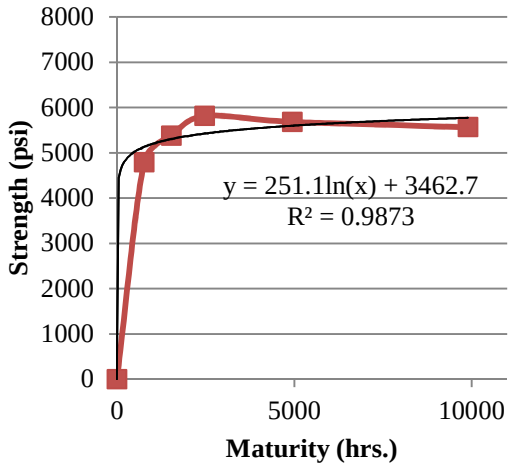
F-ash	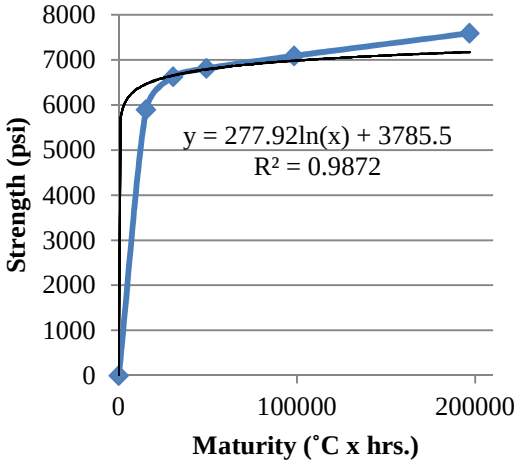	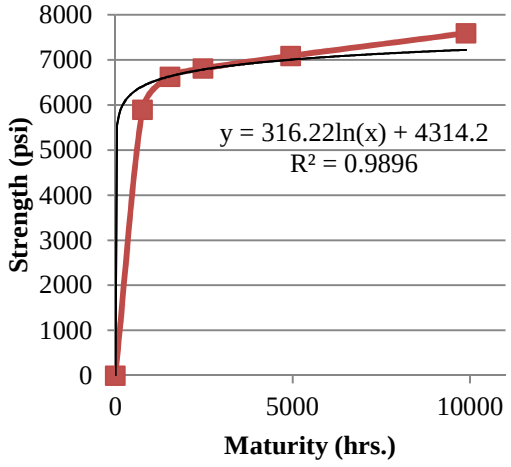
C-ash	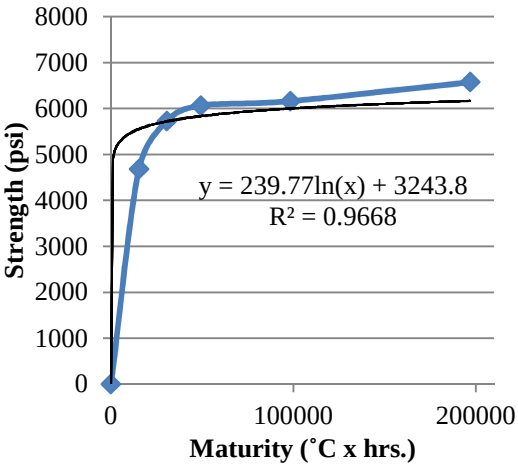	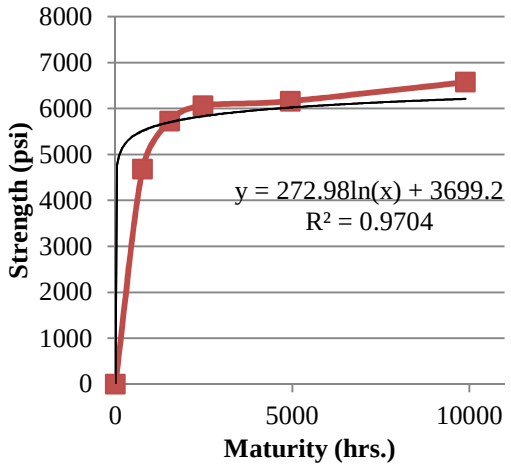

Table 6-7 Season 2 Maturity Curves

	Nurse-Saul	Equivalent Age
OPC	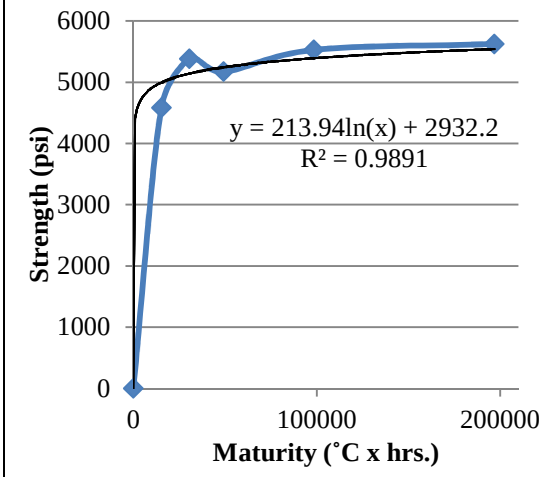	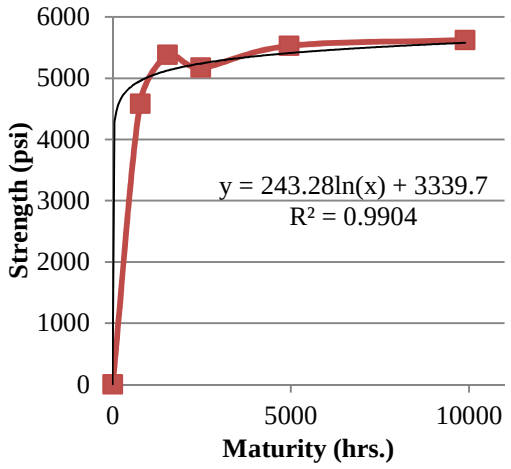
F-ash	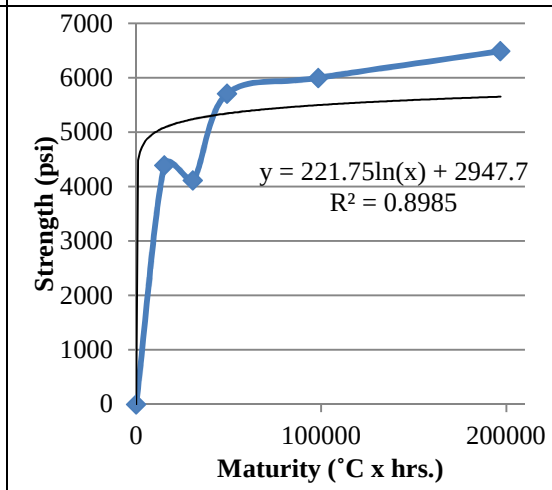	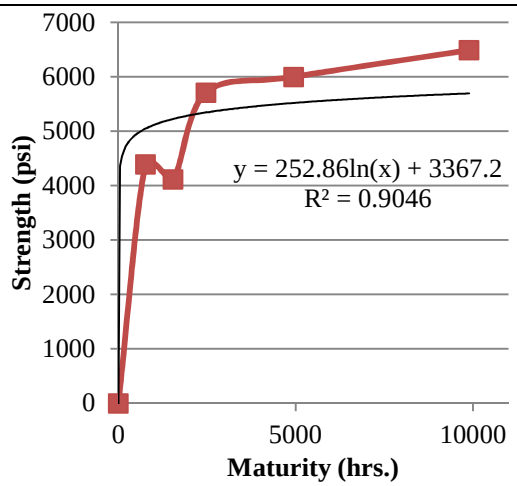
C-ash	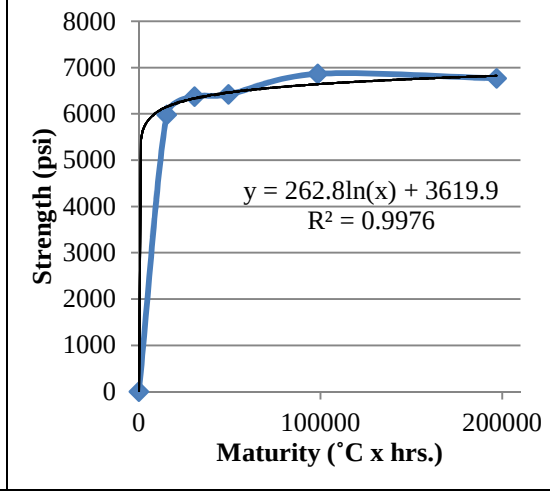	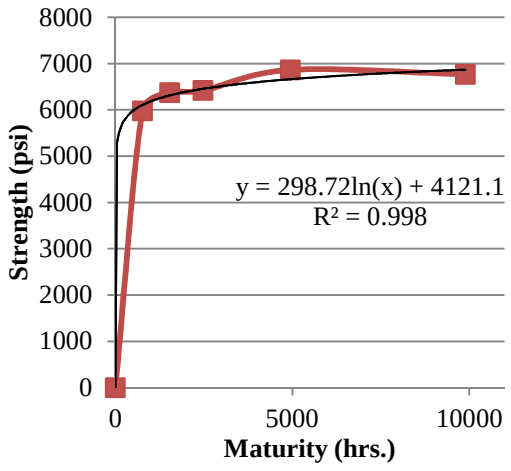

Table 6-8 Season 3 Maturity Curves

	Nurse-Saul	Equivalent Age
OPC	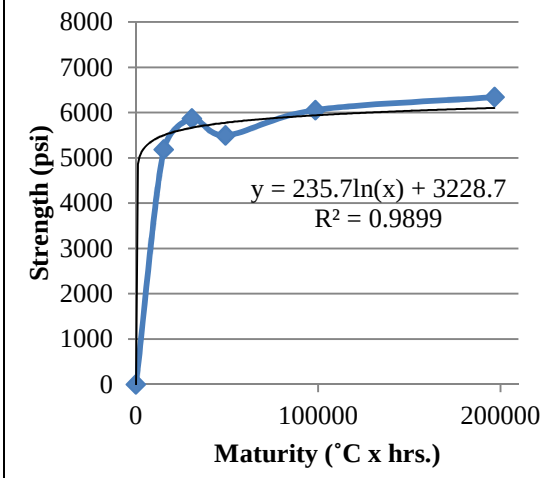	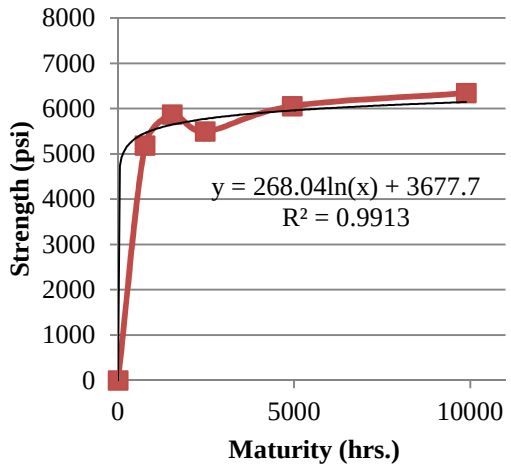
F-ash	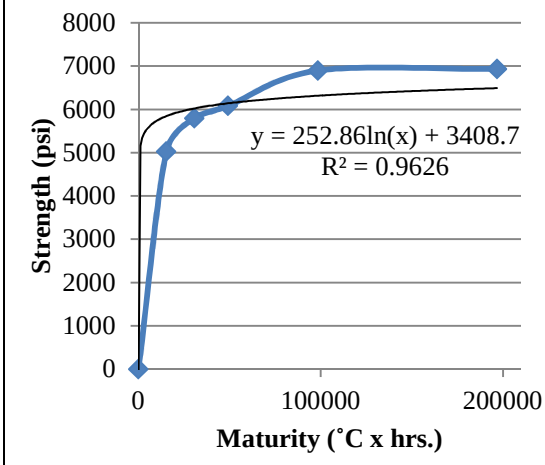	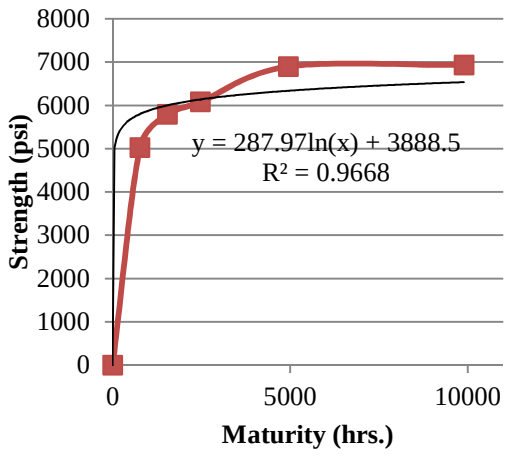
C-ash	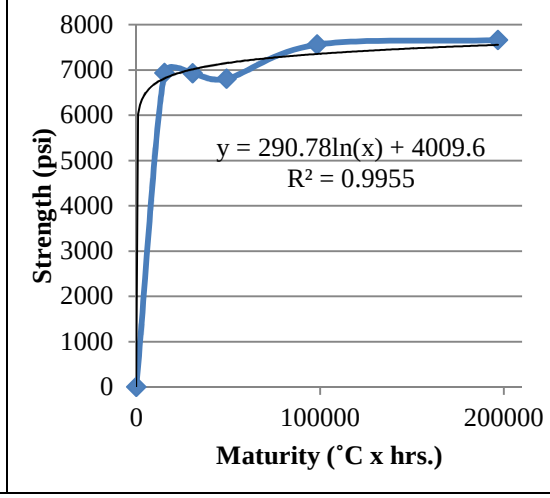	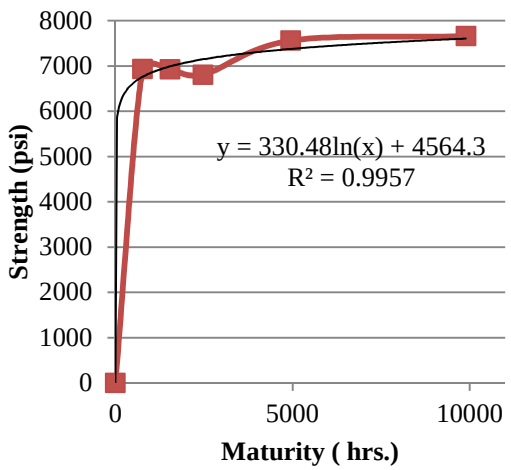

It is also evident how the use of SCMs affects the models. The models are not able to incorporate the pozzolanic reaction, and purely go off of the concrete temperature. F-ash performs much better in high temperature conditions and worse in colder temperatures which are not reflected. If the activation energies were adjusted the models may be able to be refined, but they still produce very good predications at 360 day values. The predicted values of core and cylinder strengths are in *Appendix A.*

Chapter 7 - Conclusions and Recommendations

7.1 - Conclusions

Based on the results obtained from this investigation, the following conclusions have been made regarding placements seasons, curing environments and performance tests:

1.

Incorporating supplementary cementitious materials densifies the microstructure development of both strength and permeability of concrete cured under realistic conditions. This is best seen in the percent passing of both performance standards regardless of the time parameter. The OPC only passed both tests for 16% of its samples. The Class F fly ash passed both tests for 62% of its samples and the C-ash passed both tests for 76% of its samples. The fly ash blends had a much higher rate of decreasing permeability with time and were typically much lower at early age.

2.

The F-ash blend had the highest variability between casting seasons for the in-situ core evaluation. It performed the best for season 1(summer) having RCPT values all under 1000 coulombs for the in-situ cured cores and corresponding low values of permeable voids. The F-ash also had the highest strength for all curing environments at 360 days for season 1. The F-ash had slower strength gain and permeability decrease in fall, but still very high strength and low permeability at 360 days.

3.

The C-ash consistently performed very well at early strength and low permeability regardless of the casting season and was the most resilient to placement season and differing curing effects.

4.

Average core specimens for each mix when compared to companion lab cylinder compressive strength tests were at least 90% of the lab compressive strength, indicating a good relationship between strength development of in-situ concrete.

5.

Since the RCPT and the permeable voids test are measuring different physical characteristics (electrical resistance and Archimedes' principal) a direct correlation between the two tests is unlikely. There will only be observable trends. The RCPT test shows stronger exponential correlations than linear correlations for the fly-ash blends. This furthers the position that there cannot be a direct linear correlation.

7.2 - Recommendations

Concretes containing fly ash as an SCM exhibit better long term concrete performance for both strength and permeability failure mechanisms. Use of SCMs should be encouraged in future pavement and bridge construction where a low permeability is desired.

7.3 - Future Research Needs

1.

Further research is needed to model the complex microstructure of concrete with and without SCMs to better understand the reaction kinetics, mass and ion transfer phenomena and the continuum that is the microstructure.

2.

Enhanced understanding of concrete resistivity/conductivity techniques is needed and the effects of SCMs when using such methods.

3.

Non-destructive permeability performance tests are needed that are not highly affected by the pore saturation level, surface charges and reinforcing steel

References

AASHTO T259. *Standard Method of Test for Resistance of Concrete to Chloride Ion Penetration.* Washington, D.C.: American Association of State highway and Transportation Officials, 2006.

AASHTO T260. *Standard Method of Test for Sampling and Testing for Chloride Ion in Concrete and Concrete Raw Materials.* Washingon, D.C.: American Associtions of State Highway and Transportation Officials, 2009.

AASHTO T277. *Standard Method of Test for Electrical Indication of Concrete's Ability to Resist Chloride Ion Penetration.* Washington, D.C.: American Association of State Transportation Officials, 2007.

ACI 201. *Guide to Durable Concrete.* Guide, Farmington Hills, MI: American Concrete Institute, 2008.

ACI 308. *Guide to Curing Concrete.* Technical Report, Farmington Hills, MI: American Concrete Instituite, 2008.

ACI 318. *Building Code Requirements for Structural Concrete and Commentary.* ACI Standard, Farmington Hills, MI: American Concrete Institute, 2008.

ASTM C1074. *Standard Practice for Estimating Concrete Strength by the Maturity Method.* West Conshohocken, PA: ASTM International, 2011.

ASTM C1202. *Standard Test Method for Electrical Indication of Concrete's Ability to Resist Chloride Ion Penetration.* West Conshohocken, PA: ASTM International , 2012.

ASTM C150. *Standard Specification for Portland Cement.* West Conshohocken, PA: ASTM International, 2012.

ASTM C1556. *Determinging the Apparent Chloride Diffusion Coefficient of Cementitious Mixtures by Bulk Diffusion.* West Conshohocken, PA: ASTM International, 2011.

ASTM C204. *Standard Test Methods for Fineness of Hydraulic Cement by Air-Permeability Apparatus.* West Conshohocken, PA: ASTM International, 2011.

ASTM C31. *Standard Practice for Making and Curing Concrete Test Specimens in the Field.* West Conshohocken, PA: ASTM International, 2012.

ASTM C39. *Compressive Strength of Cylindrical Concrete Specimens.* West Conshohocken, PA: ASTM International, 2012.

ASTM C42. *Standard Test Method for Obtaining and Testing Drilled Cores and Sawed Beams of Concrete.* West Conshohocken, PA: ASTM International, 2010.

ASTM C617. *Standard Practice for Capping Cylindrical Concrete Specimens.* West Conshohocken, PA: ASTM International, 2010.

ASTM C618. *Standard Specification for Coal Fly Ash and Raw or Calcined Natural Pozzolan for Use in Concrete.* West Conshohocken, PA: ASTM International, 2012.

ASTM C642. *Strandard Test Method for Density, Absorption and Voids in Hardened Concrete.* West Conshohocken, PA: ASTM International, 2006.

Atkins, Peter, and Loretta Jones. *Chemical Principles - The Quest for Insight.* Vol. 3. New York, New york: W.H. Freeman and Company, 2005.

Bamforth, P.B. "In situ Measurement of the Effect of Partial Portland Cement Replacement using either Fly Ash or Ground Granulated Blast-furnace Slag on the Performance of Mass Concrete." *Institution of Civil Engineers Proceedings* 69, no. 3 (September 1980): 777-800.

Berke, N. S., and M. C. Hicks. "Techniques to Assess the Corrosion Activity of Steel Reinforced Concrete Structures." *ASTM STP* (ASTM International), 1996: 41-57.

Bertolini, Luca, Elsener Bernhard , Elena Redaelli, and Rob Polder. *Corrosion of Steel in Concrete: Prevention, Diagnosis, Repair.* 2 vols. Weinheim, Germany: Wiley, 2013.

Castro, Javier, Robert Spragg, and William J. Weiss. *Portland Cement Concrete Pavement Permeability Performance.* Technical, Purdue University, West Lafayette: FHWA/IN/JTRP-2010/29. Joint Transportation Research Program, 2010.

Chini, A., L. Muszynski, and J. Hicks. *Determination of Acceptance Permeability Characteristics for Performance-Related Specifications for Portland Cement Concrete.* Technical, Tallahassee: Florida Department of Transportation, 2003.

Claisse, Peter. "Transport Properties of Concrete." *Concrete International* (American Concrete Institute) 27, no. 01 (2005): 43-48.

Flatt, Robert J., George W. Scherer, and Jeffery W. Bullard. "Why Alite Stops Hydrating Below 80% Relative Humidity." *Cement and Concrete Research* 41, no. 9 (September 2011): 987-995.

FM 5-578. *Florida Method of Test for Concrete Resistivity as an Electrical Indicator of Permeability.* Florida Department of Transportation, 2004.

Halstead, W. J. *Use of Fly Ash in Concrete.* Technical, National Cooperative Research Program (NCHRP), Washington, D.C.: Transportation Research Board, 1986.

Hamilton III, H. R., and Andrew J. Boyd. *Permeability of Concrete - Comparison of Conductivity and Diffusion Methods.* Technical, Civil & Coastal Engineering, University of Florida, Tallahassee: Florida Department of Transportation, 2007.

Haque, M. N., R. L. Day, and B. W. Langan. "Realistic Strength of Air-Entrained concretes with and without Fly Ash." *ACI Materials Journal*, 1988: 241-247.

KDOT 401. *Concrete.* Topeka, KS: Kansas Department of Transportation, 2007.

KDOT 501. *Portland Cement Concrete Pavement (QC/QA).* Topeka, KS: Kansas Department of Transportation, 2007.

Li, Zongjin. *Advanced Concrete Technology.* Hoboken, New Jersey: John Wiley & Sons, Inc., 2011.

McGrath, Patrick F., and Doug R. Hooton. "Re-evaluation of the AASHTO T259 90-day Salt Ponding Test." *Cement and Concrete Research*, 1999: 1239-1248.

Mindess, Sydney, J. Francis Young, and David Darwin. *Concrete.* Vol. 2 . Upper Sadle River, New Jersey, New Jersey: Prentice Hall, 2003.

Monteiro, Paulo J. M. *Concrete: Microstructure, Properties, and Materials.* Vol. 3. New York, New York: McGraw-Hill, 2006.

NT Build 443. *Concrete, Hardened: Accelerated Chloride Penetration.* Espoo, Finland: NORDTEST, 1995.

Stanish, K. D., R. D. Hooton, and M. D.A. Thomas. *Testing the Chloride Penetration Resistance of Concrete: A Literature Review.* FHWA, 2001.

Sydney Mindess, J. Francis Young, David Darwin. *Concrete.* Vol. 2 . Upper Sadle River, New Jersey: Prentice Hall, 2003.

Appendix A - Maturity Data

Season 1 Maturity for Slabs (Cores)

Lab Maturity		From Lab Temperature (˚C x hrs.)		From Slab Temperature (˚C x hrs.)		Predicted Slab Str. (psi)		
Season 1 OPC								
Time (hrs.)	**Lab Strength (psi)**	**Nurse-Saul**	**Equivalent Age**	**Nurse-Saul**	**Equivalent Age**	**Nurse-Saul**	**Equivalent Age**	**Actual Slab Str. (psi)**
0	0	0	0	0	0	0	0	0
672	4789	15308	769	21174	1180	5242	5239	4941
1344	5378	30616	1538	36578	1951	5362	5365	5298
2160	5811	49205	2472	49869	2461	5431	5423	4991
4320	5682	98410	4945	59366	2520	5469	5429	5299
8640	5566	196819	9890	144834	6595	5666	5671	5475
Season 1 F-ash								
Time (hrs.)	**Lab Strength (psi)**	**Nurse-Saul**	**Equivalent Age**	**Nurse-Saul**	**Equivalent Age**	**Nurse-Saul**	**Equivalent Age**	**Actual Slab Str. (psi)**
0	0	0	0	0	0	0	0	0
672	5896	15308	769	14777	818	6454	6435	5966
1344	6625	30616	1538	30029	1582	6651	6644	6268
2160	6809	49205	2472	43368	2094	6753	6732	6076
4320	7088	98410	4945	50902	2130	6797	6738	6652
8640	7591	196819	9890	136519	6219	7072	7077	6948
Season 1 C-ash								
Time (hrs.)	**Lab Strength (psi)**	**Nurse-Saul**	**Equivalent Age**	**Nurse-Saul**	**Equivalent Age**	**Nurse-Saul**	**Equivalent Age**	**Actual Slab Str. (psi)**
0	0	0	0	0	0	0	0	0
672	4681	15308	769	9870	555	5449	5424	5435
1344	5728	30616	1538	24850	1300	5670	5657	5247
2160	6062	49205	2472	37889	1786	5772	5743	5691
4320	6162	98410	4945	45097	1815	5813	5748	5639
8640	6574	196819	9890	130824	5921	6069	6070	6535

Season 1 Maturity for Field Cylinders

Lab Maturity		From Lab Temperature (˚C x hrs.)		From Cylinder Temperature (˚C x hrs.)		Predicted Field Cylinder Str. (psi)		
Season 1 OPC								
Time (hrs.)	**Lab Strength (psi)**	**Nurse-Saul**	**Equivalent Age**	**Nurse-Saul**	**Equivalent Age**	**Nurse-Saul**	**Equivalent Age**	**Actual Field Cyl. Str. (psi)**
0	0	0	0	0	0	0	0	0
672	4789	15308	769	19526	1085	5224	5218	3928
1344	5378	30616	1538	34361	1786	5349	5343	4136
2160	5811	49205	2472	48177	2369	5423	5414	4558
4320	5682	98410	4945	57518	2608	5462	5438	4809
8640	5566	196819	9890	145715	6996	5668	5686	4332
Season 1 F-ash								
Time (hrs.)	**Lab Strength (psi)**	**Nurse-Saul**	**Equivalent Age**	**Nurse-Saul**	**Equivalent Age**	**Nurse-Saul**	**Equivalent Age**	**Actual Field Cyl. Str. (psi)**
0	0	0	0	0	0	0	0	0
672	5896	15308	769	13879	783	6436	6421	5266
1344	6625	30616	1538	28674	1481	6638	6623	5947
2160	6809	49205	2472	42308	2052	6746	6726	5199
4320	7088	98410	4945	50037	2227	6793	6752	5850
8640	7591	196819	9890	138881	6678	7076	7099	6496
Season 1 C-ash								
Time (hrs.)	**Lab Strength (psi)**	**Nurse-Saul**	**Equivalent Age**	**Nurse-Saul**	**Equivalent Age**	**Nurse-Saul**	**Equivalent Age**	**Actual Field Cyl. Str. (psi)**
0	0	0	0	0	0	0	0	0
672	4681	15308	769	9280	531	5434	5412	5377
1344	5728	30616	1538	23724	1201	5659	5635	4529
2160	6062	49205	2472	37162	1758	5767	5739	4934
4320	6162	98410	4945	44193	1907	5808	5761	4651
8640	6574	196819	9890	133131	6389	6073	6091	5576

Season 2 Maturity for Slabs (Cores)

Lab Maturity		From Lab Temperature (˚C x hrs.)		From Slab Temperature (˚C x hrs.)		Predicted Slab Str. (psi)		
Season 2 OPC								
Time (hrs.)	**Lab Strength (psi)**	**Nurse-Saul**	**Equivalent Age**	**Nurse-Saul**	**Equivalent Age**	**Nurse-Saul**	**Equivalent Age**	**Actual Slab Str. (psi)**
0	0	0	0	0	0	0	0	0
672	4583	15308	769	9449	291	4891	4720	5135
1344	5382	30616	1538	12223	299	4946	4727	4456
2160	5171	49205	2472	13901	301	4973	4728	4497
4320	5528	98410	4945	33118	905	5159	4996	5341
8640	5624	196819	9890	144128	6634	5473	5481	4889
Season 2 F-ash								
Time (hrs.)	**Lab Strength (psi)**	**Nurse-Saul**	**Equivalent Age**	**Nurse-Saul**	**Equivalent Age**	**Nurse-Saul**	**Equivalent Age**	**Actual Slab Str. (psi)**
0	0	0	0	0	0	0	0	0
672	4390	15308	769	8068	219	4942	4618	3793
1344	4113	30616	1538	10253	224	4996	4620	5483
2160	5708	49205	2472	11373	225	5019	4622	4491
4320	5999	98410	4945	34979	1020	5268	5171	5194
8640	6488	196819	9890	146839	6806	5586	5595	5805
Season 2 C-ash								
Time (hrs.)	**Lab Strength (psi)**	**Nurse-Saul**	**Equivalent Age**	**Nurse-Saul**	**Equivalent Age**	**Nurse-Saul**	**Equivalent Age**	**Actual Slab Str. (psi)**
0	0	0	0	0	0	0	0	0
672	5977	15308	769	5474	141	6152	6106	5243
1344	6370	30616	1538	7056	142	6334	6313	5219
2160	6418	49205	2472	8375	143	6459	6455	5650
4320	6864	98410	4945	37508	1252	6641	6662	6209
8640	6770	196819	9890	145432	6715	6823	6869	6947

Season 2 Maturity for Field Cylinders

Lab Maturity		From Lab Temperature		From Cylinder Temperature (˚C x hrs.)		Predicted Field Cylinder Str. (psi)		
Season 2 OPC								
Time (hrs.)	**Lab Strength (psi)**	**Nurse-Saul**	**Equivalent Age**	**Nurse-Saul**	**Equivalent Age**	**Nurse-Saul**	**Equivalent Age**	**Actual Field Str. (psi)**
0	0	0	0	0	0	0	0	0
672	4583	15308	769	7875	261	4852	4694	5336
1344	5382	30616	1538	10431	312	4912	4737	4986
2160	5171	49205	2472	13159	385	4961	4788	5696
4320	5528	98410	4945	35733	1257	5175	5076	5704
8640	5624	196819	9890	145627	6976	5476	5493	4831
Season 2 F-ash								
Time (hrs.)	**Lab Strength (psi)**	**Nurse-Saul**	**Equivalent Age**	**Nurse-Saul**	**Equivalent Age**	**Nurse-Saul**	**Equivalent Age**	**Actual Field Str. (psi)**
0	0	0	0	0	0	0	0	0
672	4390	15308	769	6114	152	4881	4463	3752
1344	4113	30616	1538	7402	169	4923	4533	4198
2160	5708	49205	2472	8766	196	4961	4634	4616
4320	5999	98410	4945	33942	1119	5261	5207	5240
8640	6488	196819	9890	143187	6762	5580	5604	5362
Season 2 C-ash								
Time (hrs.)	**Lab Strength (psi)**	**Nurse-Saul**	**Equivalent Age**	**Nurse-Saul**	**Equivalent Age**	**Nurse-Saul**	**Equivalent Age**	**Actual Field Str. (psi)**
0	0	0	0	0	0	0	0	0
672	5977	15308	769	3362	76	6152	6106	6110
1344	6370	30616	1538	5452	101	6334	6313	6203
2160	6418	49205	2472	7292	150	6459	6455	5937
4320	6864	98410	4945	38618	1445	6641	6662	6948
8640	6770	196819	9890	144824	6940	6823	6869	6735

Season 3 Maturity for Slabs (Cores)

Lab Maturity		From Lab Temperature (˚C x hrs.)		From Slab Temperature (˚C x hrs.)		Predicted Slab Str. (psi)		
Season 3 OPC								
Time (hrs.)	**Lab Strength (psi)**	**Nurse-Saul**	**Equivalent Age**	**Nurse-Saul**	**Equivalent Age**	**Nurse-Saul**	**Equivalent Age**	**Actual Slab Str. (psi)**
0	0	0	0	0	0	0	0	0
672	5188	15308	769	13808	655	5476	5416	4858
1344	5872	30616	1538	29068	1420	5651	5623	4896
2160	5496	49205	2472	50689	2543	5782	5779	4776
4320	6054	98410	4945	112316	5844	5970	6002	4975
8640	6341	196819	9890	139592	6438	6021	6028	5399
Season 3 F-ash								
Time (hrs.)	**Lab Strength (psi)**	**Nurse-Saul**	**Equivalent Age**	**Nurse-Saul**	**Equivalent Age**	**Nurse-Saul**	**Equivalent Age**	**Actual Slab Str. (psi)**
0	0	0	0	0	0	0	0	0
672	5025	15308	769	13775	669	5819	5762	4562
1344	5791	30616	1538	30468	1524	6019	5999	5351
2160	6080	49205	2472	53841	2771	6163	6171	5984
4320	6898	98410	4945	113643	5947	6352	6391	6588
8640	6934	196819	9890	139565	6407	6404	6413	6758
Season 3 C-ash								
Time (hrs.)	**Lab Strength (psi)**	**Nurse-Saul**	**Equivalent Age**	**Nurse-Saul**	**Equivalent Age**	**Nurse-Saul**	**Equivalent Age**	**Actual Slab Str. (psi)**
0	0	0	0	0	0	0	0	0
672	6932	15308	769	15163	760	5939	6757	6204
1344	6920	30616	1538	31883	1617	6158	7006	6822
2160	6806	49205	2472	56621	2961	6334	7206	6501
4320	7559	98410	4945	112330	5830	6531	7430	6772
8640	7657	196819	9890	135349	6180	6548	7449	7457

Season 3 Maturity for Field Cylinders

Lab Maturity		From Lab Temperature		From Cylinder Temperature (˚C x hrs.)		Predicted Field Cylinder Str. (psi)		
Season 3 OPC								
Time (hrs.)	**Lab Strength (psi)**	**Nurse-Saul**	**Equivalent Age**	**Nurse-Saul**	**Equivalent Age**	**Nurse-Saul**	**Equivalent Age**	**Actual Field Cyl. Str. (psi)**
0	0	0	0	0	0	0	0	0
672	5188	15308	769	12294	520	5448	5354	5469
1344	5872	30616	1538	27951	1289	5642	5597	5735
2160	5496	49205	2472	50347	2492	5781	5774	5178
4320	6054	98410	4945	111337	5850	5968	6003	5275
8640	6341	196819	9890	138235	6739	6019	6041	5481
Season 3 F-ash								
Time (hrs.)	**Lab Strength (psi)**	**Nurse-Saul**	**Equivalent Age**	**Nurse-Saul**	**Equivalent Age**	**Nurse-Saul**	**Equivalent Age**	**Actual Field Cyl. Str. (psi)**
0	0	0	0	0	0	0	0	0
672	5025	15308	769	12596	544	5796	5703	4676
1344	5791	30616	1538	29428	1406	6011	5976	4611
2160	6080	49205	2472	53647	2763	6162	6170	5238
4320	6898	98410	4945	110594	5803	6345	6384	5312
8640	6934	196819	9890	131673	6461	6389	6415	5162
Season 3 C-ash								
Time (hrs.)	**Lab Strength (psi)**	**Nurse-Saul**	**Equivalent Age**	**Nurse-Saul**	**Equivalent Age**	**Nurse-Saul**	**Equivalent Age**	**Actual Field Cyl. Str. (psi)**
0	0	0	0	0	0	0	0	0
672	6932	15308	769	13888	648	5892	6704	6080
1344	6920	30616	1538	31101	1544	6145	6991	6322
2160	6806	49205	2472	56514	2999	6338	7210	7284
4320	7559	98410	4945	110697	5835	6531	7430	6559
8640	7657	196819	9890	132355	6511	6563	7466	7470

Appendix B - Permissions

Paul,

As a Masters student, I am pleased to grant you permission to reproduce these figures free of charge.
Good luck with your work.
Best wishes
Ben

Ben Ramster
Journals Editorial Manager
ICE Publishing
t +44 (0)20 7665 2242

To whom it may concern,

I am writing to gain permission to use figures in the below article for use in my master's thesis at Kansas State University, and for use in a report to the Kansas Department of Transportation. Could you please email me back permission or advise me on further action?

IN SITU MEASUREMENT OF THE EFFECT OF PARTIAL PORTLAND CEMENT REPLACEMENT USING EITHER FLY ASH OR GROUND GRANULATED BLAST-FURNACE SLAG ON THE PERFORMANCE OF MASS CONCRETE.

Authors: PB BAMFORTH, BS 1881

Source: ICE Proceedings, PART 2 Volume 69, Issue 3, September 1980, pages 777 - 800
Type: Article

Thank You,